

Analysis and optimization of a metamaterial for noise reduction

Master's Thesis Nr. 70

Scientific Thesis for Acquiring the
Master of Science Degree
at the Department of Mechanical Engineering
of the Technical University of Munich.

Thesis Advisor Laboratory for Production Development and Lightweight Design
Prof. Dr. Markus Zimmermann

Supervisor Laboratory for Production Development and Lightweight Design
M. Sc. Duo Xu

Submitted by B. Sc. Weiwei Wang
Christoph-Probst-Straße 8, 80805, Munich
Matriculation number: 03694919
ga27god@mytum.de

Submitted on Februar, 26 2020

Declaration

I assure that I have written this work autonomously and with the aid of no other than the sources and additives indicated.

Place

Date

Signature

Project Definition(1/2)

Initial Situation

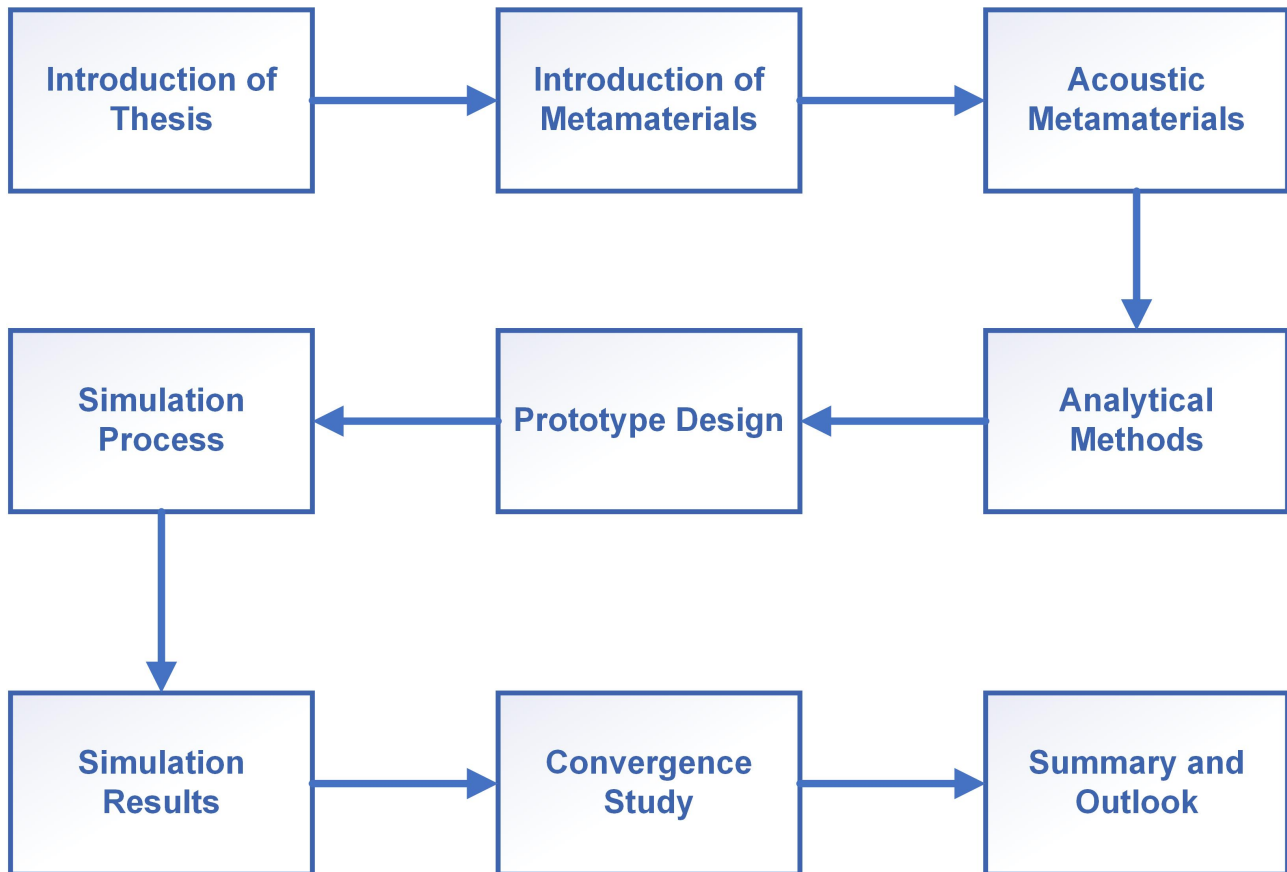
In the last twenty years, many researches and experiments have been executed in the field of acoustic metamaterials. The acoustic metamaterial is one of the most important metamaterial branch, which has remarkable performance in reducing vibration and noise, especially for light-weight design applications. Metamaterials are known with their periodic structures, which is also general property in all metamaterial varieties. In most literatures, the acoustic metamaterial models are manufactured by 3D-printing technique, which is recently a relative mature manufacturing method for acoustic metamaterial experiments. However, the execution of simulations for acoustic metamaterial is still a challenge for today's work. By simulating models and environments rather than experiments a lot of time can be saved. Moreover, the simulation process in software is relatively flexible. Due to some influence factors, there are always deviations between experimental and simulation results, which is a common problem in literatures.

Goals

In this thesis, based on the literature research a prototype design is drawn up. After that, different variants for experiment and simulation process are further designed. By using commercial software COMSOL® Multiphysics, several typical models are built up to analyze their dispersion relations. In order to match the experimental results, several models are further improved by executing convergence study. This thesis aims to give a guidance for simulating two-dimensional acoustic metamaterials to analyze the stop band property. Different models are built up by same principles. In the end, challenges and suggestions for the future work are also illustrated.

Project Definition(2/2)

Contents of this Thesis



The work remains a property of the Laboratory for Product Development and Lightweight Design.

Project Note

Master's Thesis

Nr. 70

Supervisor

M. Sc. Duo Xu

Time period

Juli, 26 2019 - Februar, 26 2020

My supervisor Mr. Duo Xu mentored me during the compilation of the work and gave continuous input. We exchanged and coordinated approaches and results weekly.

Restriction notice without participation of industry partner

The present work contains confidential information which is subject to confidentiality. Therefore, publication, reproduction, modification, storage in a retrieval system or retransmission, in any form or by any means, electronic, mechanical or otherwise, is strictly prohibited without prior written permission of the supervisor at the Laboratory for Product Development and Lightweight Design. (If applicable recourse claims of the university and/or of the supervisor arise.) Only persons who correct or assess the work are allowed to gain access to it. The restriction notice is indefinite (submission date: Februar, 26th. 2020). In case of any queries, contact the supervisor of the thesis. Alternatively you may contact the office of the Laboratory for Product Development and Lightweight Design.

Publication // I consent to the laboratory and its staff members using content from my thesis for publications, project reports, lectures, seminars, dissertations and postdoctoral lecture qualifications.

Signature of student

Signature of supervisor

Abstract

Good acoustical behavior is one of the most important factor in the light-weight design. The acoustic metamaterials are promising solutions to achieve the improvements in this field. With their repeating structure in periodicity, an excellent sound reduction effect can be achieved. According to the literature research, there are various of acoustic metamaterial designs with different materials and structures. However, there are still challenges to find a model, which can be both manufactured and simulated and meanwhile the results agree with each other.

On the one hand, the manufacturing method (3D-printing technology) has error potentials when building small-size models. This will lead to a wrong value in experiments. On the other hand, the simulation environment is idealized, which cause a deviation between simulation results and experimental results. Obviously, the acoutic physical domain has some unavoidable uncertenties. It is difficult to explore the propagation of acoustic waves in different media materials.

This thesis aims to propose possible acoustic metamaterial designs based on the literature research. These models can be both manufactured by 3D-printing technology and simulated in software. The focus of thesis is to find a simulation process, in which the experiments machted results can be calculated. The properties of acoustic metamaterials, which can be evaluataed and compared by experiments and simulations, are also explained and analyzed.

The first few chapters give an overview about state of the art. The history and development as well as categories of metamaterials are introduced. After that, the important physical parameters and academica models as well as possible analytical methods of acoustical metamaterials are explained. Possible mathematical calculation methods are compared with Finite-element method specially for software. Based on the literature research different prototype designs are proposed. Before explain the simulation process in details, the possible simulated properties are analyzed and compared. In order to improve the simulation results, the convergence study is executed. In the end, the challenges and possible improvements are summarized.

Contents

1 Introduction	3
1.1 Motivation.....	3
1.2 Structure of the work	4
2 Introduction and categories of metamaterials	6
2.1 History and development.....	6
2.2 Elastic metamaterials.....	6
2.3 Structural metamaterials	6
2.4 Nonlinear metamaterials	7
2.5 Electromagnetic metamaterials	8
2.6 Acoustic metamaterials.....	8
3 Concept of acoustic metamaterials	10
3.1 Acoustic parameters	11
3.1.1 Bulk modulus.....	11
3.1.2 Mass density	11
3.2 Typical academic models in 1D and 2D	12
3.2.1 One-dimensional model.....	12
3.2.2 Two-dimensional model	13
3.3 Typical structures and designs.....	15
3.3.1 Rod-type acoustic metamaterials	15
3.3.2 Membrane-type acoustic metamaterials	16
3.3.3 Plate-type acoustic metamaterials	17
3.3.4 Other types	18
4 Calculation methods and Finite-element-method in software	20
4.1 Calculation methods	20
4.1.1 Plane wave expansion method	20
4.1.2 Multiple scattering method	21
4.1.3 Finite-difference-time-domain method	22
4.1.4 The Korringa-Kohn-Rostoker Method	23
4.2 Finite-element-method in software	24
4.2.1 Mathematical principles of Finite-element-method	24
4.2.2 Possible software based on Finite-element-method	26
5 Design and construction of prototype	27
5.1 Physical principles	27

5.2 Design of demonstrators	28
6 Simulation process	39
6.1 Theories for simulation process	39
6.1.1 Physical properties.....	39
6.1.2 The Brillouin zone and wave vector	42
6.1.3 The Floquet-Bloch boundary condition	44
6.2 Simulation steps.....	45
6.2.1 Model environment.....	46
6.2.2 Geometric objects.....	46
6.2.3 Definitions and parameters.....	48
6.2.4 Material properties.....	48
6.2.5 Periodic boundary conditions	49
6.2.6 Meshing	51
6.2.7 Study	52
6.3 Verification of simulation process.....	53
7 Simulation results.....	54
7.1 Diagrams of the dispersion relation	54
7.2 Discussion about simulation results.....	58
7.3 Correlation between simulation and experiment results.....	59
7.4 Potentials for convergence study	63
8 Convergence study	64
8.1 Convergence study of the meshing size for small resonators	64
8.2 Convergence study of the model geometry	67
9 Discussion and summary	72
9.1 Discussion of results.....	72
9.2 Conclusion and outlook	72
References	74
List of Figures.....	77
List of Tables	80
List of abbreviations	81

1 Introduction

1.1 Motivation

Ecological trends and efficiency requirements give the lightweight design a significant meaning in today's development. To satisfy customer's expectations, good acoustical behavior turns into one of the most important design criteria. The vibration and noise reduction measures usually require heavy and bulky systems, which in general have conflicts with the lightweight design. Therefore, the acoustic metamaterial is treated as a promising solution to achieve Noise Vibration and Harshness (NVH.) improvement, especially for automobile and aerospace applications.

Acoustic metamaterials are regarded as a new type of artificial composite acoustic material that is closely related to the concept of phononic crystals at a subwavelength scale (LU et al., 2014, p.1). The impressive character of them is the repeating structural patterns. The periodic arrangement of scatterers causes the destructive interference of waves in the band of frequencies, which leads to sound attenuation (Gupta, 2014, p.1).

Yet, there exists a variety of metamaterials in literature. This thesis aims to get an overview of acoustic metamaterial for noise isolation through a literature research. The typical structures of acoustic metamaterial will be summarized and a prototype design will be suggested based on the literature research. The prototype, which will be built by a 3D printing technique, should also be simulated on the basis of relevant numerical principles. In the end, the simulation results will be validated and improved by comparing with experimental results, where the prototype will be installed into a mess system and the effectiveness of the metamaterial in noise reduction will be evaluated.

So far, there has been some researches on both experiments and simulations of acoustic metamaterial. However, the structures and properties of them studied in each paper vary greatly. Moreover, 3D printing manufacturing and simulation processes are not always possible for some complex structures. For models that can be both 3D printed and simulated, the experimental results and simulation results are more or less different.

Currently, there are three typical 3D printing technologies for acoustic metamaterial manufacturing: Selective Laser Sintering (SLS.), Fused Deposition Modelling (FDM.) and Selective Laser Melting (SLM.). Among them, SLS. and FDM. are more commonly used. Usually, it is necessary to build a corresponding CAD model before manufacturing the sample. Experiments are generally executed in an acoustic impedance tube or based on self-built experimental platforms. And the reflection of sound waves should be avoided during experiments.

The most simulations of acoustic metamaterials are achieved by building a finite element model in COMSOL ® Multiphysics, the software Abaqus and LMS VL Acoustics software environment are also used in pieces of literature. In addition to finite element model, other basic simulation models include the Heckls model and the Helmholtz model. The difficulty of simulation is to create a same model environment as experimental test. Generally, the simulation environment is idealized, and the test environment will have a certain influence on experimental results, which also causes a deviation between experimental results and simulation results to some extent.

In general, there are two properties of acoustic metamaterials that can be evaluated through simulation process and meanwhile compared with experimental results: the dispersion relation and Sound Transmission Loss (STL). On the one hand, the dispersion curve expresses a relation between eigenfrequency and wave vector of metamaterial structure. On the other hand, the bandgap of a prototype can also be visualized through the dispersion relation. Those bandgaps are also referred to as stopbands, there are frequency zones for which free wave propagation is prevented through the metamaterial, resulting in frequency zones of pronounced wave attenuation (Claeys, Deckers, Plutmers, & Desmet, 2016, p.1). STL expresses a relationship between incident sound energy and transmitted sound energy, which reflects noise reduction effect of a metamaterial structure. So far very little simulation has been done for these two properties. It is difficult to find a relatively mature simulation step for a prototype.

The idea of prototype built in this thesis comes from a numerical study on the behavior of partition panels with micro-resonator-type metamaterials (Amado-Mendes, Godinho, Dias, Amaral, & Pinho, 2018, p.1). Each resonator on the basis plate can be considered as a mass-spring element. This numerical modelling concept allows straightforward control of the resonance frequency of the first bending mode (Claeys et al., 2016, p.2) and can be applied with the Floquet-Bloch boundary conditions, which enables modelling only a unitary cell of the periodic system (Amado-Mendes et al., 2018, p.5).

To visualize the sound insulation effect of acoustic metamaterial prototype and to compare with the experimental results. It is decided to use commercial software COMSOL® Multiphysics to simulate the dispersion curve, which reflects band gap structure at a certain frequency range. The focus of this thesis is try to build a exactly same model as the prototype design and execute the corresponding analytical solution for the simulation process.

Due to the Floquet-Bloch boundary condition the simulation model can be simplified and considered as a periodic structure. After defining the necessary coordinate system and parameters to set up the first Brillouin zone, the geometry and material properties of the model can be built up in the corresponding physical module. In the end, the simulated results will be compared with experimental results and then be improved. In order to prove the correctness of the simulation process used in this thesis, a phononic crystal structure is additionally simulated to compare with the results from a paper. By changing some parameters and settings, the results of improved models are showed and discussed.

1.2 Structure of the work

The first two chapters give an overview about state of the art. At first, chapter 2 introduces the history and development of metamaterials. Different variants of metamaterials are classified and explained briefly. Chapter 3 then goes into the concepts of acoustic metamaterials. Physical properties and academic models as well as typical structures of them are explained. In chapter 4, calculation methods for the dispersion relation and Finite-element method specially for the simulation are compared. Based on principles each method is explained.

Then, chapter 5 describes different prototype designs as well as their work principles. Chapter 6 presents the physical parameters and simulation steps for the selected models. Chapter 7 then analyzes the results of simulation and experiments. The similarities and deviation are

discussed. In chapter 8, simulation process is improved to reduce the deviation by executing convergence study. In the end, chapter 9 contains a discussion about suggestions for the future work.

2 Introduction and categories of metamaterials

In this chapter, the history and development of metamaterials will be introduced. Based on that different kinds of metamaterials will be shortly explained. After that, the next chapter will focus on acoustic metamaterials.

2.1 History and development

Scientists and engineers started to research metamaterials since the 19th century. Metamaterials are known with their periodic patterns which don't exist in nature. In the case of periodic structures, only a single computational sample needs to be studied because the sample precisely describes the periodic structure, as the object that repeats in space is always of the same size (Maldovan & Thomas, 2009, p.26). Therefore, the cost of simulation for metamaterials is greatly reduced.

In recent years, metamaterials can be applied in different fields such as microwave, optoelectronics and material science etc.. In general, metamaterials can be divided into following categories: elastic metamaterials, structural metamaterials, nonlinear metamaterials, electromagnetic metamaterials and acoustic metamaterials. In the following sections, each category will be briefly introduced.

2.2 Elastic metamaterials

Elastic metamaterials are also called mechanical metamaterials, whose mechanical properties are defined by their structure that can not be found in nature. By exploring locally resonant effect of the building units, they are able to possess negative values of effective mass, effective bulk or shear modulus (X. Zhou, Liu, & Hu, 2012, p.1). With these properties elastic metamaterials can be used for cloaking and superlensing effects. Typical examples of them are like:

- Acoustic/phononic metamaterials
- Materials with negative Poisson's ratio (auxetics)
- Metamaterials with negative longitudinal and volume compressibility transitions
- Pentamode metamaterials or meta-fluids
- Cosserat and Micropolar Metamaterials

2.3 Structural metamaterials

Structural metamaterial plays an important role in light-weight design. With the same density, they have much better properties than conventional materials, that means they are much harder and can withstand more loads. This property comes from their remarkable compact structure shaped like a truss.

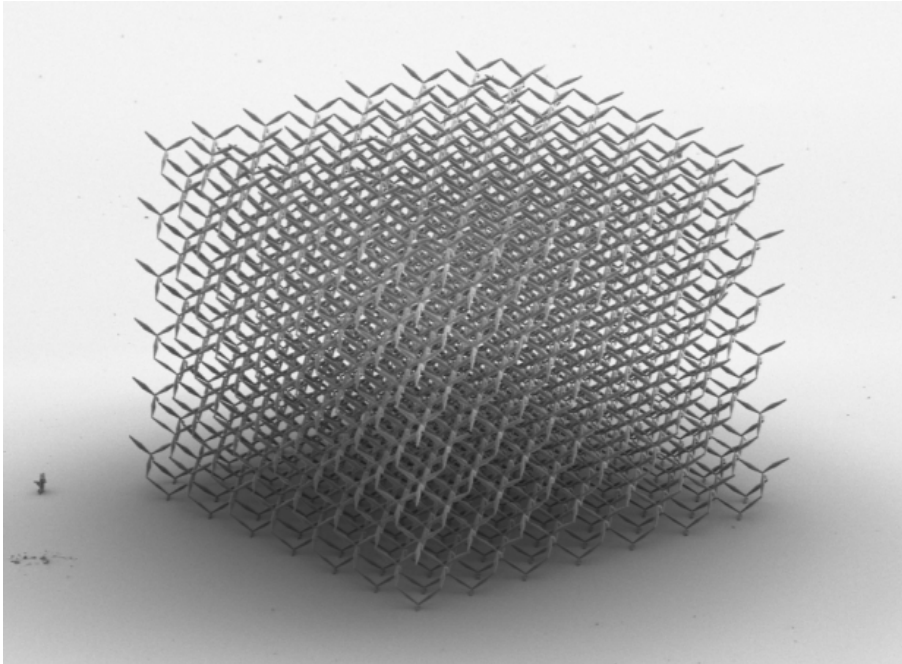


Figure 2.1: Example of elastic metamaterial: pentamode metamaterial (<https://en.wikipedia.org/wiki/File:Pentamode.png>)

2.4 Nonlinear metamaterials

Nonlinear metamaterials are important for the study in nonlinear optics field. The typical properties of nonlinear metamaterials are electric permittivity and magnetic permeability in electromagnetic fields, which can generate the refractive index. Because of this property nonlinear metamaterials can generate more remarkable nonlinear behavior in response to electromagnetic radiation than conventional materials.

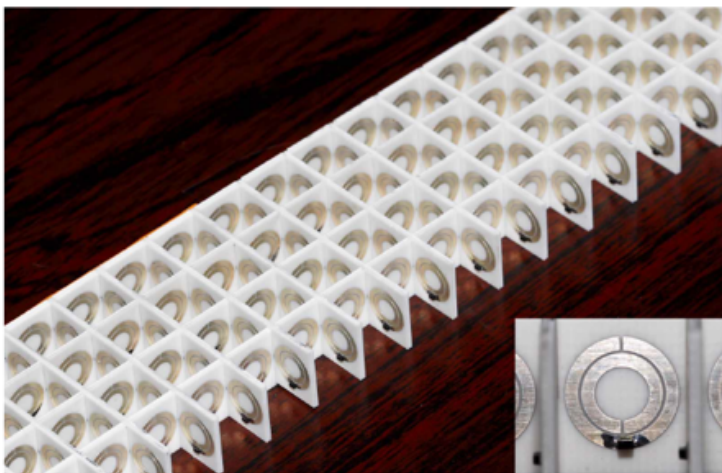


Figure 2.2: Photograph of the nonlinear tunable magnetic created by a square lattice of nonlinear Split Ring Resonator (SRR.) resonator (Shadrivov, Kozyrev, van der Weide, & Kivshar, 2008, p.6)

2.5 Electromagnetic metamaterials

Electromagnetic metamaterials are arrays of structured subwavelength elements which may be described as effective materials via the electric permittivity and magnetic permeability respectively (Watts, Liu, & Padilla, 2012, p.3). They are able to generate pronounced electromagnetic responses which are not possible in natural materials. This negative response comes from the negative refraction index generated by their periodic structure in subwavelength scale rather than their chemical composition. In general, electromagnetic metamaterials can be divided into several classes:

- Negative index
- Single negative
- Hyperbolic
- Bandgap
- Double positive medium
- Bi-isotropic and bianisotropic
- Chiral
- Frequency Selective Surface (FSS.) based

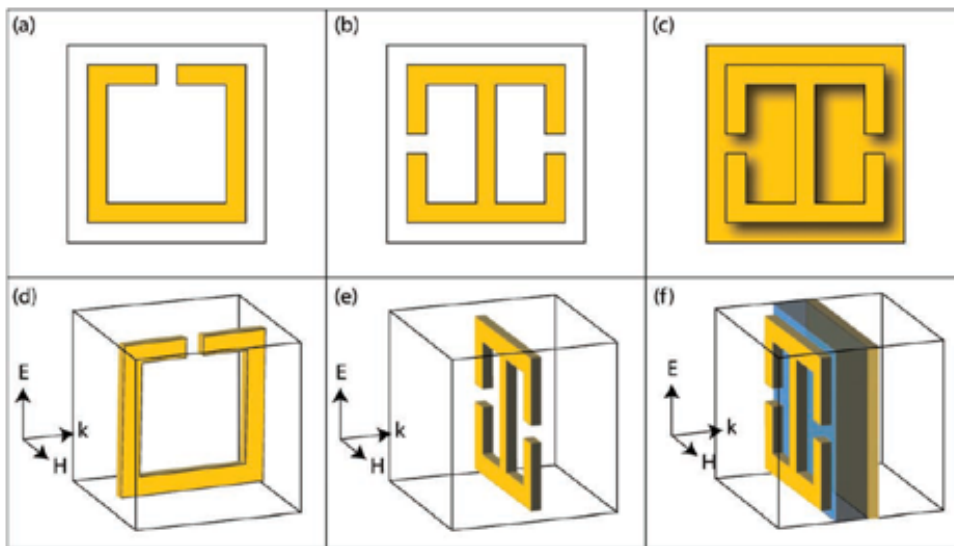


Figure 2.3: Schematic of the two canonical metamaterial unit cells used to create magnetic and electric response

(Watts et al., 2012, p.3)

2.6 Acoustic metamaterials

Same as electromagnetic metamaterials, acoustic metamaterials also have negative refraction index. The difference is that acoustic metamaterials affect sound waves through mechanical properties such like bulk modulus and mass density. The periodic structures with these material properties form a resonant system, which can block the transmission of sound waves within a certain frequency range. The structural features of acoustic metamaterials can be

significantly smaller than the wavelength of the waves they are affecting (Deymier, 2013, p.8).

As acoustics is a new application field of metamaterials, it is difficult to execute simulation process of acoustic metamaterials due to the lack of literatures. Based on the properties of acoustic metamaterials and some physical principles, there are several calculation methods to analyze the behavior of acoustic metamaterials. However, how to model them and simulate their behavior in specific software, is still a challenge. The further details about acoustic metamaterials will be described in the next section.

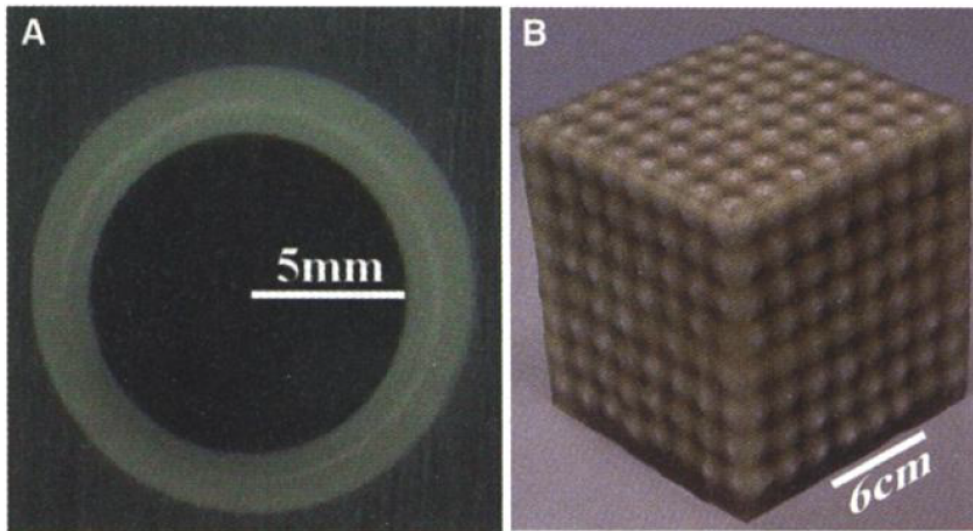


Figure 2.4: Locally Resonant Sonic Crystals
(Liu et al., 2000, p.2)

3 Concept of acoustic metamaterials

In 1967, the Russian physicist Victor Veselago firstly proposed the concept of metamaterials. After that, the study and researches of metamaterials developed quickly in different fields, especially in acoustics. The main goal of acoustic metamaterial applications is to enhance the response of materials to sound waves.

The history of acoustic metamaterials began two decades ago. The study of them mainly involves the control and reduction of sound noise, creation of useful sounds for medical diagnosis and measurement of other physical properties. The focus of this thesis is the first option.

The principle of acoustic metamaterials can be explained by the principle of general metamaterials. Similar with other metamaterial categories, the interest in acoustic metamaterials is mainly focused on their negative refraction index. This parameter is generated by changing the bulk modulus and density. Due to the floating of these micro structural and physical characteristics, the impact on macro sound waves is achieved.

The study of acoustic metamaterials began with the manufacturing of them. Early in 2000 acoustic metamaterials are firstly fabricated as sonic crystals based on the idea of localized resonant structures (Liu et al., 2000, p.1). Later in 2004 the existence of acoustic metamaterials, in which both the effective density and bulk modulus are simultaneously negative, is confirmed (Li & Chan, 2004, p.1).

With the development of 3D printing technology, the manufacturing of acoustic metamaterials is becoming mature. In recent years, scientists have begun to execute experiments on them to analyze their properties and industrial application possibilities. Early in 2016, the potential of metamaterial as vibration insulation along known transmission paths is investigated, which verified that different stop bands can be combined (Melo, Claeys, Deckers, Pluymers, & Desmet, 2016, p.7). Later in 2018, an additional structure based on acoustic metamaterial for the reduction of vibro-acoustic transfer function of a car body panel is designed (Jung, Kim, Chol, & Wang, 2018, p.1). In the same year, a host structure with the resonant elements is demonstrated to isolate vibrations at low frequencies with multiple transmission paths (Sangluliano, Claeys, Deckers, Pluymers, & Desmet, 2018, p.1). Recently in 2019, a laminate acoustic metamaterial design with multi-stopband for structural-acoustic coupled system was proposed (Xiao, He, Li, & Cheng, 2019, p.1).

Because of the long experiment period and many uncertainties during experiment process, researchers began to attempt the simulation of acoustic metamaterials in recent years. Early in 2013, three novel metal Periodic Cellular Material Structures (PCMS.) types have been studied by using finite element simulation, by getting natural frequencies and mode shapes their acoustic response and vibration behavior are evaluated (Al-Zubi et al., 2013, p.15). Later in 2016, a metastructure which combines local resonances with structural modes of a periodic architected lattice is demonstrated, by using finite-element simulations the application in controlling structural vibrations and noise is confirmed (Matlack, Bauhofer, Kröder, Palermo, & Daraio, 2016, p.1). In 2019, a design of ring-shaped acoustic black holes in plates for broadband vibration isolation is simulated separately by using Gaussian expansion method and finite element method (Deng, Guasch, & Zheng, 2019, p.1). In the meantime, on the basis of finite element simulations the frequencies of cylindrical metamaterials for tubular

structures at broadband vibration damping are analyzed (Yeh & Harne, 2019, p.1).

Most simulations of acoustic metamaterials demonstrate their superior performance in reducing vibrations. However, there are still challenges to prove the effectiveness in acoustic insulations. On the one hand, it is not easy to build an exactly same simulation environment as experiments. On the other hand, the idealized simulation conditions lead to the deviation between simulation and experiment results.

In the following sections, firstly the properties and general parameters of acoustic metamaterials will be shortly claimed. After that, the typical 1D and 2D models of acoustic metamaterial mainly for academic study will be illustrated. In the end, typical structures and designs of acoustic metamaterials will be introduced.

3.1 Acoustic parameters

The propagation of sound waves through a medium is described by the acoustic wave equation. The acoustic wave equation in a homogeneous medium absent of a source is given by (Ma & Sheng, 2016, p.1):

$$\nabla^2 P - \frac{\rho}{\kappa} \frac{\partial^2 P}{\partial t^2} = 0 \quad (3.1)$$

where P is pressure, and the two parameters are the mass density ρ and the bulk modulus κ . For acoustic metamaterials, bulk modulus and mass density are important parameters to define their refraction index. In the following, both of them will be briefly explained.

3.1.1 Bulk modulus

Bulk modulus has an essential meaning to fluids. It reflects the compression resistance of an object. In physics, the bulk modulus can be defined as:

$$\kappa = \rho \frac{dP}{d\rho} \quad (3.2)$$

where $\frac{dP}{d\rho}$ is the derivation of pressure with respect to density.

3.1.2 Mass density

The mass density can also be called just density. It is defined as mass per volume and changes with the temperature and pressure value. In a fluid, the bulk modulus κ and the density ρ define the speed of sound c :

$$c = \sqrt{\frac{\kappa}{\rho}} \quad (3.3)$$

Negative refraction of acoustic waves may be achieved with double negative acoustic meta-

materials in which both the effective mass density and bulk modulus are negative (Li & Chan, 2004, p.1). The dipolar resonance of heavy inclusions coated with a soft material embedded in a stiff matrix can result in a displacement of the center of mass of the metamaterial that is out of phase with the acoustic wave, leading to an effective negative dynamical mass density (Deymier, 2013, p.5).

3.2 Typical academic models in 1D and 2D

At the beginning, the researches of acoustic metamaterials are mainly based on academic models, which actually don't exist for real and work on a theoretical basis. For these models, scientists have found several analytical solutions to analyze their physical properties. In general, academic models of acoustic metamaterial can be divided into 1D and 2D. For each category there is a typical structure in the literature. In the following subsections, each model will be briefly introduced.

3.2.1 One-dimensional model

The typical one-dimensional model of acoustic metamaterial is the mass-spring-unit, which can be regarded as a resonant unit cell of a metamaterial structure. The principle of this model is based on the interaction between mass unit and basic plate by combining them with a spring:

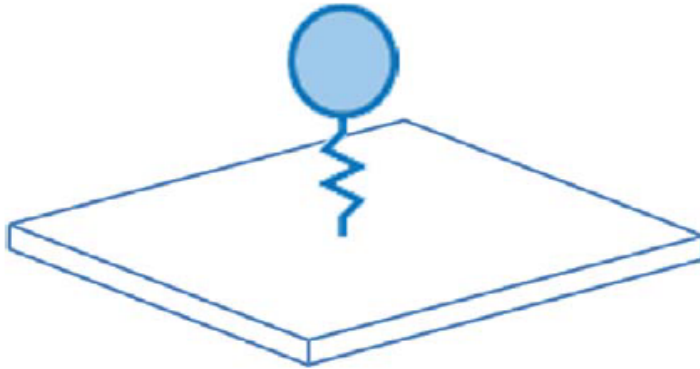


Figure 3.1: Principle of mass-spring-unit in 3D-version (Nateghi et al., 2017, p.6)

In order to clarify the effect of this model mathematically, a simple one-dimensional coupled oscillator under an external harmonic excitation force $F(\omega)$ from the literature (Ma & Sheng, 2016, p.2) is considered. By regarding the motion equation, the following equations can be derived for the model (Ma & Sheng, 2016, p.2):

$$F = \left(M_1 + \frac{K}{\omega_0^2 - \omega^2} \right) \ddot{x}_1 \quad (3.4)$$

$$\omega_0 = \sqrt{K/M_2} \quad (3.5)$$

where M_1 and M_2 are masses of structure. ω_0 is the local resonance frequency of M_2 . x_1 is displacement of M_1 , where the double overdot denotes a second-order time derivative. By applying Newton's second law, the system's inertial response $\bar{M}(\omega)$ and the dynamic mass density $\bar{\rho}$ can be then defined as (Ma & Sheng, 2016, p.2):

$$\bar{M}(\omega) = M_1 + \frac{K}{\omega_0^2 - \omega^2} \quad (3.6)$$

$$\bar{\rho} = f/\ddot{x} \quad (3.7)$$

where f is the force density, x is the sample (unit cell) displacement.

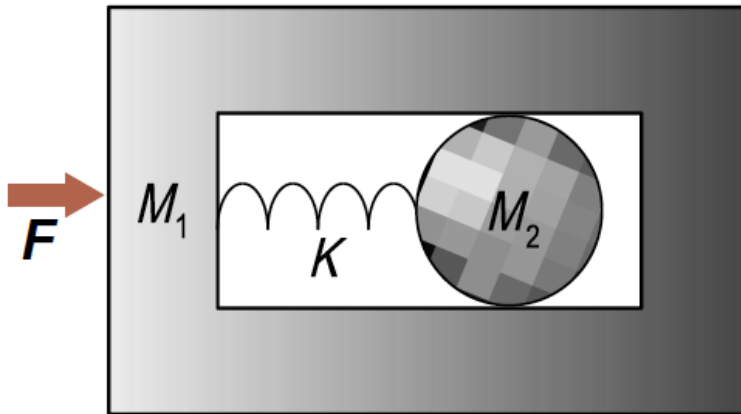


Figure 3.2: A spring-coupled mass-in-mass oscillator (Ma & Sheng, 2016, p.3)

3.2.2 Two-dimensional model

There are different types of two-dimensional phononic crystals made of different materials. The most common type is that made of solid and fluid materials. As exsamples, two comprehensive 2D models from the book "Periodic Materials and Interference Lithography" (Maldovan & Thomas, 2009) will be introduced. Because of different principles of mechanical waves in the solid and fluid material, it is difficult to study the band gap of these models, so that some approximations must be made in order to apply simple numerical techniques (Maldovan & Thomas, 2009, p.198). It is assumed that the two-dimensional phononic crystals extend infinitely in the xy plane.

The first type is vacuum cylinders in a solid background arranged on the square and triangular lattices. In this model mechanical waves propagate only through the solid background material. Therefore, in order to get the band gap of this model, the elastic wave equation for

nonhomogeneous solid materials is considered (Maldovan & Thomas, 2009, p.195):

$$\nabla \cdot (\rho c_T^2 \nabla u_i + \rho c_T^2 \frac{\partial u}{\partial x_i}) + \frac{\partial}{\partial x_i} ((\rho c_L^2 - 2\rho c_T^2) \nabla \cdot u) = -\rho (\omega(k))^2 u_i \quad (3.8)$$

where $\rho = \rho(r)$ is density, $c_T = c_T(r)$ is transverse velocity, $c_L = c_L(r)$ is longitudinal velocity. $u = u_k(r)$ is the spatial part of the displacement vector of the elastic Bloch wave.

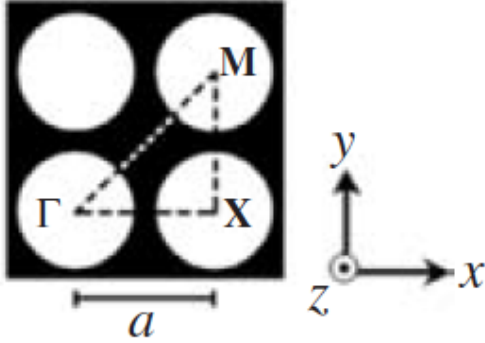


Figure 3.3: Two-dimensional solid-vacuum phononic crystals (Maldovan & Thomas, 2009, p.199)

The second type is solid cylinders in air arranged in the square and triangular lattices. Different from the last model, in this model mechanical waves propagate as acoustic waves mainly through the air region. Therefore, the propagation of these acoustic Bloch waves is governed by the acoustic wave equation. Combining with the equation describing the Bloch waves, band gap can be analyzed. Bloch waves can be described with following equation (Maldovan & Thomas, 2009, p.203):

$$p_k(r,t) = \text{Re}[f_k(r)e^{i(k \cdot r - \omega(k)t)}] \quad (3.9)$$

where $f_k(r)$ is a periodic scalar function, k is the wave vector.

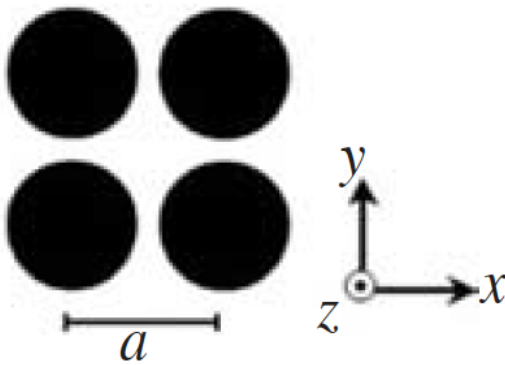


Figure 3.4: Two-dimensional air-solid phononic crystals (Maldovan & Thomas, 2009, p.203)

3.3 Typical structures and designs

Acoustic metamaterials have remarkable performance in vibration and noise insulation applications. In general, acoustic metamaterials can be divided into those periodic structures with and without resonators, which are small masses attached on the host structure. Depending on the type of structure, the field of application can vary. In the following subsections, different typical structures of acoustic metamaterials based on the literature research will be introduced.

3.3.1 Rod-type acoustic metamaterials

As an impressive geometric property, the rod-type acoustic metamaterials generally have a structure arranged in axial periodicity. Due to this property the rod-type acoustic metamaterials have excellent vibration reduction performance in the axial direction. In 2006, the band gaps in Euler-Bernoulli beams with locally resonant structures with two degrees of freedom are analyzed (Yu, Liu, Zhao, Wang, & Qiu, 2006, p.1). Recently in 2018, a substructure is fabricated and clamped on a panel in order to evaluate the vibration reduction effect (Oltmann, Hartwich, & Krause, 2018, p.1). The rod-type acoustic metamaterials are expected to be widely used in the vibrational attenuation of transmission components. According to Wu et al., the rod-type acoustic metamaterials can be structurally divided into two types (Wu, Ma, Zhang, & L., 2016, p.6):

- Two or more materials are arranged alternatively in the axial direction to form a periodic structure
- Local resonance units distributed on the periodic structure

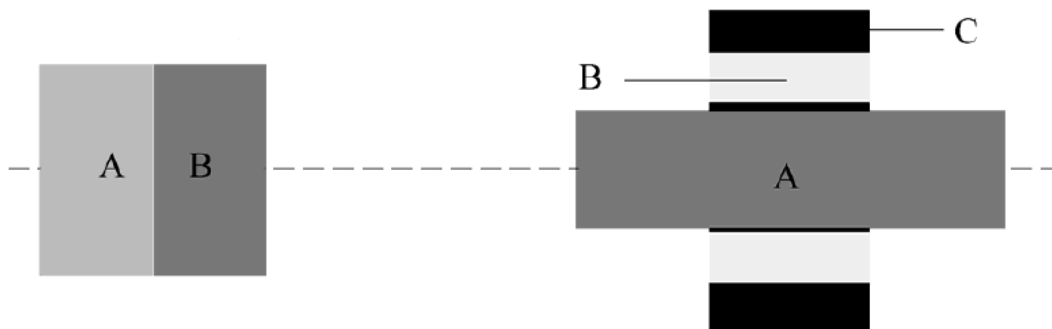


Figure 3.5: Two types of rod-type acoustic metamaterials according to Wu et al. (Wu et al., 2016, p.6)

The first type of acoustic metamaterials can be considered as a one-dimensional spring-mass system, and the second type can be considered as a dynamic vibration absorber. From the perspective of engineering application, the first kind of metamaterial structure is difficult to be applied. In contrast, the application of the second type of metamaterial structure is relatively flexible (Wu et al., 2016, p.6).



Figure 3.6: Principles of two rod-type acoustic metamaterials (Wu et al., 2016, p.6)

3.3.2 Membrane-type acoustic metamaterials

The membrane-type acoustic metamaterials are generally composed of masses arranged on the membrane cell unit. In order to get a better sound insulation effect, the cell size and shape can be changed. The resonance frequency of the whole system is greatly affected by the weight, quantity and position of the mass unit.

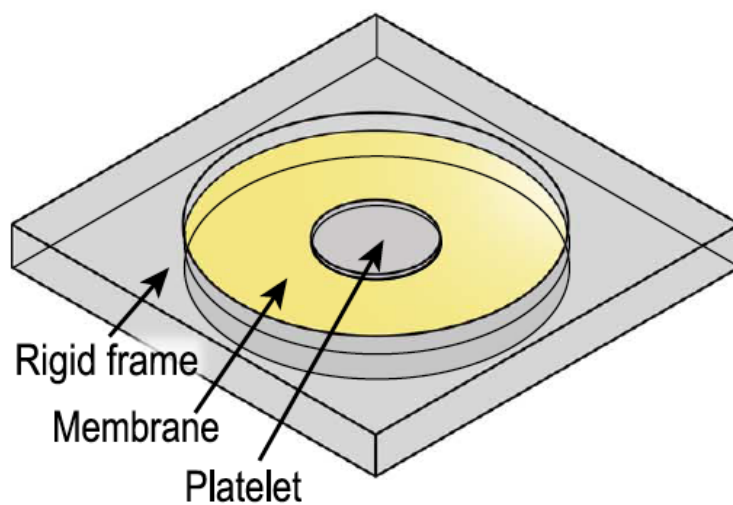


Figure 3.7: Single membrane with negative effective mass density (Ma & Sheng, 2016, p.4)

The study of membrane-type acoustic metamaterials has a long history. In 2008 Yang et al. have presented the experimental realization and theoretical understanding of a membrane-type metamaterial with negative dynamic mass characteristics, operative in the 100-1000 Hz frequency regime (Yang, Mei, Yang, Chan, & Sheng, 2008, p.1). In 2010 Naify et al. have examined the transmission loss of membrane-type metamaterials to understand the effect of material parameters on the resonant and peak transmission frequencies (Naify, Chang, McKnight, & Nutt, 2010, p.2). In 2012 Mei et al. have presented a thin-film acoustic metamaterial that aims to totally absorb low-frequency airborne sound at selective resonance frequencies ranging from 100 – 1000 Hz (Mei et al., 2012, p.2). In 2014 Chen et al. have

developed an analytical vibroacoustic membrane model to study sound transmission behavior of the membrane acoustic metamaterial under a normal incidence (Y. Chen, Huang, Zhou, Hu, & Sun, 2014, p.1). Recently in 2020, a finite element simulation for the acoustic-structural interaction of the membrane-type acoustic metamaterial with eccentric masses is developed, the results are validated experimentally (Lu, Yu, Lau, Khoo, & Cui, 2020, p.11).

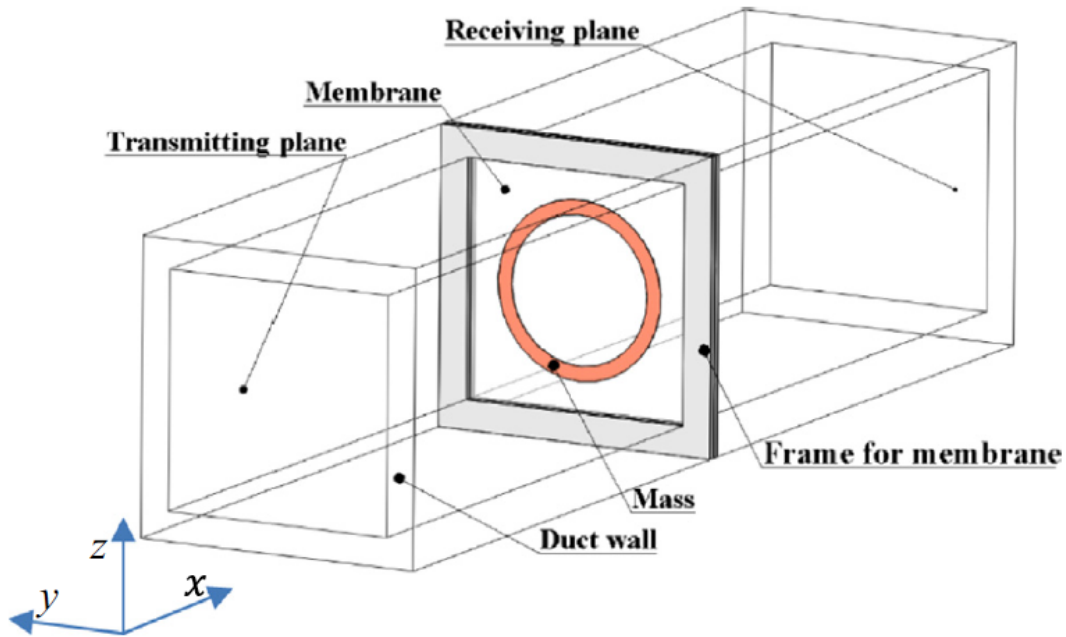


Figure 3.8: Schematics of the simulation configuration for the membrane-type acoustic metamaterial

(Lu et al., 2020, p.2)

3.3.3 Plate-type acoustic metamaterials

In 2012 Stenger et al. have designed, fabricated and experimentally characterized a broadband elastic free-space cloak in thin plates at acoustic frequencies (Stenger, Wilhelm, & Wegner, 2012, p.4). In 2015 Nouh et al. have presented a theoretical and experimental investigation of the wave propagation and vibration attenuation characteristics of metamaterial plates manufactured from assemblies of periodic cells with built-in local resonances (Nouh, Aldraihem, & Baz, 2015, p.20). Recently in 2019 Wang et al. have studied the sound insulation performance and mechanism of a simple large-scale plate-type acoustic metamaterial panel by using finite-element-analysis (Wang, Chen, Zhou, Chen, & Ma, 2019, p.14).

The plate-type acoustic metamaterials are generally composed of periodic holes or resonators with different shapes arranged on a plate. They are typical two-dimensional acoustic metamaterials and have remarkable performance. According to Huang et al., the mechanism of membrane- and plate-type acoustic metamaterials can be considered as (Huang, Shen, & Jing, 2016, p.3):

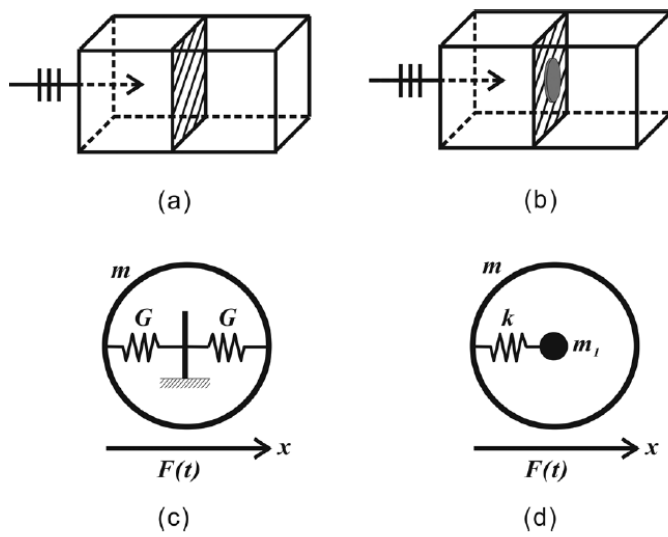


Figure 3.9: Membrane or plate clamped in a waveguide: a) Without mass attached. b) With mass attached. c) The corresponding mass-spring diagram for a). d) The corresponding mass-spring diagram for b).

(Huang et al., 2016, p.3)

3.3.4 Other types

In addition to the three mentioned common acoustic metamaterial structures, there are some other types of structures. In 2013, Chen et al. presented an acoustic meta-atom model of hollow steel tube (H. Chen, Zeng, Ding, Luo, & Zhao, 2013, p.1). In 2018, Guild et al. have presented and discussed a thin functionally-graded acoustic metamaterial sound absorber (Guild, Rohde, Tothko, & Sieck, 2018, p.1). Recently in 2020 Rice et al. have analyzed a single open kelvin cell and then determined a lossy Helmholtz model of the same structure (Rice, Kennedy, Göransson, Dowling, & Trimble, 2020, p.1). They have also designed and manufactured a model based on a benchmark periodic metamaterial structure (Dowling, Flanagan, Rice, Trimble, & Kennedy, n.d., p.1).

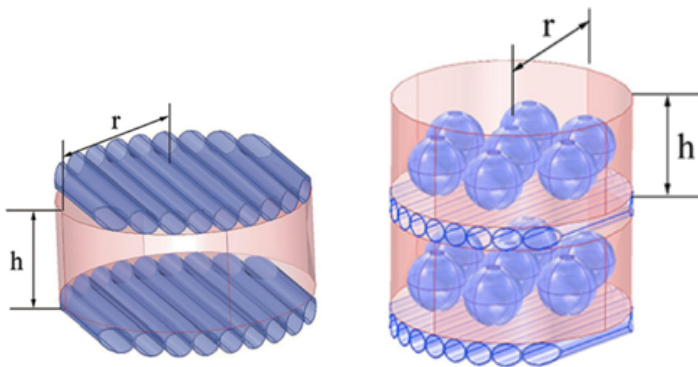


Figure 3.10: Schematic of acoustic meta-atom model of hollow steel tube: 2D and 3D model (H. Chen et al., 2013, p.5)

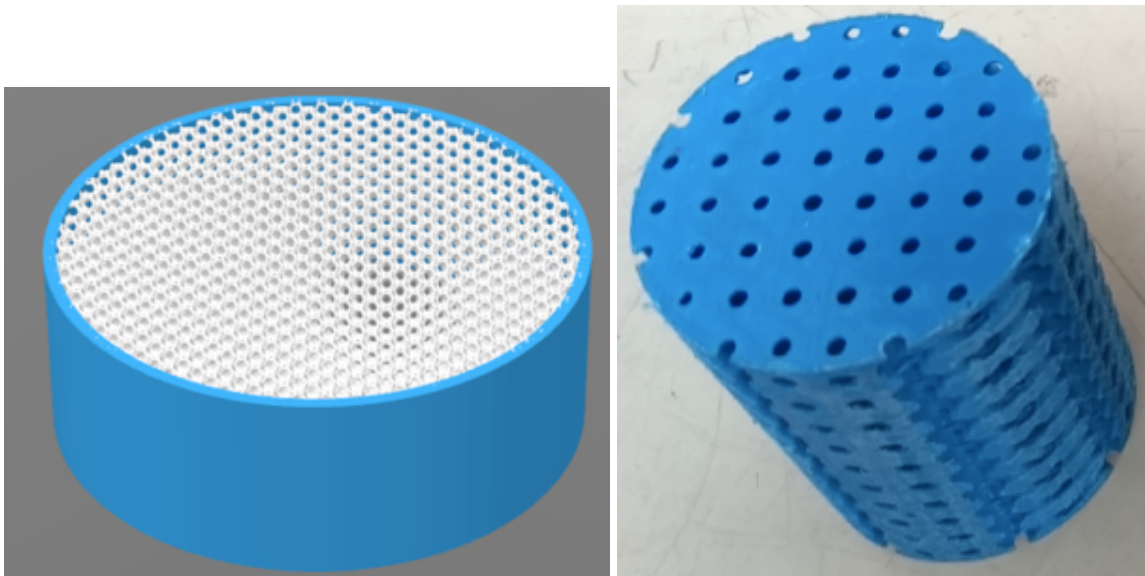


Figure 3.11: CAD Sample based on a Kelvin Cell; 3D-printed Sample based on a benchmark structure
(Rice et al., 2020, p.9); (Dowling et al., n.d., p.12)

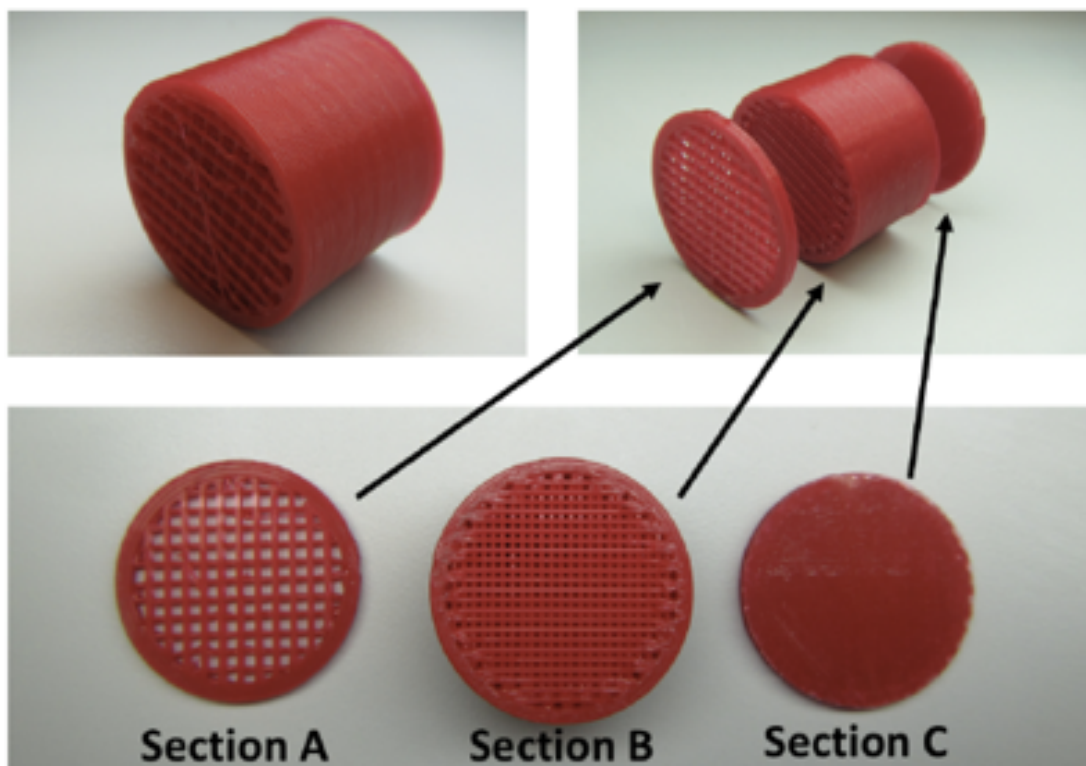


Figure 3.12: Compact 3D printed functionally-graded acoustic metamaterial sound absorber, consisting of 3 sections
(Guild et al., 2018, p.2)

4 Calculation methods and Finite-element-method in software

4.1 Calculation methods

In order to calculate the properties of acoustic metamaterials and to compare with the experimental results, scientists began to use mathematical methods to solve the metamaterial problem. Generally, there are two parameters which can be analyzed both in experiments and in numerical methods: the band gap and the noise prediction. For each parameter, there are different methods for the calculation. The most applications of the acoustic metamaterial are based on the analysis of the band structure. The band gap is characterized by the position (center frequency) and the width of the band gap (Gupta, 2014, p.6).

For calculating the band structure, there are four typical methods: Plane wave expansion method (PWEM.), Multiple scattering method (MSM.), Finite difference time domain (FDTD.) method and Korringa Kohn Rostoker (KKR.) method. For the noise prediction, there are approaches such like: Finite Element Method (FEM.), Boundary Element Method (BEM.) and Statistical Energy Analysis (SEA.). Because the main focus in this thesis is to simulate the dispersion curve, in the following four typical calculation methods for the band gap will be explained.

4.1.1 Plane wave expansion method

PWEM. comes from electromagnetics by solving eigenvalue problem. It is based on the Maxwell's equations. PWEM. was primarily described by Dr. Danner (Danner, 2002) and applied for photonic crystals. Later on, it is widely used for sonic crystals and in other fields.

Plane waves are solutions to the homogeneous Helmholtz equation. These solutions are based on a periodic environment. PWEM. was used in some of the earliest studies of photonic crystals and is simple enough to be easily implemented (Danner, 2002). Maxwell's equation describes how electric and magnetic fields are generated. According to Faraday's law of induction the Maxwell-Faraday equation is:

$$\nabla \times E = -\frac{\partial B}{\partial t} \quad (4.1)$$

where E and B are field vectors, and t is time. If it is assumed that the fields are time-harmonic, then (Danner, 2002):

$$\frac{1}{\varepsilon} \nabla \times \nabla \times E = \frac{\omega^2}{c^2} E \quad (4.2)$$

where ε is the relative permittivity. The goal is to find the energies and electromagnetic field configurations that are allowed to exist in a periodic structure (Danner, 2002). That means to solve for ω and the fields. The fields themselves and the dielectric function can be expanded in Fourier series along the directions in which they are periodic (Danner, 2002).

In real applications, the model will be simplified and then the calculation will be reduced under some assumptions. By expanding through Fourier series the eigenvalue problem will be solved. When the eigenvalues are calculated employing standard numerical methods, it is straightforward to use the eigenvalues to find the allowed propagation frequencies, and the eigenvectors to calculate the field distributions (Danner, 2002).

PWEM. is an efficient method to calculate the periodic structures by expanding in Fourier series. From 1D to 2D there are plenty of applications based on PWEM. since 19th century. Early in 2004 Shi et al. have combined the PWEM. with perfectly matched layers for calculating band structure of photonic crystal slabs (Shi, Chen, & Prather, 2004, p.1). In 2011 Bin et al. have combined Cartesian coordinates and polar coordinates wave number eigenvalue equations to calculate the band structure of the two-dimensional metal photonic crystals (Bin, Wen-Jun, Wei, An-Jin, & Wan-Hua, 2011, p.1). In 2013 the students of TU Graz applied the PWE on a specific photonic crystal: a two-dimensional, hexagonal arrangement of air holes in a dielectric material (*Application of the plane wave expansion method to a two-dimensional, hexagonal photonic crystal*, 2013, p.2).

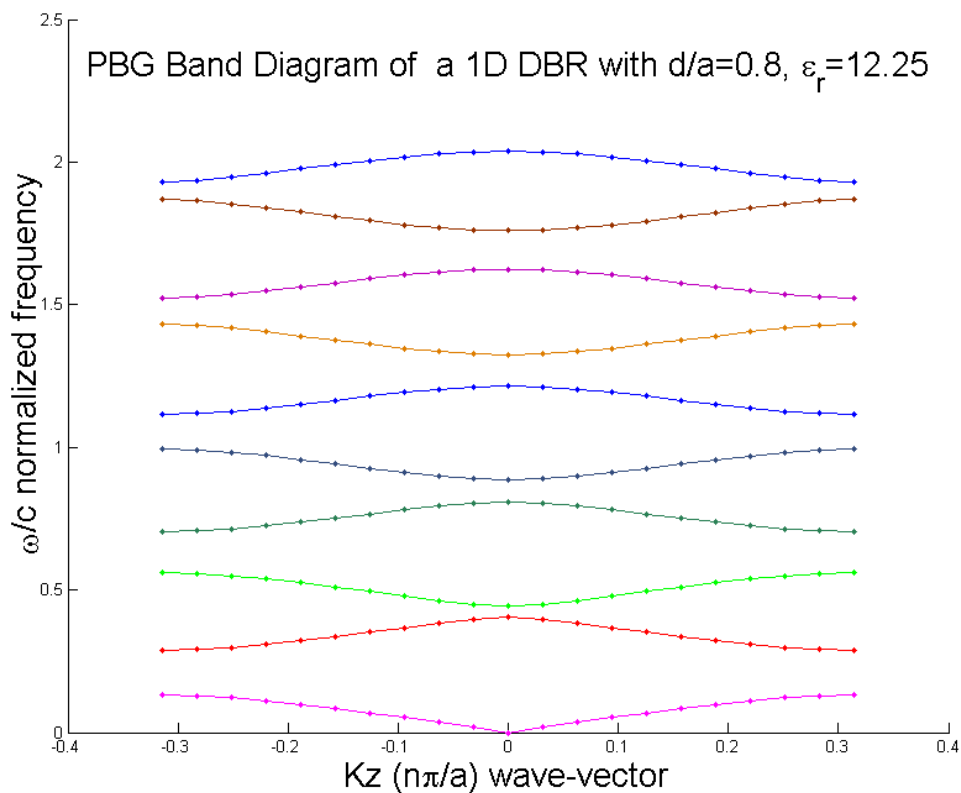


Figure 4.1: Band structure of a 1D Photonic Crystal based on PWEM.
<https://en.wikipedia.org/wiki/Plane-wave-expansion-method/media>

4.1.2 Multiple scattering method

MSM. is used to explain the propagation of a wave through scatterers. Early in 18th century scientists have already written articles about its theories. After that, researchers began to put

it in real applications. The first important theory of MSM. was made by the German physicist Paul Peter Ewald. Later on, it is widely used for electronic structure calculations.

The principle of MSM. is to derive the one-electron Green's functions. In order to calculate the band structure of photonic crystals, same like PWEM., the first thing is to solve the Maxwell equations for the electric field (Zhang, Chan, & Sheng, 2001, p.2):

$$\nabla \times \nabla \times E(r, \omega) - \kappa^2 \varepsilon(r, \omega) E(r, \omega) = 0 \quad (4.3)$$

where κ and ε is the position dependent dielectric function. This equation can be put into an integral equation form (the dyadic Green's function), instead of integrating over the outer surface of the whole crystals, the integration can be carried out as the sum of surface integrations over individual scatterers (Zhang et al., 2001, p.2):

$$E_0(r, \omega) = \Sigma \oint dS' \cdot (d_0(r - r') \times (\nabla' \times E(r', \omega)) + (\nabla' \times d_0(r - r')) \times E(r', \omega)) \quad (4.4)$$

Under some assumptions this equation can be further reduced. Firstly it can be simplified as a linear equation. After considering the Wronskian-like surface integral and applying a Fourier transformation, the physical solution can be picked up by counting the number of positive pseudo-eigenvalues for each frequency (Zhang et al., 2001, p.3). In 2006 Cai et al. have analyzed the band structure of elastic wave propagating in a binary phononic crystal by employing MSM. (Cai, Xiaoyun, & Xisen, 2006).

4.1.3 Finite-difference-time-domain method

The FDTD. is one of the most important methods to solve the electromagnetic problems. It was first described by Chinese American mathematician K. Yee and then applied in various fields. The most fascinating character of FDTD. method is that it can calculate a wide frequency range.

The FDTD. method is a differential numerical modelling method, which is based on grids. With this method 1D, 2D and 3D problems can be solved. The time-dependent Maxwell's curl equations are discretized for the rectangular grids, FDTD. updating electric and magnetic field expressions can be then derived using time-dependent Maxwell's curl equations (Singh & Jain, 2012, p.6). In photonic band structure material where the dielectric constant is periodically modulated, the electric and magnetic fields of the electromagnetic waves can be described as (Dastjerdi & Ghanaatshoar, 2013, p.3):

$$E_{n,k}(r) = u_{n,k}(r) \exp(ik \cdot r), u_{n,k}(r + R) = u_{n,k}(r) \quad (4.5)$$

$$H_{n,k}(r) = v_{n,k}(r) \exp(ik \cdot r), v_{n,k}(r + R) = v_{n,k}(r) \quad (4.6)$$

where $E(r)$ and $H(r)$ are electric and magnetic fields, n is band index, k is wave vector, R is the lattice constant, $u(r)$ and $v(r)$ are periodic functions. Based on this equation, one can find eigenvalues of the periodic structure for a given periodic boundary condition (Dastjerdi &

Ghanaatshoar, 2013, p.3).

Similar works have been done after FDTD method was proposed. In 2000 Qiu and He have studied a photonic crystal with a dielectric layer coated on a metallic cylinder as an inclusion (Qiu & He, 2000). In 2004 Cao et al. have calculated the band structure of two-dimensional phononic crystals based on FDTF method (Cao, Hou, & Liu, 2004). In 2007 Zhou et al. have computed the photonic band-structure of three dimensional crystals based on FDTD scheme (M. Zhou et al., 2007).

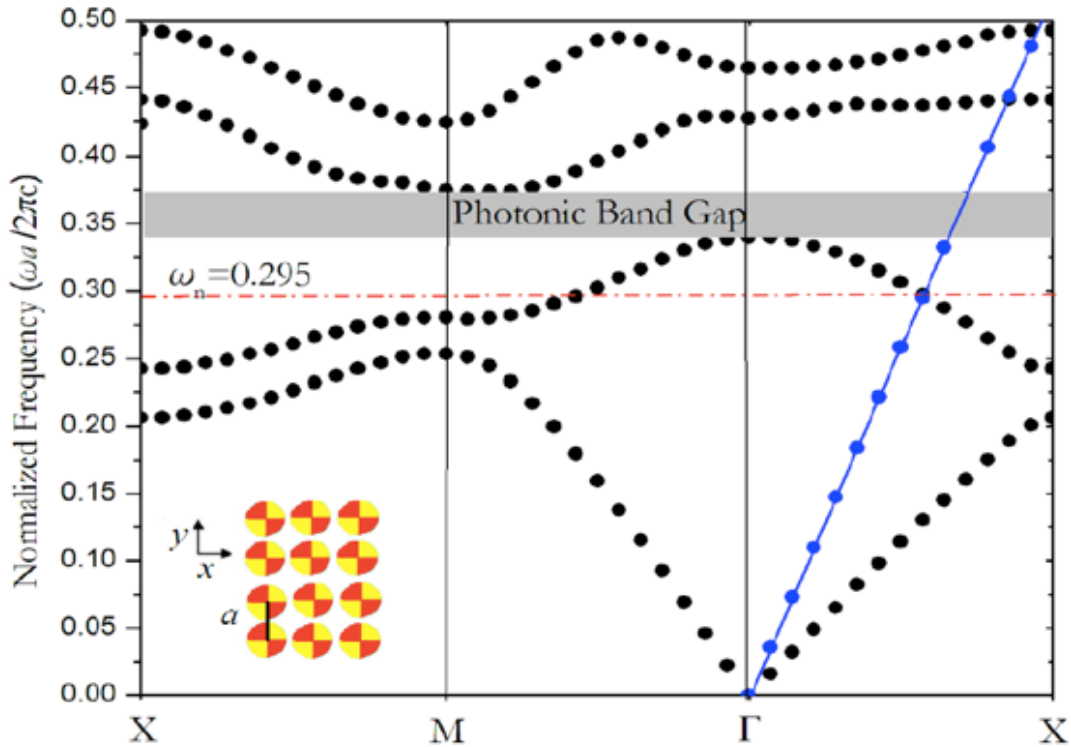


Figure 4.2: Band diagram based on FDTD.

(Dastjerdi & Ghanaatshoar, 2013, p.3)

4.1.4 The Korringa-Kohn-Rostoker Method

The KKR. method was proposed to analyze the electronic band structure of solid crystals which are arranged in periodic forms. The real applications of KKR. method are not as much as other methods. The principle of KKR. method is to solve the Green's function by using multiple scattering theory. Consider the Green function of a periodic array of spherically symmetric, non-overlapping potentials, the Green function is defined as (Mavropoulos & Papanikolaou, 2006, p.15):

$$(-\nabla^2 + V^n(r) - E)G(r + R^n, r' + R^{n'}; E) = -\delta_{nn'}, \delta(r - r') \quad (4.7)$$

After considering the homogeneous Schrödinger equation and using a subsequent Fourier

transform, it can be written as (Mavropoulos & Papanikolaou, 2006, p.16):

$$G_{LL'}(k; E) = \sum G_{LL'}^{nn'}(E) e^{-ik \cdot (R^n) - R^{n'}} \quad (4.8)$$

Under some assumptions such as translational symmetry, this equation can be combined with Dyson equation and then be solved (Mavropoulos & Papanikolaou, 2006, p.16).

4.2 Finite-element-method in software

The industry relies dominantly on the usage of computational software rather than analytically obtaining results from mathematical formulations (Ang, Koh, & Lee, 2016, p.17). Because the analytical solutions always require complicated calculation process and need a long time period, more and more scientists try to use simulation software to solve the metamaterial problem. In addition, the most of calculation methods for metamaterials are based on electromagnetic domains and proposed to solve the electronic and magnetic problems. It is difficult to transform them to solve the acoustic problems.

For acoustic metamaterial problems, the most softwares are based on Finite-Element method. The Finite-Element method is the most widely used method for analyzing mathematical models. This analyzing process is also called Finite-Element analysis. In the following subsections, the mathematical principles of Finite-Element method will be explained. And the possible software which can be used to simulate the acoustic metamaterials will be illustrated.

4.2.1 Mathematical principles of Finite-element-method

Finite-Element method is an approximate numerical method developed based on the rapid development of computer technologies, which is used to solve partial differential equation problems with specific boundary conditions in mechanics and mathematics. The core principles of Finite-element method are numerical approximation and discretization. The general steps of Finite-element analysis can be divided into following points:

- Discretization of the entire model structure
- Analysis of the unit mechanics
- Units assembling
- Analysis of the entire model structure
- Applying boundary conditions
- Units assembling
- Reaction of the entire model structure
- Reaction analysis of a single unit within structure

The convergence study of discretization and unit characteristics is an important research field of Finite-element analysis. In general, finite elements and the assembled entire structure can be mainly divided into 1D, 2D and 3D elements:

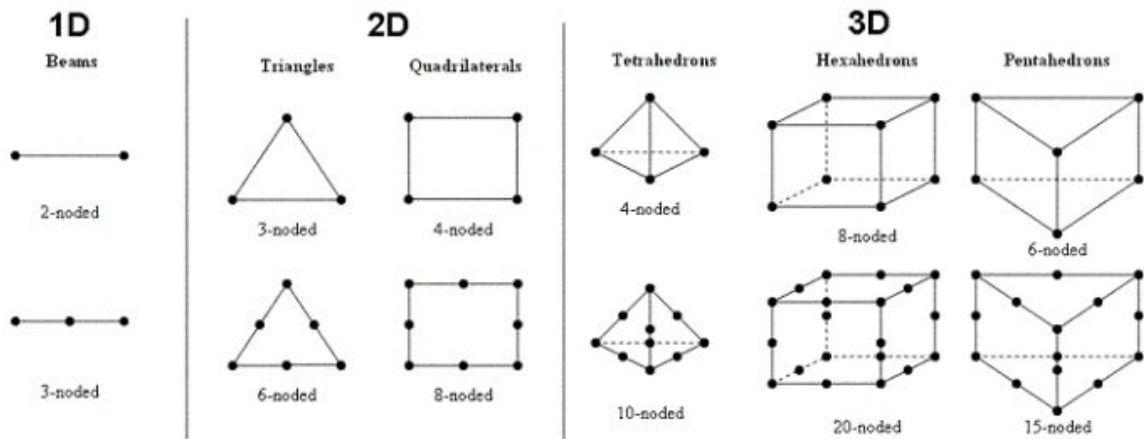


Figure 4.3: Categories of finite elements

<http://www.studioseed.net/research/estructuras/calculo-dinamico/what-does-shape-function-mean-in-finite-element-formulation/>

The main point of Finite-element method is to solve the partial differential equation of each element and then combine to an assembled structure. For different problem cases, various field equations are considered to solve the structure problem. These equations include for example the conservation equations, classical equations of mechanics and equations of electromagnetism. For software applications, Finite-element method mainly focuses on the structural mechanics and fluid mechanics.

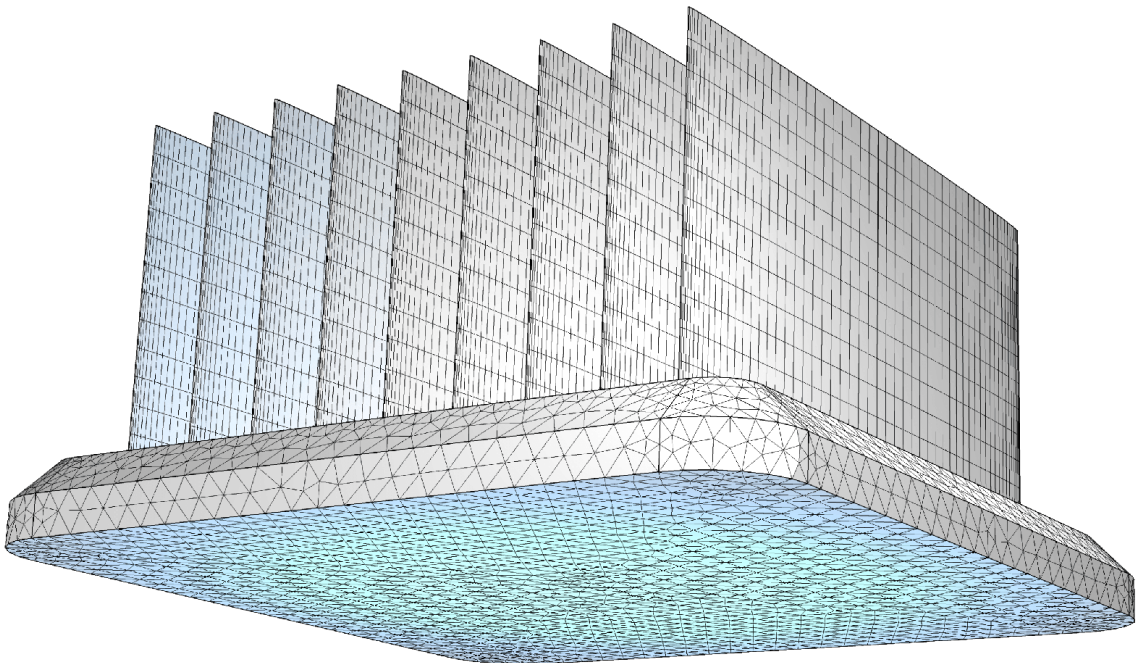


Figure 4.4: Finite-element discretization of radiator model

<https://cn.comsol.com/multiphysics/fea-software>

The concept of Finite-element method began several centuries ago and developed in these

years quickly. With the rapid development of computer simulating technology, the Finite-element method can solve various complicated problems. Abaqus and COMSOL ®Multiphysics are among the latest software, which use Finite-element method to solve problems. Finite-element analysis software can help to reduce the number of prototypes and test times in the design and optimization processes, which leads to a cost reduction.

4.2.2 Possible software based on Finite-element-method

At present, there are two commonly used softwares which are able to simulate the acoustic metamaterials: Abaqus and COMSOL ®Multiphysics. In addition, the team from KU Leuven has used LMS Virtual. Lab Acoustics to establish an acoustic environment and then coupled with a Nastran structural solver and a Sysnoise acoustic solver to perform the needed simulation process (Claeys et al., 2016, p.15).

Today, the realistic applications in simulating acoustic metamaterials by using software Ansys are rare. It is difficult to create an acoustic environment and then couple with boundary conditions. In order to calculate the band structure in Abaqus, it is necessary to establish two single cells with identical meshing and boundary conditions. Recently in 2019, Dong et al. have numerically simulated the dispersion relation of a metamaterial structure in ABAQUS 6.14-1 (Dong et al., 2019, p.7).

The most simulations of acoustic metamaterials are created in commercial software COMSOL ®Multiphysics. It is powerful and relatively simple to create an acoustic domain. Based on that, different parameters and properties can be analyzed.

Early in 2011, Elford et al. have computed the band structure of a C-shaped locally resonant sonic crystal (Elford, Chalmers, Kusmartsev, & Swallowe, 2011). In 2013, Chen et al. have simulated 2D and 3D model composed of hollow steel tube (H. Chen et al., 2013). In 2019, Wang et al. have analyzed the sound transmission loss of a large plate with and without mass unit (Wang et al., 2019). In the same year, Dong et al. have simulated the acoustic subwavelength imaging of a structure optimized by topology method (Dong et al., 2019).

An advantage of using COMSOL ®Multiphysics to compute the acoustic band structure is the capability of modelling more complex scatterer geometries (Elford et al., 2011). Moreover, it can be easily extended with additional functional modules and has an external integration interface such as MATLAB. It is possible to set models through scripts, use MATLAB functions in model Settings, conduct interactive modelling between COMSOL ®Multiphysics and MATLAB, analyze results in MATLAB and create model interfaces.

5 Design and construction of prototype

Based on the literature research a prototype design is proposed. The idea comes from a numerical study on the behavior of partition panels with micro-resonator-type metamaterials (Amado-Mendes et al., 2018).

In order to put the prototype in an impedance tube, the base structure is designed as a circle plate whose diameter matches the size of the impedance tube. On the one side of the plate, there are some square holes in periodic arrangements. The basic design of the resonator is a cube which directly connects to the bottom of holes.

Each resonator of this prototype can be considered as a mass-spring element. This numerical modeling concept allows straightforward control of the resonance frequency of the first bending mode (Claeys et al., 2016, p.2) and can be applied with the Floquet-Bloch boundary conditions, which enables modeling only a unitary cell of the periodic system (Amado-Mendes et al., 2018, p.5).

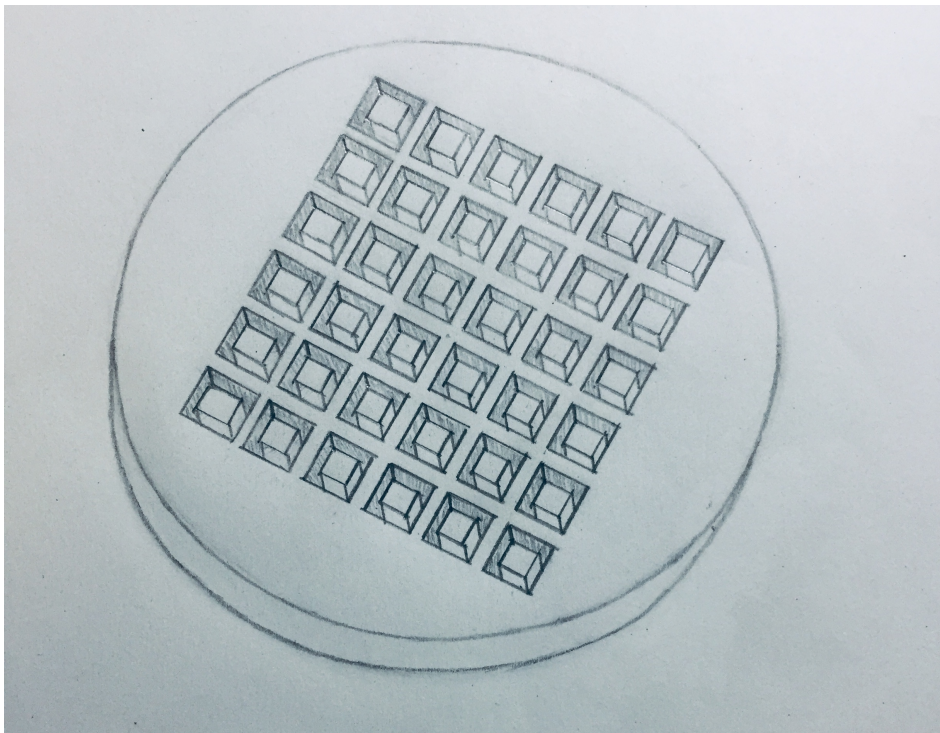


Figure 5.1: Sketch of the first prototype

5.1 Physical principles

Conceptually the designed prototype is based on a mass-spring system. In this system the propagating wave effect is reduced. The resonator can be considered as a small mass unit, which is connected to the base plate. The plate is modelled as infinite in a longitudinal (vertical) direction, with the incorporation of periodic discrete resonators (Amado-Mendes et

al., 2018, p.5). With this concept, the following motion equation can be applied to the model (Amado-Mendes et al., 2018, p.5):

$$\mathbf{K}\mathbf{u} - \omega^2\mathbf{M}\mathbf{u} = \mathbf{F} \quad (5.1)$$

where \mathbf{u} is the displacement vector, \mathbf{K} and \mathbf{M} represent the stiffness and mass matrices, \mathbf{F} is the external forces, ω is the angular frequency. By applying Floquet boundary condition, the following relations between displacements of adjacent nodes are imposed (Amado-Mendes et al., 2018, p.5):

$$u_1 = u_2 \cdot e^{-k_x a} \quad (5.2)$$

where a is the spatial periodicity of the system, k_x is the wavenumber in the periodic direction.

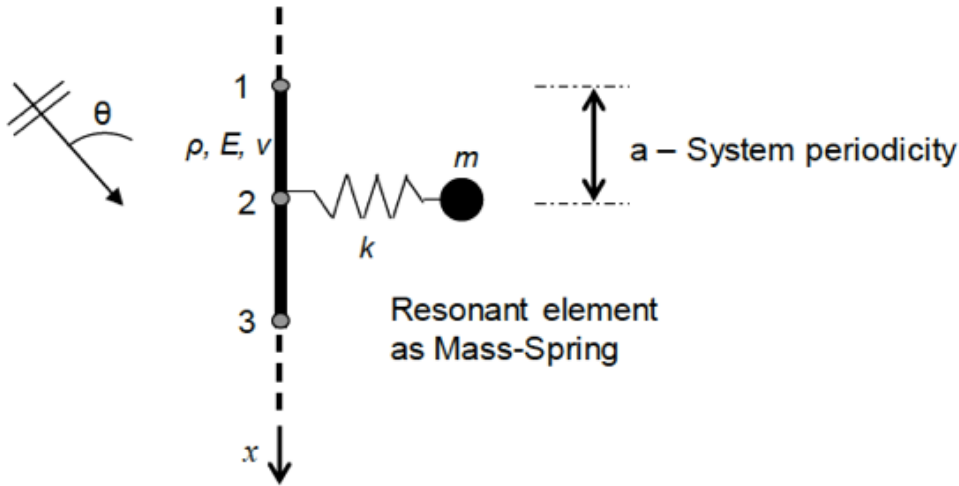


Figure 5.2: Schematic representation of mass-spring system (Amado-Mendes et al., 2018, p.5)

5.2 Design of demonstrators

In order to investigate and analyze the parameter influence of acoustic metamaterial on the eigenfrequency, further different resonators in various forms and sizes are designed. In the following pictures and tables, all designed models will be showed. All these models are first drawn in a CAD software and then imported, finally printed by a 3D printer. The same material resin (tough) is used for all models.

In order to study the effect of a single variable on the eigenfrequency more precisely, the volumes of all models are kept at a fixed value (around 20 mm^3). The variables are: the thickness of plate, the shape and size of resonators, the shape and thickness of holes on the plate. For a better comparison of different models, each model is numbered according to their characteristics.



Figure 5.3: Model 1: Panel-Flat-Sides

Table 5.1: Parameters of Model 1

Parameter	Value
Diameter of panel	40mm
Thickness of panel	16mm

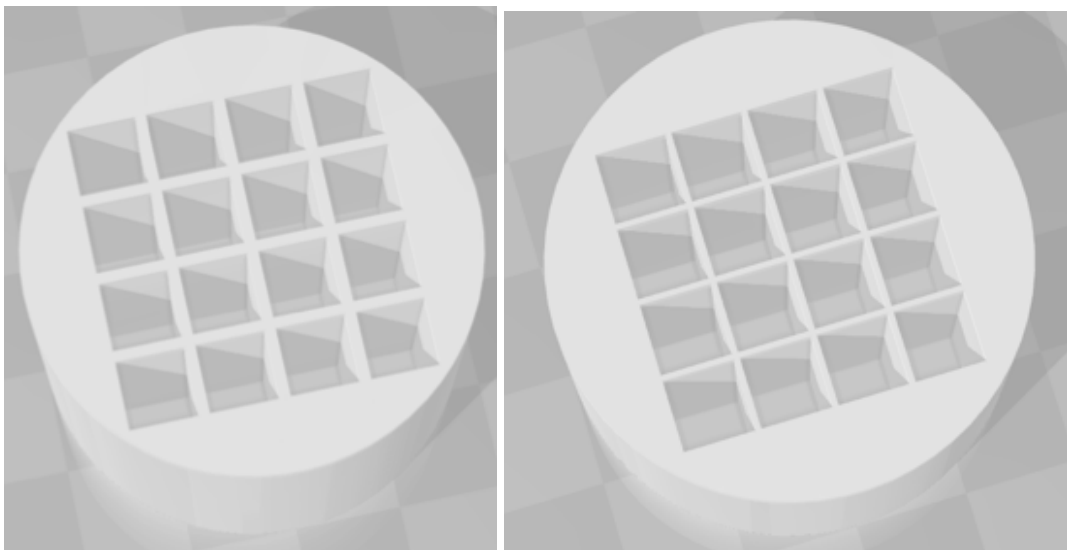


Figure 5.4: Model 2a: Panel-4x4-Length6-T30; Model 2b: Panel-4x4-Length6

Table 5.2: Parameters of **Model 2a**

Parameter	Value
Diameter of panel	40mm
Thickness of panel	30mm
Hole length x depth	6x20mm
Distance between holes	0.5mm

Table 5.3: Parameters of **Model 2b**

Parameter	Value
Diameter of panel	40mm
Thickness of panel	22mm
Hole length x depth	6x20mm
Distance between holes	0.5mm

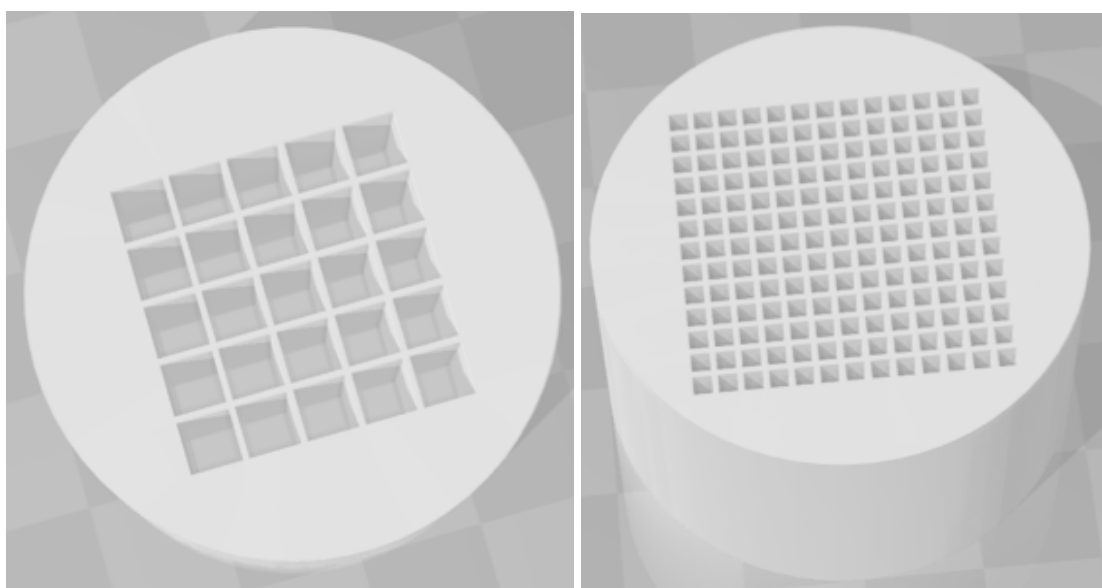


Figure 5.5: Model 2c: Panel-Grid-Without-Resonator; Model 3a: Panel-Grid-13x13

Table 5.4: Parameters of *Model 2c*

Parameter	Value
Diameter of panel	40mm
Thickness of panel	22mm
Hole length x depth	4x20mm
Distance between holes	0.5mm

Table 5.5: Parameters of *Model 3a*

Parameter	Value
Diameter of panel	40mm
Thickness of panel	22mm
Hole length x depth	1.5x20mm
Distance between holes	0.5mm

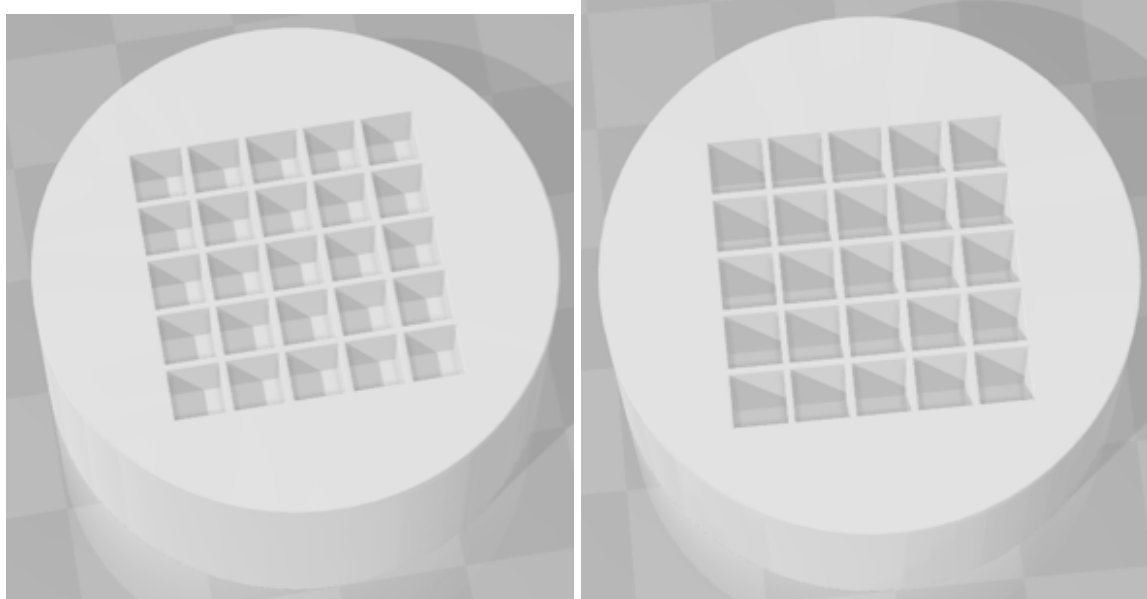


Figure 5.6: Model 4a: Panel-Grid-5x5-Depth-5; Model 4b: Panel-Grid-5x5-Depth-10

Table 5.6: Parameters of *Model 4a*

Parameter	Value
Diameter of panel	40mm
Thickness of panel	17.7mm
Hole length x depth	4x5mm
Distance between holes	0.5mm

Table 5.7: Parameters of *Model 4b*

Parameter	Value
Diameter of panel	40mm
Thickness of panel	19.2mm
Hole length x depth	4x10mm
Distance between holes	0.5mm

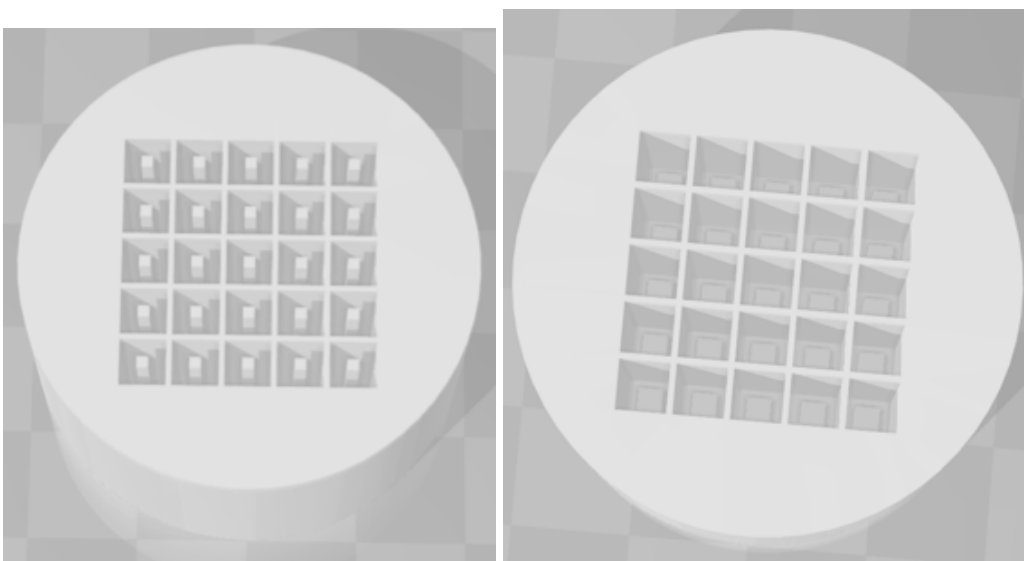
Figure 5.7: *Model 5a: Panel-Grid-Cube-Fixed-On-Bottom; Model 5b: Panel-Grid-Cube-Fixed-On-Bottom-5b*

Table 5.8: Parameters of *Model 5a*

Parameter	Value
Diameter of panel	40mm
Thickness of panel	22mm
Hole length x depth	4x20mm
Distance between holes	0.5mm
Resonator length x width x height (cubic)	1x1x20mm

Table 5.9: Parameters of *Model 5b*

Parameter	Value
Diameter of panel	40mm
Thickness of panel	22mm
Hole length x depth	4x20mm
Distance between holes	0.5mm
Resonator length x width x height (cubic)	2x2x5mm

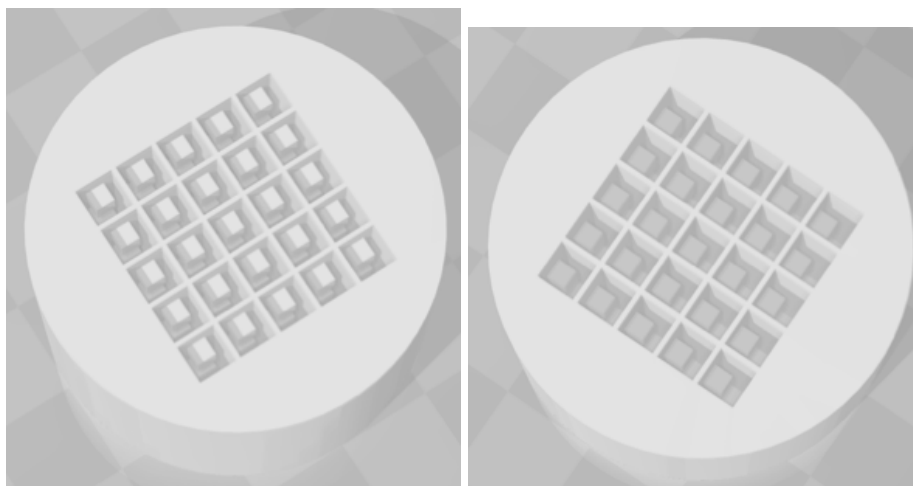
Figure 5.8: *Model 6a: Panel-Grid-Cube-Fixed-On-Sidewall-6a; Model 6b: Panel-Grid-Cube-Fixed-On-Sidewall-6b*

Table 5.10: Parameters of **Model 6a**

Parameter	Value
Diameter of panel	40mm
Thickness of panel	22mm
Hole length x depth	4x20mm
Distance between holes	0.5mm
Resonator length x width x height (cubicx2)	2x2x2.5mm

Table 5.11: Parameters of **Model 6b**

Parameter	Value
Diameter of panel	40mm
Thickness of panel	22mm
Hole length x depth	4x20mm
Distance between holes	0.5mm
Resonator length x width x height (cubic)	2x2x5mm

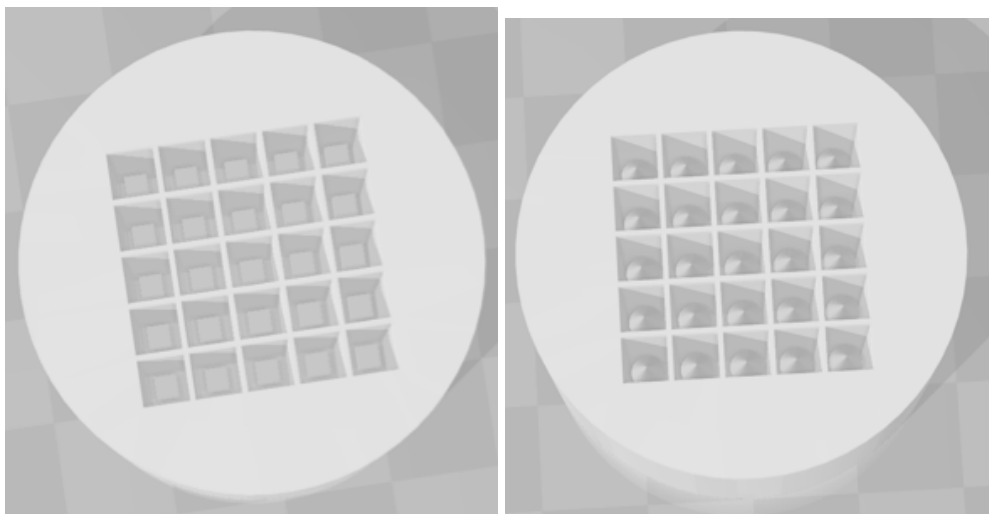


Figure 5.9: Model 7a: Panel-Grid-With-Cubic-Bridge; Model 7b: Panel-Grid-With-Conical-Resonator

Table 5.12: Parameters of **Model 7a**

Parameter	Value
Panel diameter x thickness	40x22mm
Hole length x depth	4x20mm
Distance between holes	0.5mm
Bridge	1x1x10mm
Resonator length x width x height (cubic)	2x2x2.5mm

Table 5.13: Parameters of **Model 7b**

Parameter	Value
Panel diameter x thickness	40x22mm
Hole length x depth	4x20mm
Distance between holes	0.5mm
Bridge	1x1x10mm
Conical resonator	3x4mm

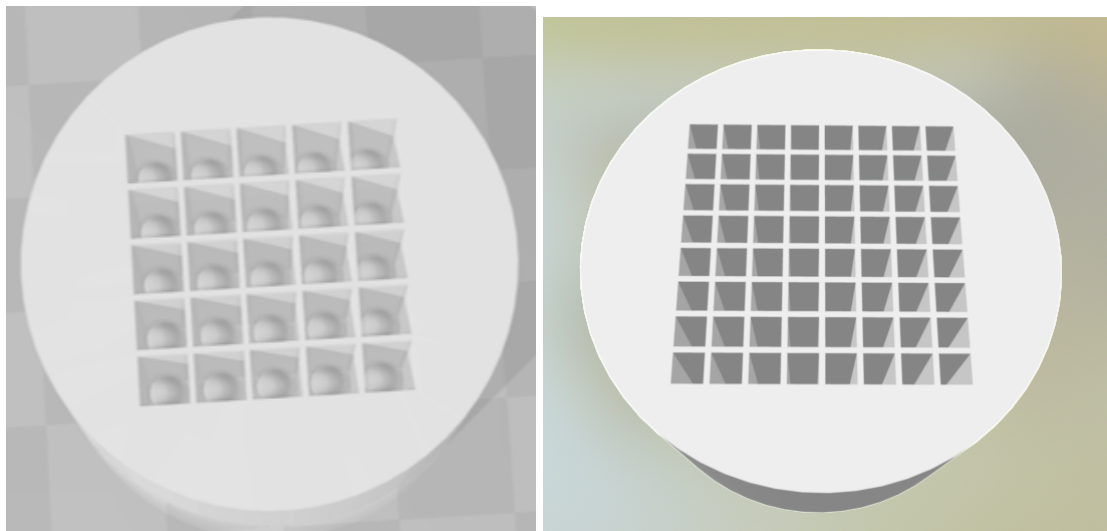


Figure 5.10: Model 7c: Panel-Grid-Hemispherical-Resonator; Model 8a: Panel-8x8-Length2.5

Table 5.14: Parameters of **Model 7c**

Parameter	Value
Panel diameter x thickness	40x22mm
Hole length x depth	4x20mm
Distance between holes	0.5mm
Bridge	1x1x10mm
Hemispherical resonator	3x1.5mm

Table 5.15: Parameters of **Model 8a**

Parameter	Value
Panel diameter x thickness	40x22mm
Hole length	2.5mm
Hole depth	20mm
Distance between holes	0.5mm

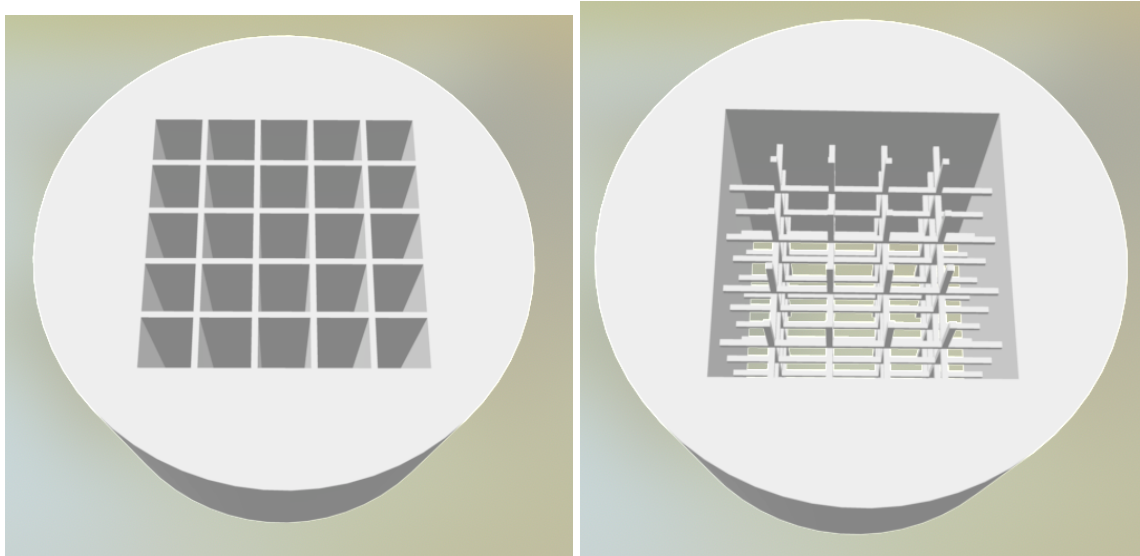


Figure 5.11: Model 8b: Panel-5x5-Length4-Without-Bottom; Model 8c: Panel-5x5-Length4-Lattice-Edges

Table 5.16: Parameters of **Model 8b**

Parameter	Value
Panel diameter x thickness	40x24mm
Hole length	4mm
Hole depth	24mm
Distance between holes	0.5mm

Table 5.17: Parameters of **Model 8c**

Parameter	Value
Panel diameter x thickness	40x22mm
Hole length	4mm
Hole depth	22mm
Distance between holes	0.5mm

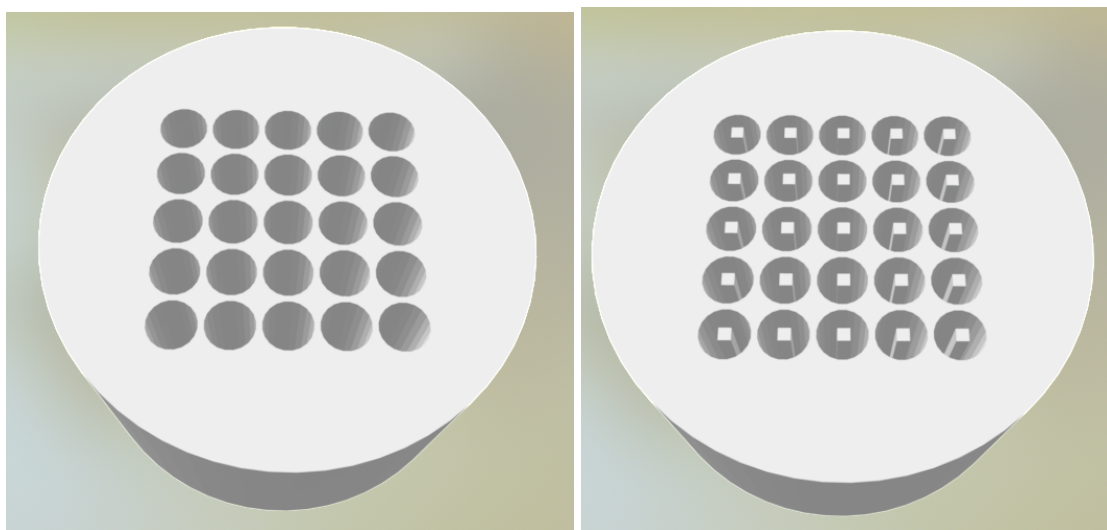


Figure 5.12: Model 9a: Panel-Cylindricalgrid; Model 9b:
Panel-Cylindricalgrid-Cube-Fixed-On-Bottom

Table 5.18: Parameters of *Model 9a*

Parameter	Value
Panel diameter x thickness	40x22mm
Hole diameter	4mm
Hole depth	20mm
Distance between holes	0.5mm

Table 5.19: Parameters of *Model 9b*

Parameter	Value
Panel diameter x thickness	40x22mm
Hole diameter	4mm
Hole depth	20mm
Distance between holes	0.5mm
Resonator length x width x height (cubic)	1x1x20mm

6 Simulation process

6.1 Theories for simulation process

In this section, various physical properties, which can be evaluated in the simulation process, will be introduced. Moreover, the important physical principles and boundary conditions for acoustic metamaterials will be described.

6.1.1 Physical properties

- **The absorption coefficient:**

The absorption coefficient describes the sound absorption effect of a metamaterial structure. It can be written as the ratio of absorbed sound energy to incident sound energy. After considering the equation of motion and the continuity equation, the acoustic absorption coefficient for normal incidence may be obtained as (Al-Zubi et al., 2013, p.3):

$$a_0 = \frac{4\text{Re}(z/\rho_0 c_0)}{(\text{Re}(z/\rho_0 c_0) + 1)^2 + (\text{Im}(z/\rho_0 c_0))^2} \quad (6.1)$$

In order to get the absorption coefficient in the simulation, some approximations such as Rayleigh's approximate energy method are taken into consideration. In 2013, Al-Zubi et al. have simulated the sound absorption of different acoustic materials by using Abaqus and Matlab and compared with experimental results, the performance of different materials vary greatly (Al-Zubi et al., 2013).

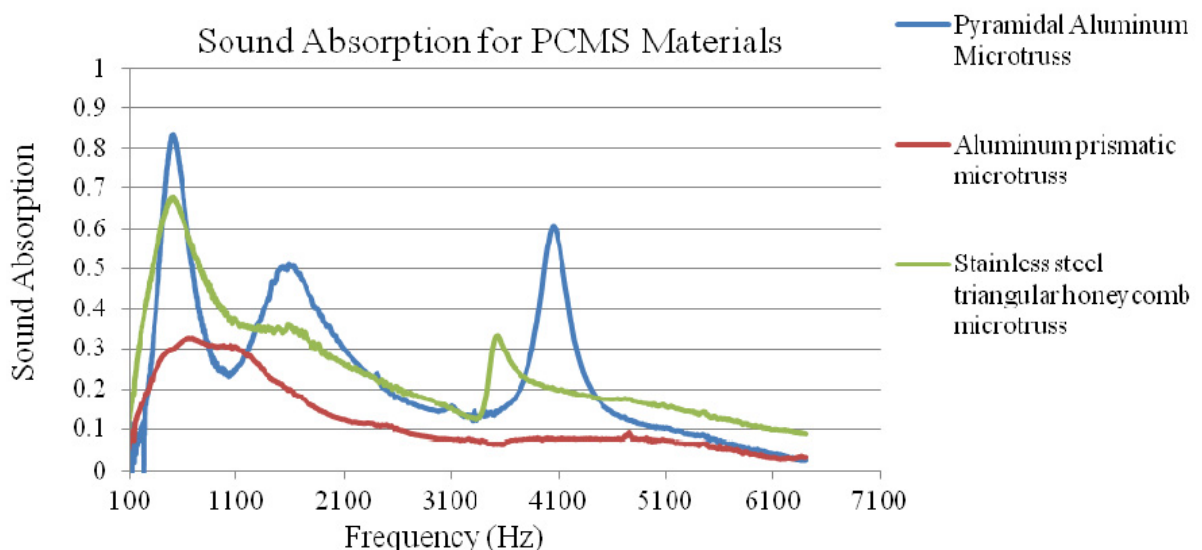


Figure 6.1: Sound absorption of some periodic cellular material structures based on Abaqus and Matlab (Al-Zubi et al., 2013, p.6)

- **Dispersion relation:**

The dispersion relation describes the physical relation between wavenumber k and frequency ω of a structure. It is usually illustrated in a diagram with the x-axis as wave number and the y-axis as frequency. To some extent it reflects the band gap of a structure. By combining an acoustic plane wave propagating equation and an acoustic wave equation, the relation between the frequency ω and the wave vector k of the acoustic plane wave can be given by (Maldovan & Thomas, 2009, p.188):

$$k = \frac{\omega}{c_0} \quad (6.2)$$

where c_0 is the velocity of the acoustic wave, which is determined by the mechanical properties: the wave length and mass density. In the literature, the dispersion relation of acoustic metamaterials is limited to two-dimensional modeling. In 2011, Elford et al. have simulated the band gap of a C-shaped locally resonant crystal by using COMSOL [®]Multiphysics, it shows that resonance bands can be combined to form broad regions of attenuation (Elford et al., 2011).

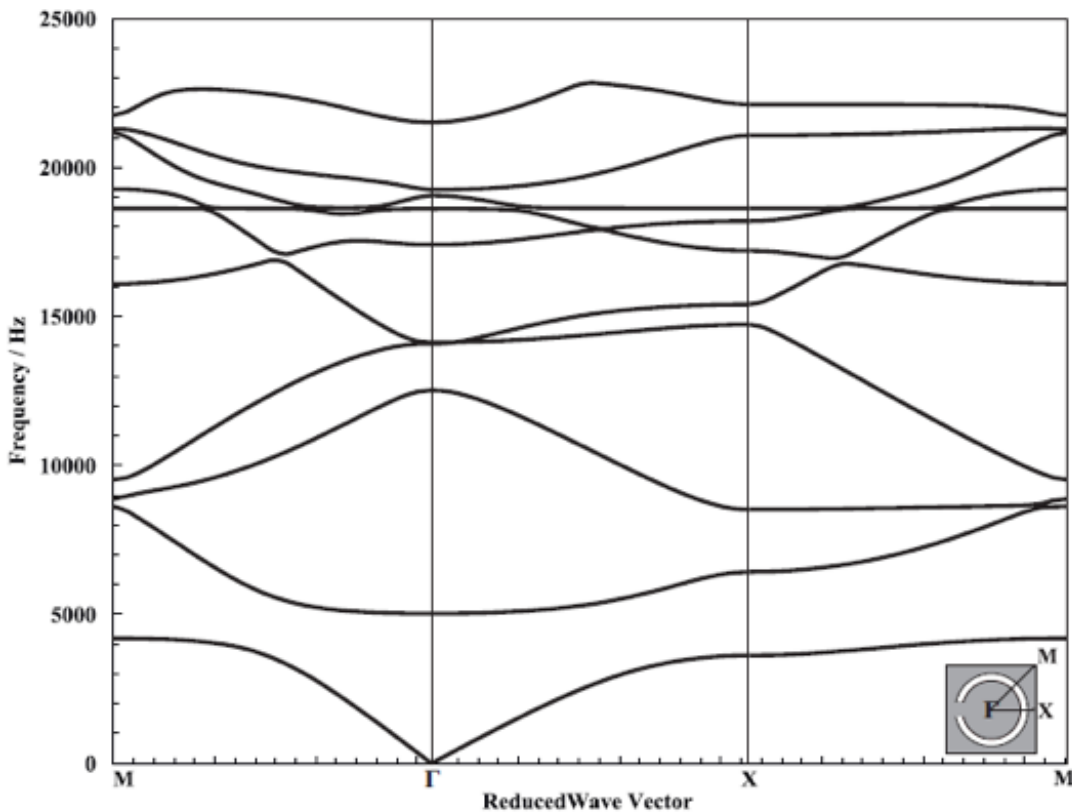


Figure 6.2: Band structure for a C-shaped locally resonant sonic crystal based on COMSOL [®]Multiphysics (Elford et al., 2011, p.4)

- **Sound transmission loss:**

At a specific frequency, sound transmission loss describes the reduction of sound intensity caused by a structure. It can be defined as a ratio of the sound energy transmitted through a

treatment versus the amount of sound energy on the incident side of the material (Wang et al., 2019, p.4):

$$STL = 10 \log\left(\frac{W_{in}}{W_{out}}\right) \quad (6.3)$$

$$W_{in} = \frac{|P_i|^2}{2\rho_0 c_0}, W_{out} = \frac{|P_t|^2}{2\rho_0 c_0} \quad (6.4)$$

where W_{in} is incident sound energy, W_{out} is transmitted sound energy. By giving the incident sound pressure value and the scanning frequency band range, the sound transmission loss value of a specific structure can be calculated. In 2019, Wang et al. have simulated the sound transmission loss of a plate-type acoustic metamaterial panel to analyze sound insulation effect by using COMSOL ®Multiphysics, the simulation results are verified by the experiment (Wang et al., 2019).

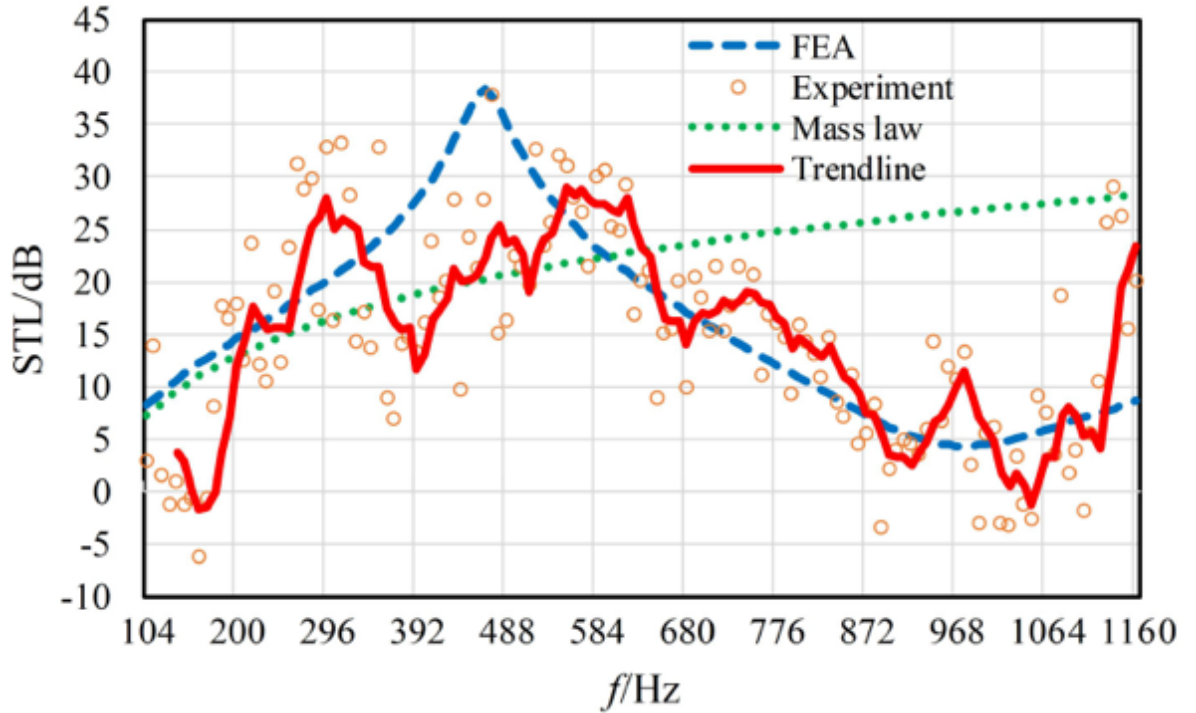


Figure 6.3: Results of STL. based on COMSOL ®Multiphysics (Wang et al., 2019, p.31)

- **Frequency response:**

The frequency response of an acoustic metamaterial can be described as the measurement of the frequency spectrum in response to a stimulus. In the simulation process, this stimulus is usually given as a sound pressure or an external force. The governing equation can be described in a matrix form as (Yeh & Harne, 2019, p.5):

$$(-\omega^2 M + j\omega C + K)q = F \quad (6.5)$$

where F is the forcing vector, M is the mass matrix, K is the stiffness matrix, C is the damping matrix. By simulating the frequency response of an acoustic metamaterial, the eigenfrequencies of a structure within a specific frequency range can be analyzed. In 2019, Yeh and Harne have simulated a series of cylindrical hollow tubes with different metamaterial inclusions based on COMSOL [®]Multiphysics, the results are validated by experiments (Yeh & Harne, 2019).

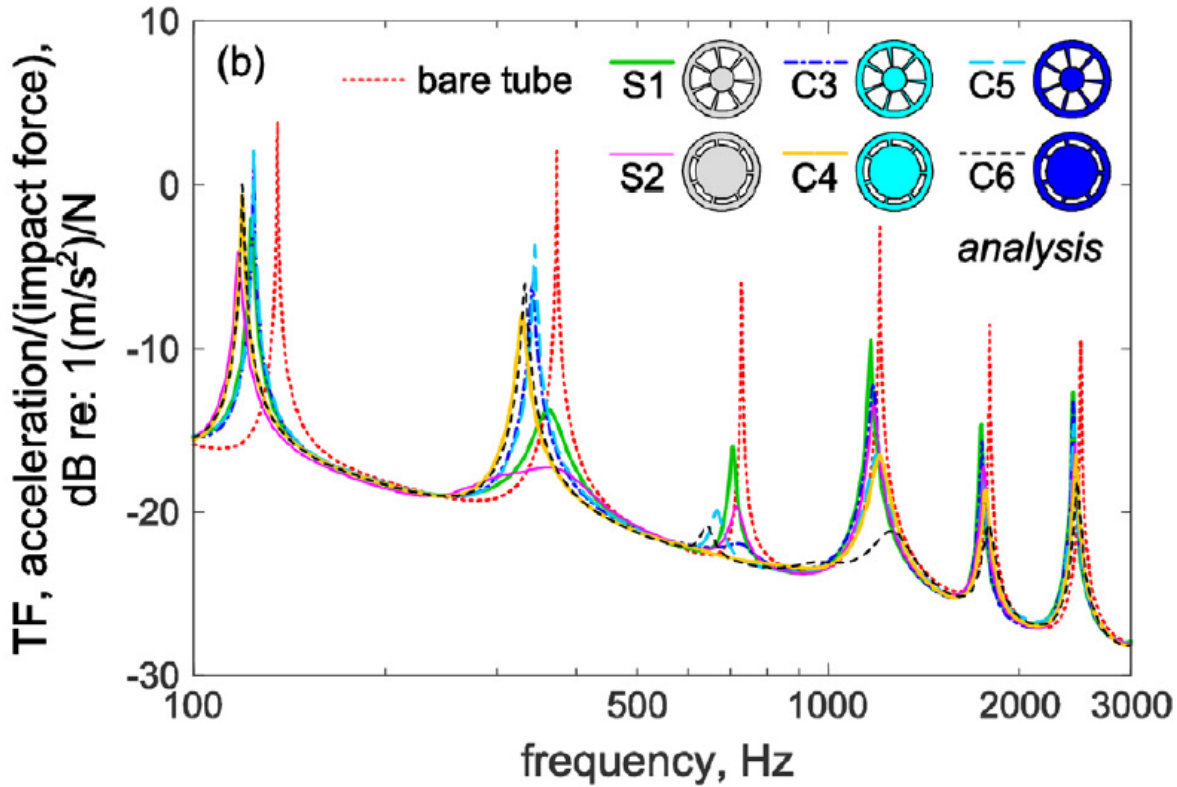


Figure 6.4: Results of frequency responses based on COMSOL [®]Multiphysics (Yeh & Harne, 2019, p.11)

6.1.2 The Brillouin zone and wave vector

The band structure can be obtained from the diagram of dispersion relation. The dispersion relation describes the relation between eigenfrequency and wave vector of sound waves. It can be written as a function depending on the variable \mathbf{k} :

$$\omega = \omega(\mathbf{k}) \quad (6.6)$$

- **Wave vector:**

Wave vector is a physic definition, which represents the vector of a wave. It is a vector whose magnitude is the angular wave number and whose direction is the direction in which the wave travels. In one-dimensional problems, it can also be called wave number. Wave number is the inverse of the wavelength. It is the number of waves per unit of length in the direction of wave. In theoretical physics, the relation of wave vector and wave number can be written

as:

$$k = |\mathbf{k}| = 2\pi/\lambda \quad (6.7)$$

where λ is the wave length. Wave vector is an important parameter for the wave equation. In two-dimensional sound wave propagating problems, the wave vector of sound wave with different magnitudes and arbitrary directions in defined plane must be considered.

- **The First Brillouin zone (Reduced Brillouin zone):**

The Brillouin zone was first proposed by the French physicist Leon Brillouin to divide the region of wave vector space. All the waves in the periodic structure generate Bragg reflection on the Brillouin boundary. For some waves, this reflection may cause discontinuous changes in electron energy on the Brillouin boundary. Since the energy of the moving electrons and magnetons of a complete crystal are all periodic functions of the reciprocal lattice, it is possible to use only the wave vector in the First Brillouin zone to describe the energy band. Due to this the First Brillouin zone is also called the Reduced Brillouin zone.

In order to calculate the dispersion relation and to investigate the band gap, the first thing is to determine the domain of the function, that is, to define the set of wave vectors required to completely describe the propagation of two-dimensional waves (Maldovan & Thomas, 2009, p.152). This set of wave vectors is also called the Brillouin zone. Only wave vectors within the Brillouin zone need to be considered to plot the dispersion relation (Maldovan & Thomas, 2009, p.155). There are different methods to define Brillouin zones. In simple 2D models, the Brillouin zone is usually considered as a square or hexagon:

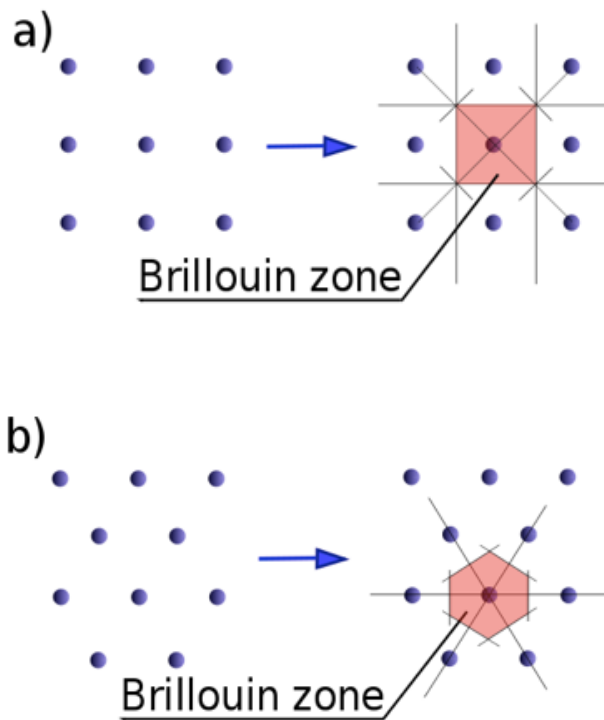


Figure 6.5: The typical Brillouin zone for two dimensional models: a) Square Brillouin zone; b) Hexagon Brillouin zone

<https://en.wikipedia.org/wiki/File:Brillouin-zone.svg>

Due to the periodicity only a structural unit will be considered in the Brillouin zone. The critical points in Brillouin zone are strictly defined. In general, Γ is the center of Brillouin zone, M is the center of an edge, X is the center of a face, K is the middle of an edge joining two hexagonal faces.

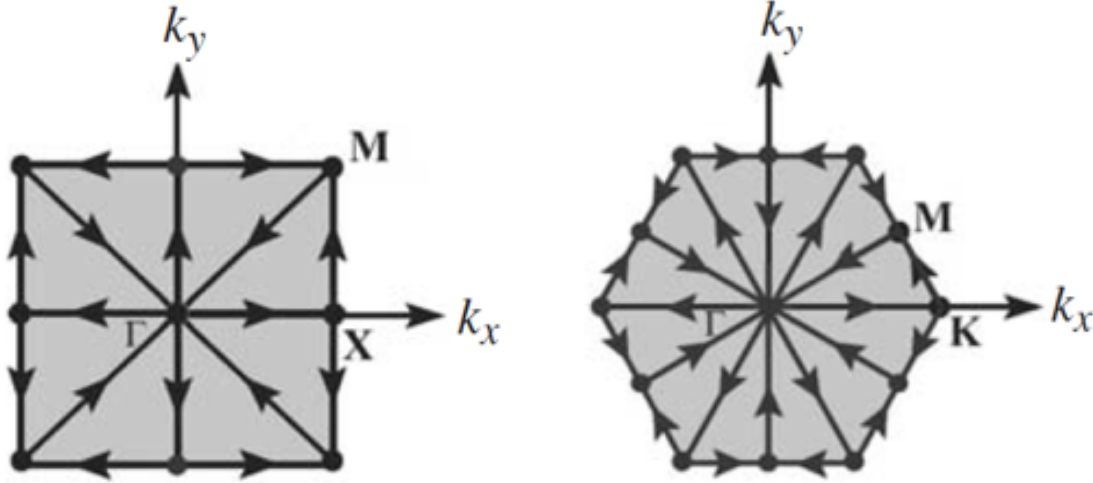


Figure 6.6: The critical points in two dimensional Brillouin zones (Maldovan & Thomas, 2009, p.156)

6.1.3 The Floquet-Bloch boundary condition

- **Bloch wave:**

In infinite periodic structures, the propagating waves are also called Bloch waves, which can be described with a periodic function. The propagation of acoustic Bloch waves within the phononic crystal is governed by the acoustic wave equation (Maldovan & Thomas, 2009, p.204):

$$\nabla \cdot \left(\frac{1}{\rho} \nabla p \right) = -\frac{1}{\rho c_L^2} (\omega(\mathbf{k}))^2 p \quad (6.8)$$

where ρ is the density, c_L is the longitudinal velocity of acoustic waves within the phononic crystal, p is the spatial part of the pressure of an acoustic Bloch wave propagating with wave vector \mathbf{k} within the phononic crystal. In order to get the dispersion relation, this equation must be numerically solved.

- **Floquet boundary condition:**

Floquet boundary condition is one of the periodic boundary conditions. With periodic conditions the surrounding environment of the unit cell can be ignored so that the simulation models can be simplified. It can also be regarded as a property that can be generalized to express the global property by the property of parts. In Floquet boundary condition, the field values of source boundary and target boundary differ by a phase factor, which is determined by the relative distance between wave vector and boundary. For the two-dimensional acoustic models, each side of the model should be combined with Floquet boundary condition.

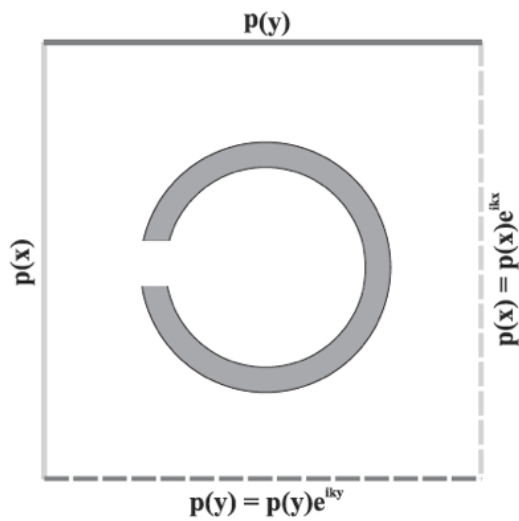


Figure 6.7: Unit cell with Floquet boundary condition (Elford et al., 2011, p.2)

6.2 Simulation steps

To visualize the sound insulation effect of acoustic metamaterial prototype and to compare with the experimental results. It is decided to use commercial software COMSOL® Multiphysics to simulate the dispersion curve, which reflects band gap structure at a certain frequency range. The focus of this thesis is try to build an exactly same model as the prototype design and execute the corresponding analytical solution for the simulation process. Due to the Floquet boundary condition the simulation model can be simplified and considered as a periodic structure. After defining the necessary coordinate system and parameters to set up the Brillouin zone, the geometry and material properties of the model can be built up in the corresponding physical module. In the end, the simulated results will be compared with experimental results and then be optimized. The steps to simulate a model in COMSOL® Multiphysics are strictly defined by the software developer, which is also a big advantage of this software tool. In general, the simulation process can be described as the following workflow:

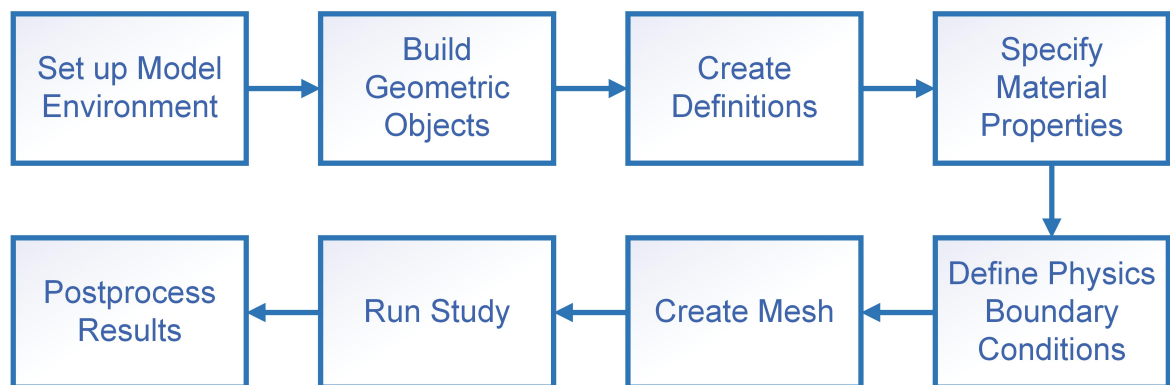


Figure 6.8: Workflow of simulation steps in COMSOL Multiphysics

In the next, the simulation model will be built as the workflow described above. Since this thesis is mainly about two-dimensional modelling, only several representative models will be selected from chapter 4 for the simulation. Through simulation results the influence of different parameters will be analyzed. The involved parameters are such as: shape, number and size of holes on the plate, shape, size and location of resonators. All selected models are simulated in a top view, so that 3D factors such as the thickness of the plate are ignored. In the next, the model 2a, model 2c, model 5a, model 5b, model 6a, model 7b, model 9a and model 9b will be simulated to analyze their band structure. In the following subsections, each simulation step for the models will be explained.

6.2.1 Model environment

Since the main focus here is to research the properties of acoustic metamaterials, the pressure acoustics module of the physical domain is selected for the simulation. In this physical module the interaction within air dominates the acoustic interaction. In this module, the plate is mainly modeled in the frequency domain through the Helmholtz equation, which reflects the relation between frequency and wave vector:

$$\nabla \cdot \left(-\frac{1}{\rho} (\nabla p - \mathbf{q}_d) \right) - \frac{k_{eq}^2 p}{\rho} = Q_m \quad (6.9)$$

$$k_{eq}^2 = \left(\frac{\omega}{c} \right)^2 - k_z^2 \quad (6.10)$$

$$-i\omega = \lambda \quad (6.11)$$

where c and ρ are sound speed and density of air, λ is the wavelength. By giving the material properties and solving the above equations the eigenfrequencies of the model can be obtained. This pressure acoustics domain is set on the entire surface of the model. The wave numbers out of plane and the initial pressure value are set as 0. In this step, the sound hard boundary is automatically used for every side of model.

6.2.2 Geometric objects

As mentioned above the two-dimensional model is built based on the experiment panel. The Floquet-Bloch boundary condition can only be set on the straight side of model. Therefore, in order to set the boundary conditions later, the basic panel is transformed into a square with the side length 40mm in the simulation, which is same as the diameter of the panel. On the surface of the square, different holes are built by removing the corresponding part. The resonators are built by adding extra parts in the holes. The additional parts (resonators) are then combined with the square. In this way they form an union so that the material properties and physical properties can be set on it, which means they use the same material property and physical property and move together as an entire part. In the following pictures, all simulated models selected from the experiment are showed.

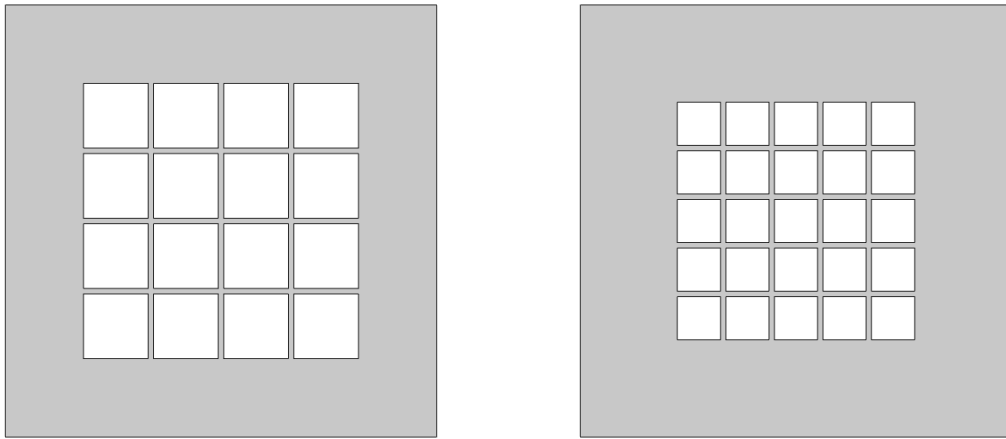


Figure 6.9: Model 2a (left) and model 2c (right)

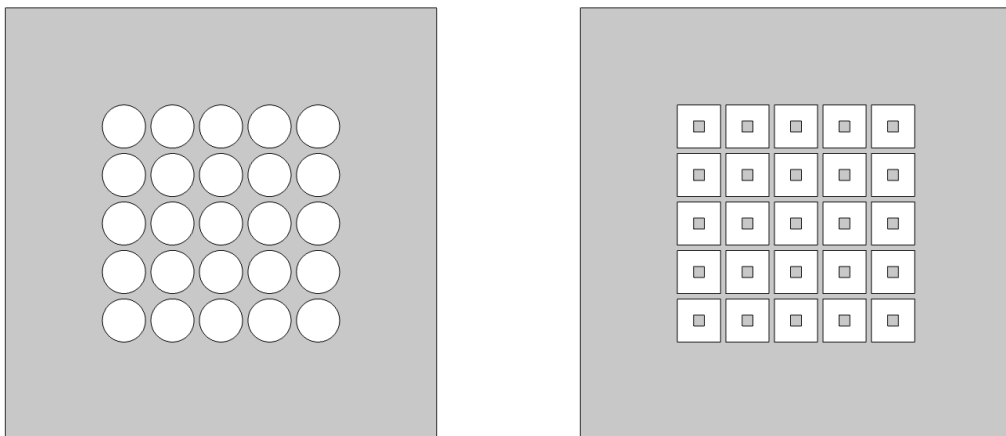


Figure 6.10: Model 5a (left) and model 5b (right)

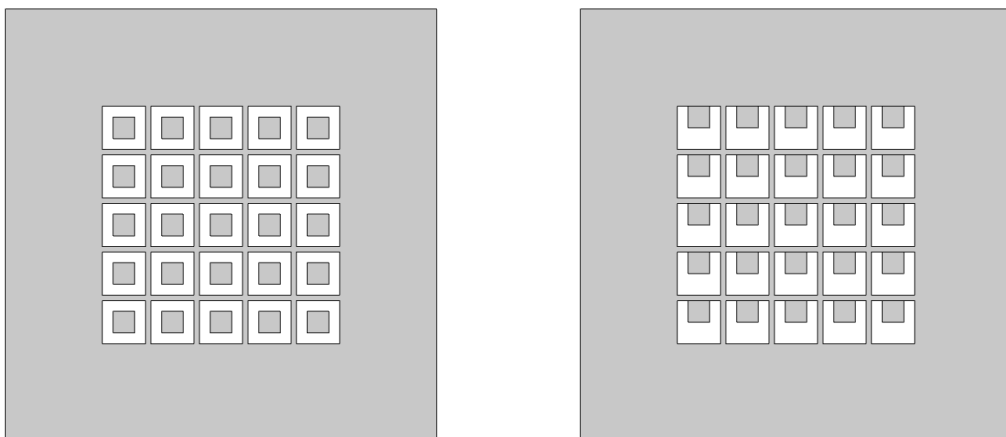


Figure 6.11: Model 6a (left) and model 7b (right)

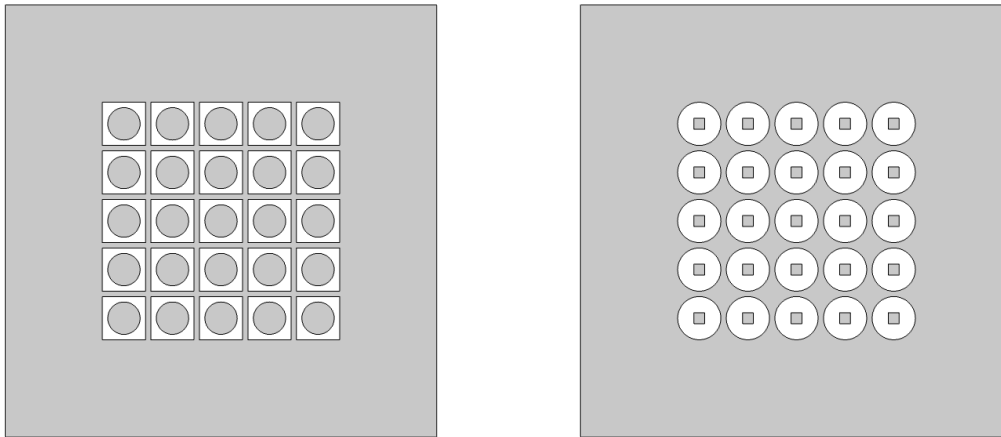


Figure 6.12: Model 9a (left) and model 9b (right)

6.2.3 Definitions and parameters

In order to set up the first Brillouin zone, some parameters need to be defined at first. For the physical parameter, $L1$ is defined as the side length of the first Brillouin zone, it is also the side length of the simulation model. For the global variables, k_x and k_y are the direction vectors of the wave vector k , which varies from 0 to 3. In the following table, the initial value of k is set as 0.5.

Table 6.1: Global parameters for the simulation model

Parameter	Value
$L1$	40mm
k	0.5
k_x	$\text{if}(k < 1, \pi/L1 * k, \text{if}(k < 2, \pi/L1, (3-k) * \pi/L1))$
k_y	$\text{if}(k < 1, 0, \text{if}(k < 2, (k-1) * \pi/L1, (3-k) * \pi/L1))$

6.2.4 Material properties

In pressure acoustics module only the material properties of air are considered: density and sound speed, which are determined by the physical formulas. These material properties are set on the entire model surface including resonators, which directly contact with air. That means, the material properties of the model itself has little influence on the results.

Table 6.2: Material parameters for the simulation model

Parameter	Value
density (ρ)	$1.29\text{kg}/\text{m}^3$
sound speed (c)	$343\text{m}/\text{s}$

6.2.5 Periodic boundary conditions

In order to set the Floquet-Bloch boundary condition, the first Brillouin zone must be defined before that. In the first Brillouin zone the direction and calculation method of wave vectors are defined. In this two-dimensional model only wave vectors k_x and k_y in x - and y -direction are considered. Here the basic square is considered as the first Brillouin zone. Firstly a coordinate system for the wave vector k is established in the basic square, the original point is the center of the square. Since the band structure diagram consists of three parts, the definition of the wave vector k can be described as: $k=0$ at the center of the square, $k=1$ at the center of the face, $k=2$ at the center of the edge, $k=3$ at the center of the square. The dispersion relation is calculated in three parts: from $k=0$ to $k=1$, from $k=1$ to $k=2$, from $k=2$ to $k=3$. These three parts join together to form the band structure diagram.

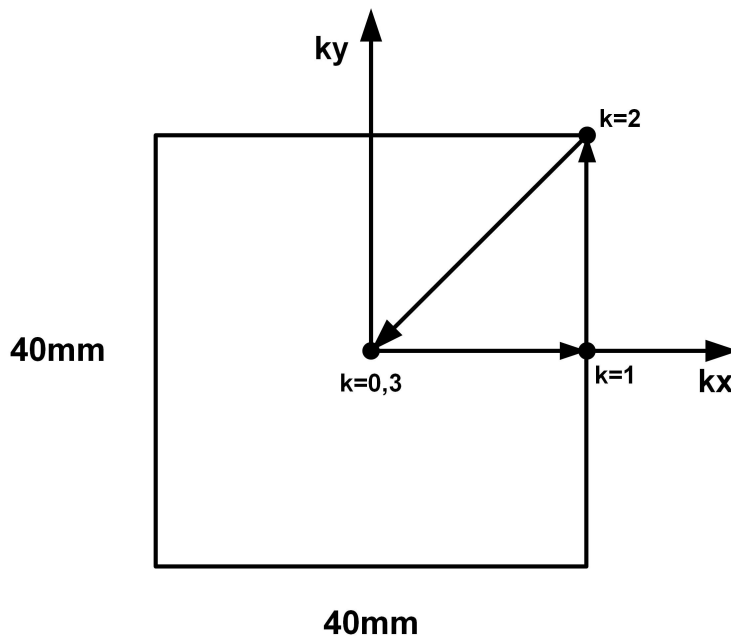


Figure 6.13: The Brillouin zone for the simulation model

For simulation models the Floquet-Bloch boundary condition is used. It is one of the important periodic conditions and set twice on the two opposite sides of the square. The sound hard boundaries are the contact boundaries between the air and model. In the following pictures, the Floquet-Bloch boundary condition and sound hard boundaries of several models are showed. For the models with resonators, the sound hard boundaries includes the boundaries of resonators.

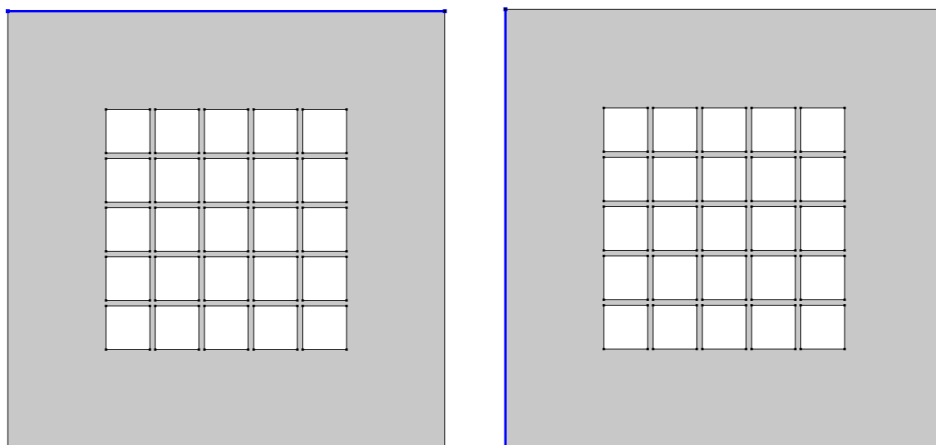


Figure 6.14: The Floquet-Bloch boundary condition for the model 2c

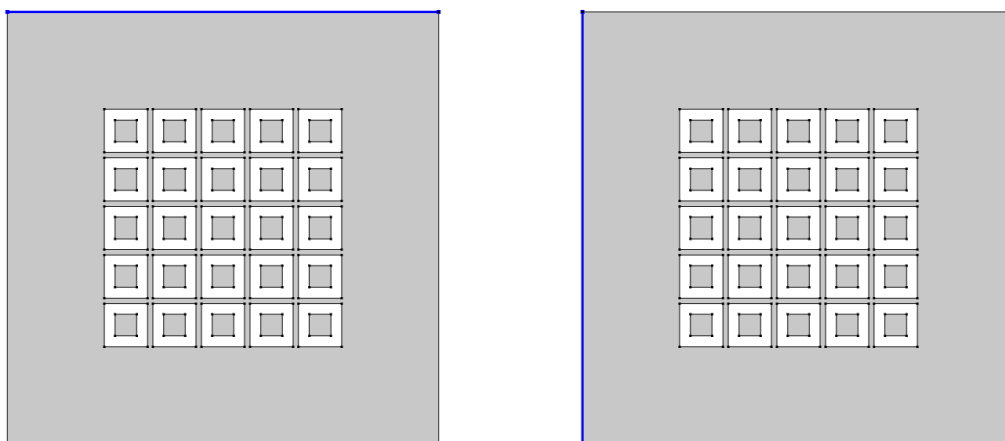


Figure 6.15: The Floquet-Bloch boundary condition for the model 6a

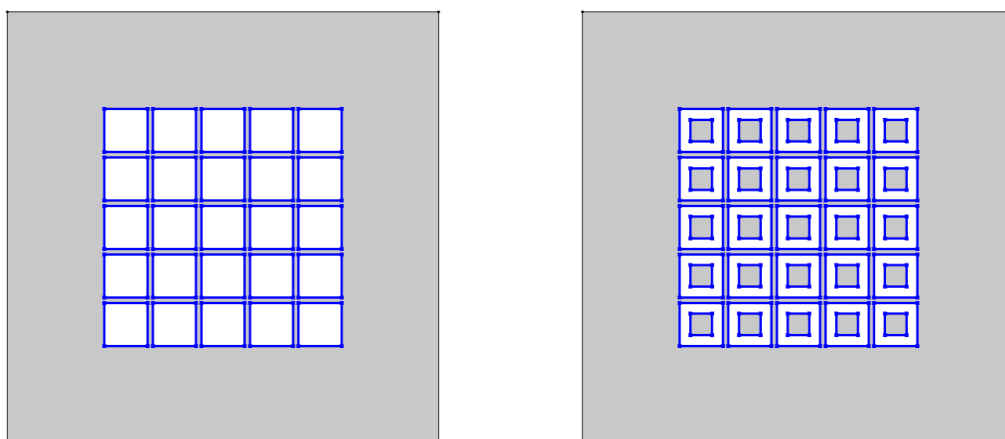


Figure 6.16: Sound hard boundaries of model 2c (left) and model 6a (right)

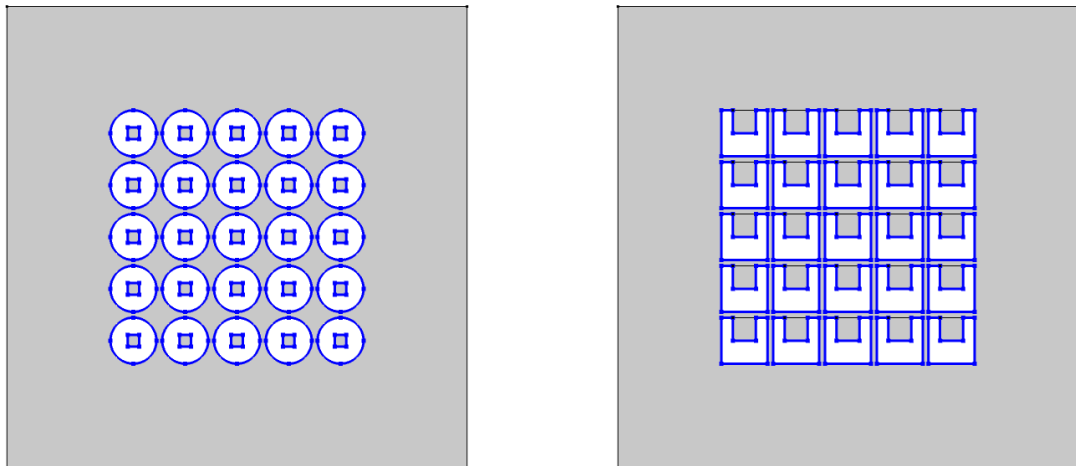


Figure 6.17: Sound hard boundaries of model 9b (left) and model 7b (right)

6.2.6 Meshing

In this step an extra fine mesh size is selected in order to get an accurate simulation result. The meshing process depends on the physical domain and corresponding formulas, which determines the smallest size of meshing unit. The square sides are extra selected, since the Floquet-Bloch boundary condition is used. Then the boundary condition is copied to the opposite square sides. As the mesh form a free triangle meshing is set on the entire model area. In the following pictures, the meshing of several models including mesh size and boundary condition are showed as exsamples. The meshing size and conditions of resonators are same as the basic square.

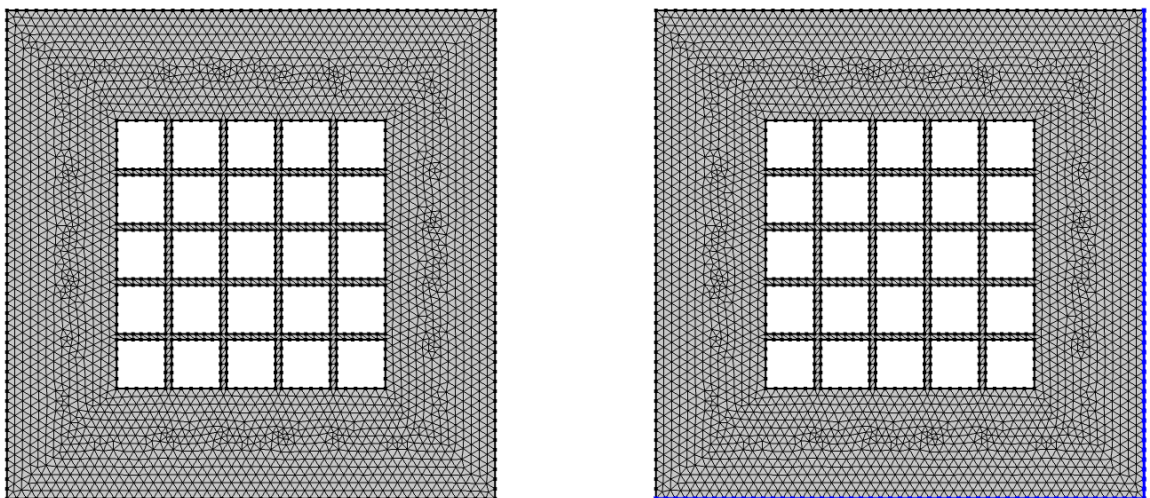


Figure 6.18: Meshing for the structure (left) and for the boundaries (right) of model 2c

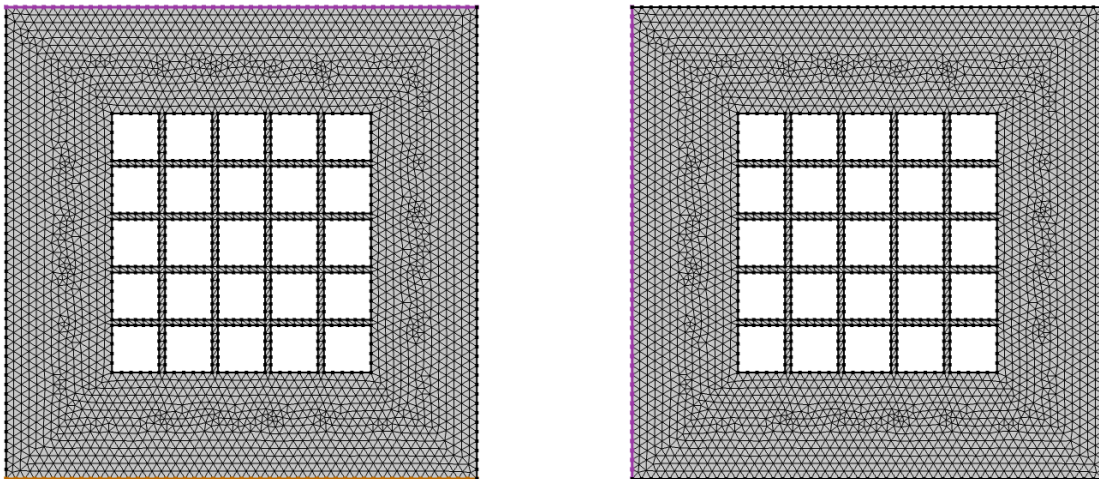


Figure 6.19: the Floquet-Bloch boundary condition for the meshing of model 2c

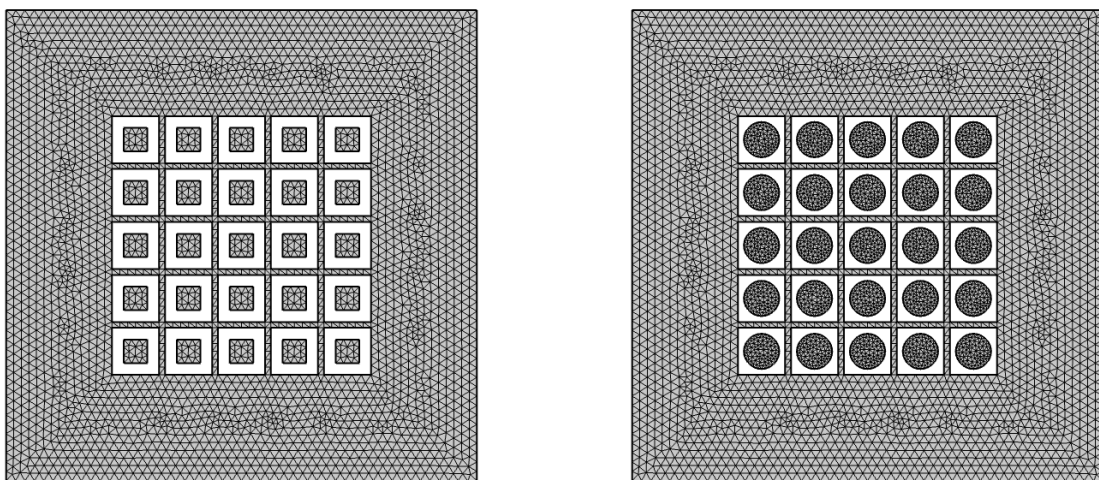


Figure 6.20: Meshing of model 6a (left) and model 9a (right)

6.2.7 Study

For the band structure analysis an eigenfrequency study is selected. At first a parameter sweep is executed to set the wave vector variable k . It is defined to vary from 0 to 3, and the two direction variables k_x , k_y change with it. The eigenfrequency numbers are set as 6, and the target frequency is around 5000Hz.

Table 6.3: Parameter sweep for the wave vector k

Parameter	Sweep
k	range(0,3/36,3)

In order to visualize the band structure, an one-dimensional diagramm is defined: the wave vector k is the x-axis, the eigenfrequency is the y-axis with the unit Hz. The values of the wave vector k are taken from the results of the parameter sweep. The eigenfrequency values are taken from solutions of the simulation process. The simulation process of each model is executed seperately. In the following subsections, the band structure diagramms of different models are analyzed and compared.

6.3 Verification of simulation process

In order to prove the simulation process of this thesis is correct and widely applicable, a normative structure of phononic crystals from the book "Periodic Materials and Interference Lithography for Photonics, Phononics and Mechanics" (Maldovan & Thomas, 2009) is simulated to compare with the results in the paper. The comparison is showed in the pictures below. It is obvious that the most important five eigenfrequency lines are successfully simulated. The stop band is easily recognizable. The most powerful advantage of this simulation method is that it can automatically ignore the useless eigenfrequency lines, so that only the import lines are showed in the diagrams, which leads to an intuitionistic visualization of the band structure. The left diagram in the following picture is from Mohammadi et al. (Mohammadi, Eftekhar, Khelif, & Adibi, 2010, p.5). The simulated eigenfrequencies are marked with dark lines.

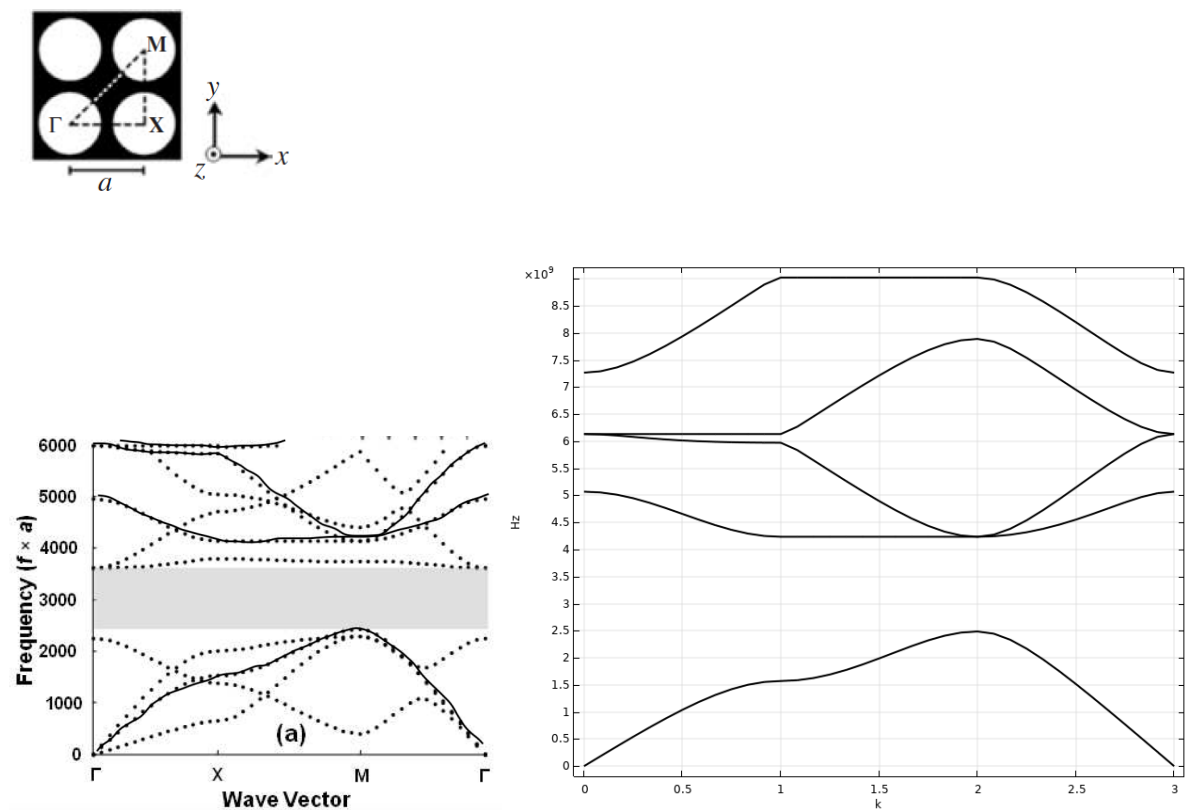


Figure 6.21: Comparison of the band structure between the paper (left) and simulation (right) in this thesis

7 Simulation results

7.1 Diagrams of the dispersion relation

In the last section, totally eight models are simulated in 2D. In the following pictures, the dispersion relations of them are showed. The stop bands are marked in the diagrams and can be summarized as:

- Model 2a: The stopband is between 4900Hz and 5300Hz.
- Model 2b: The stopband is between 5000Hz and 5500Hz.
- Model 5a: The stopband is between 5200Hz and 5600Hz.
- Model 5b: The stopband is between 4700Hz and 4800Hz.
- Model 6a: The stopband is between 5000Hz and 5500Hz.
- Model 7b: The stopband is between 4900Hz and 5500Hz.
- Model 9a: The stopband is between 5000Hz and 5500Hz.
- Model 9b: The stopband is between 4800Hz and 4900Hz.

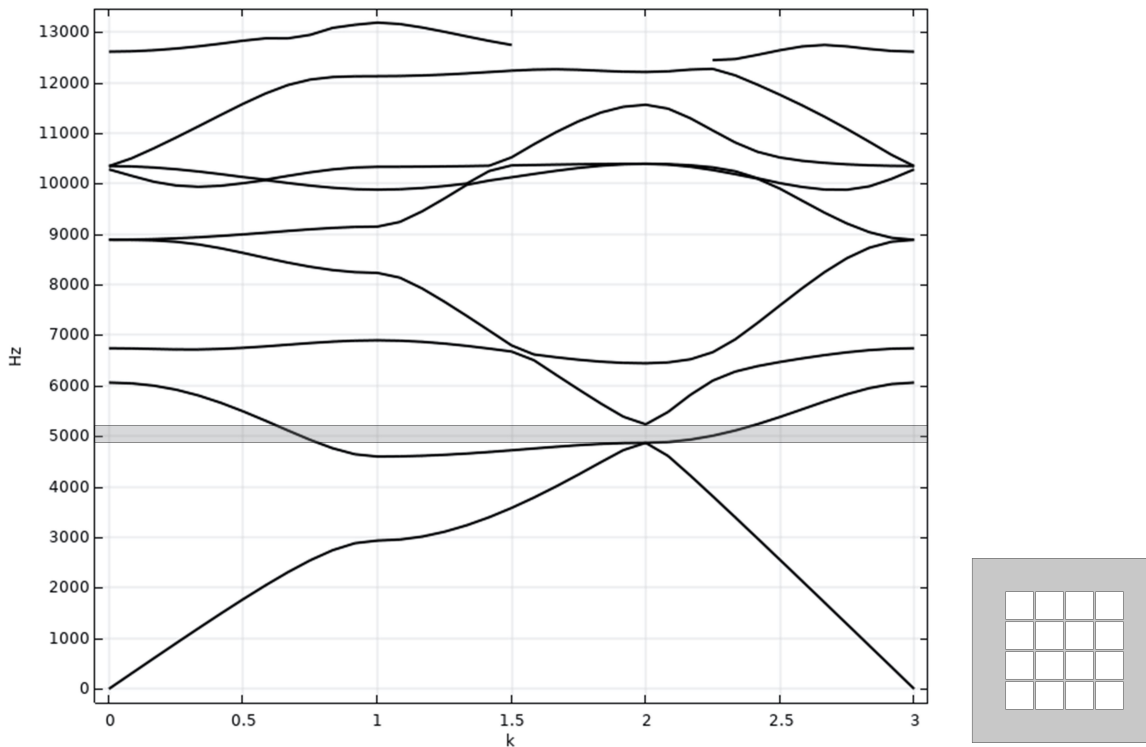


Figure 7.1: The band structure of the model 2a: with 4x4 holes and without resonators

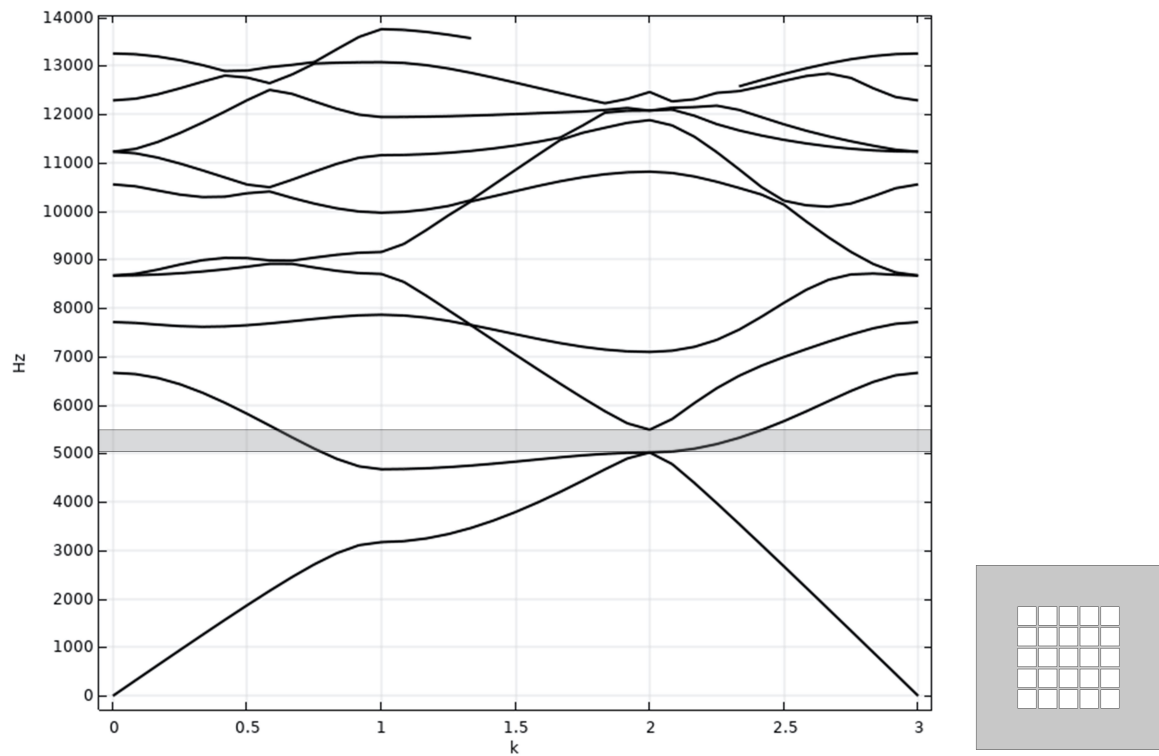


Figure 7.2: The band structure of the model 2b: with 5x5 holes and without resonators

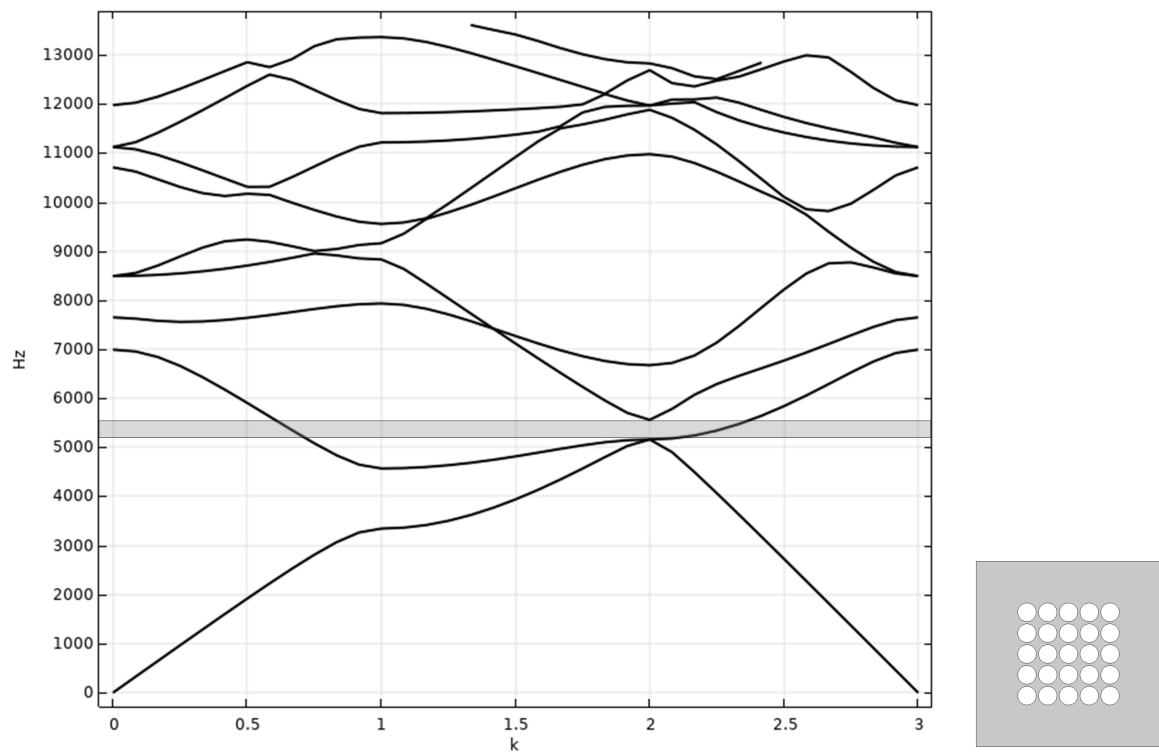


Figure 7.3: The band structure of the model 5a: with circle holes and without resonators

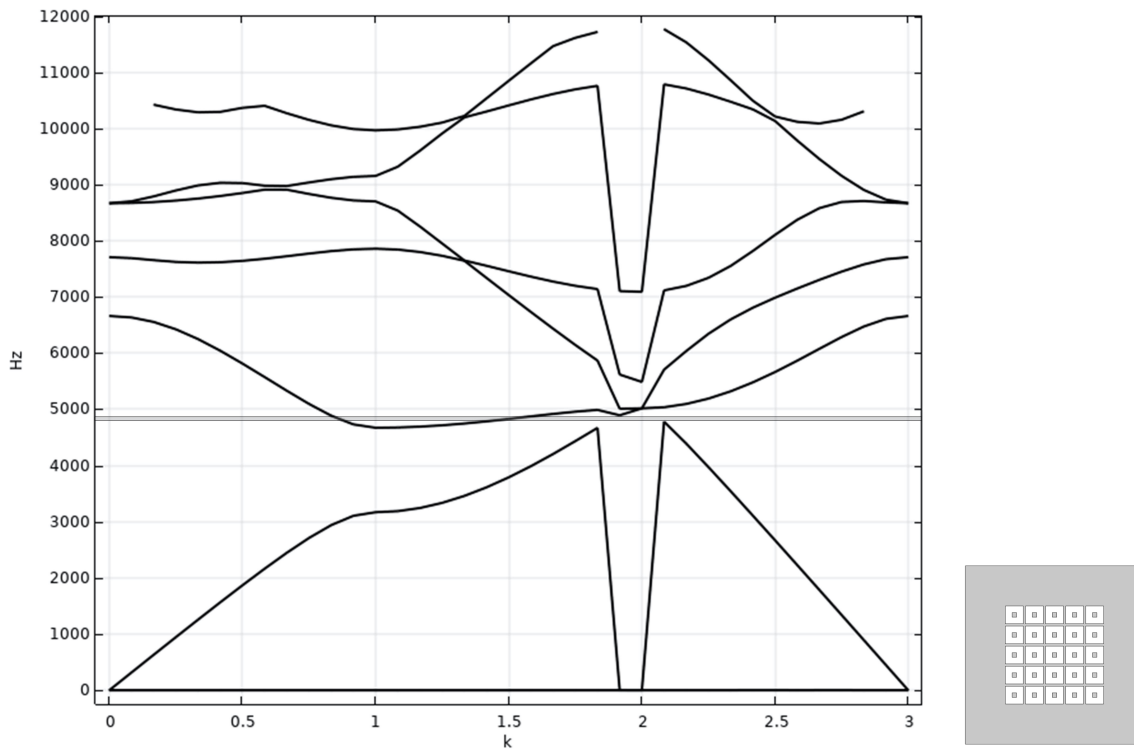


Figure 7.4: The band structure of the model 5b: with 5x5 holes and with resonators in the length of 1x1mm

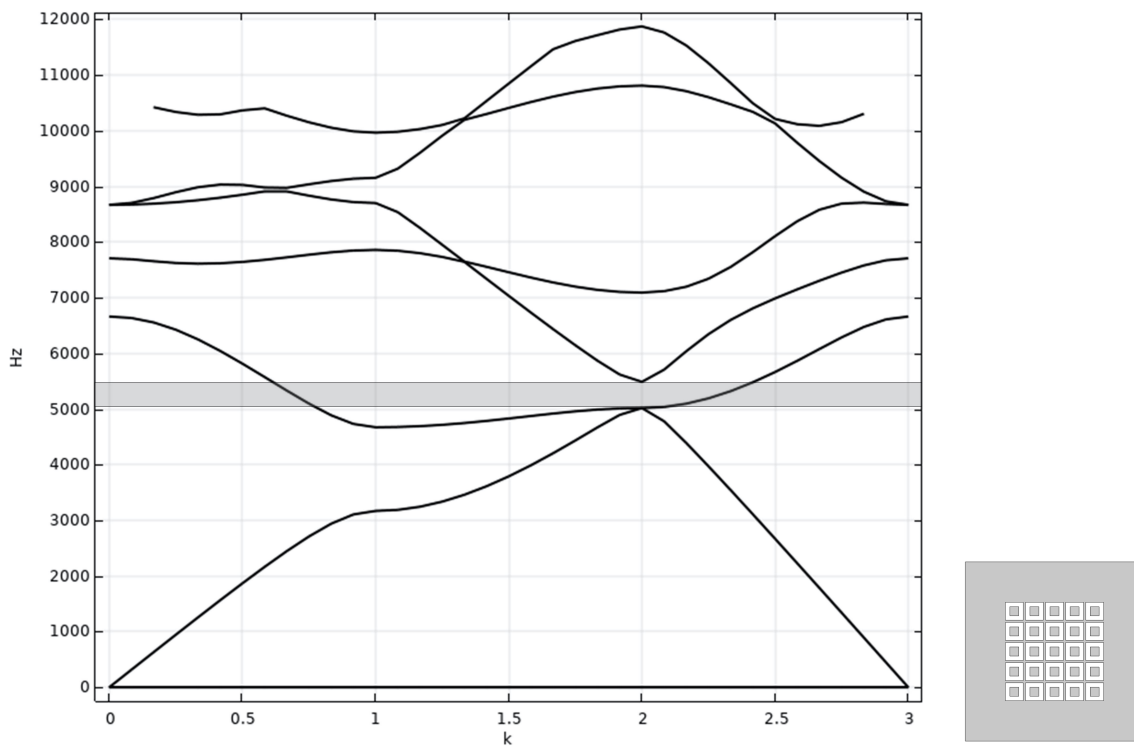


Figure 7.5: The band structure of the model 6a: with 5x5 holes and with resonators in the length of 2x2mm

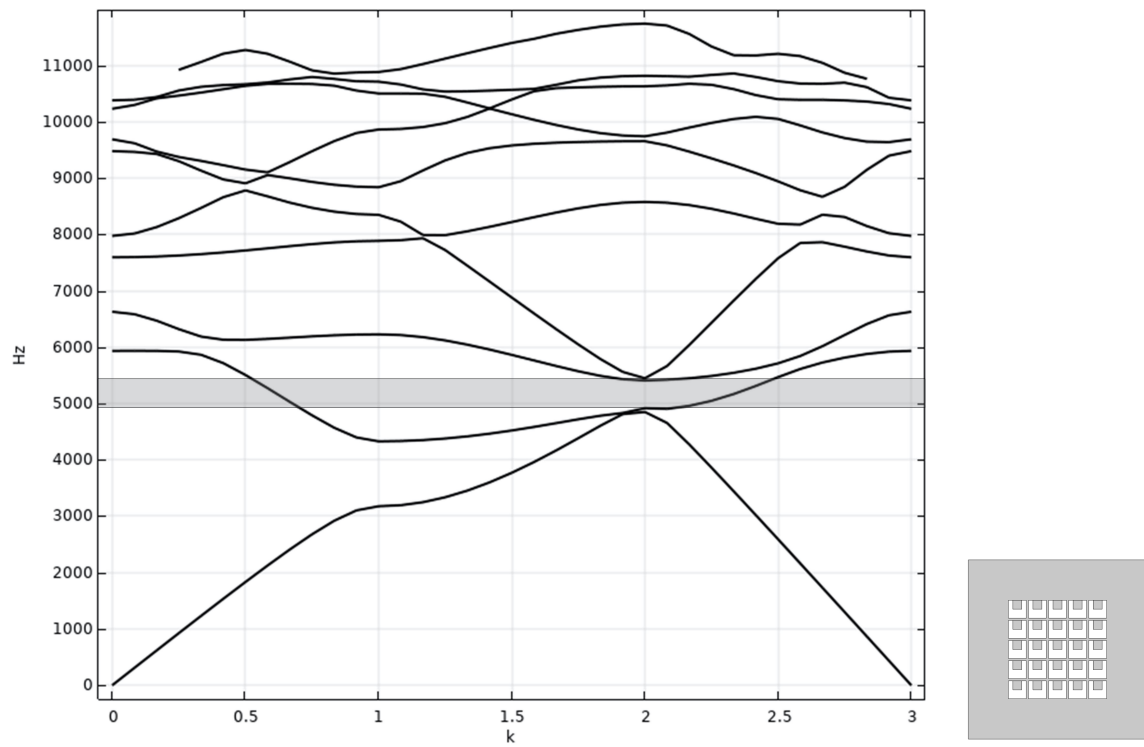


Figure 7.6: The band structure of the model 7b: with 5x5 holes and with 2x2mm resonators on the side

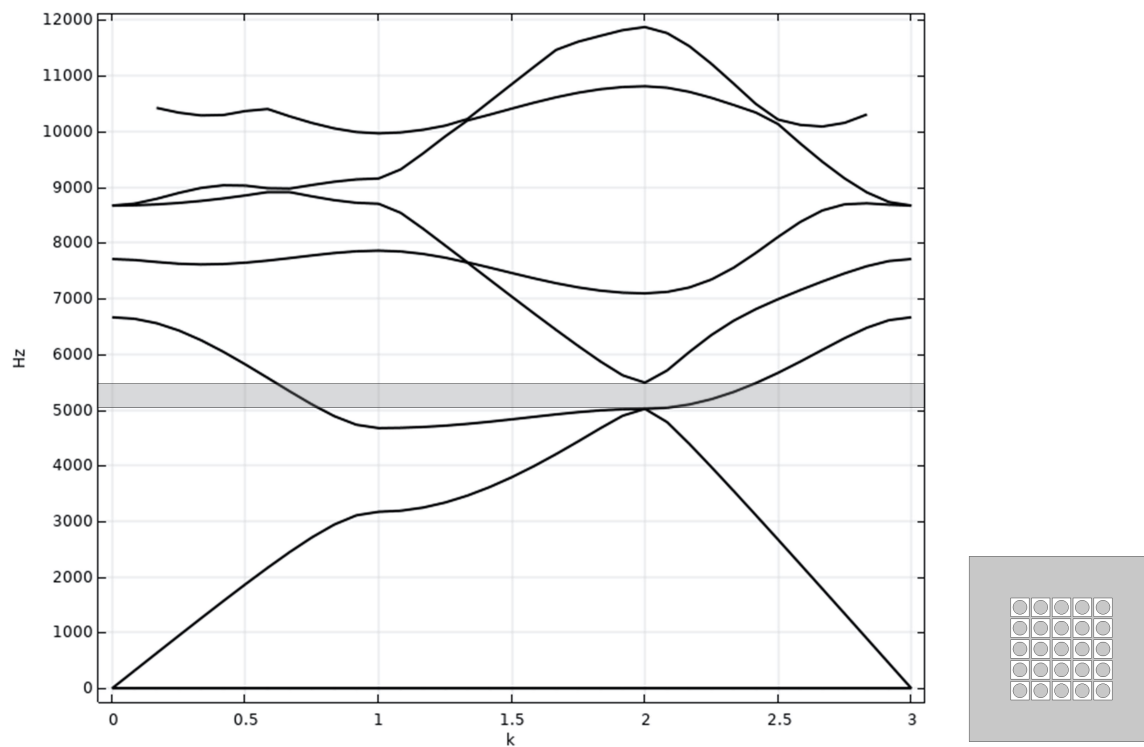


Figure 7.7: The band structure of the model 9a: with 5x5 holes and circle resonators

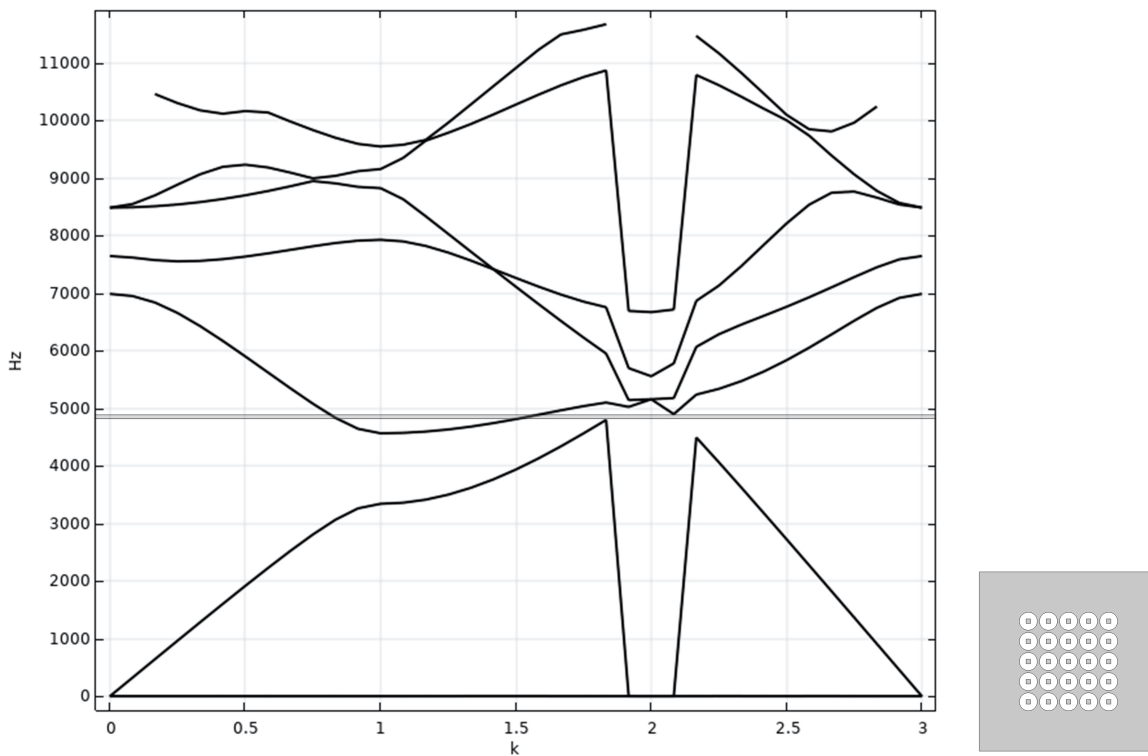


Figure 7.8: The band structure of the model 9b: with circle holes and with resonators in the length of 1x1mm

7.2 Discussion about simulation results

In the last section, the dispersion relation diagrams of all models are showed. In order to analyze the influence of single parameter on the results, at one time two of them are chosen and compared to make sure that only one variable parameter exists. The analyzed parameters are: with and without resonators, the form and shape of resonators, the size of resonators, the form and shape of holes, and the position of resonators. After comparing the simulation diagrams one by one, following summaries can be made as the first conclusion:

- If there are no resonators, the more holes in the model, the larger value of the stop band. And the circular holes have a smaller frequency band range than square holes.
- The square resonators with the size 1x1mm show a very small stop band range and an unstable noise reduction effect, not only in square holes but also in circular holes.
- The position of resonators has an influence on the frequency range. If resonators are connected to the side wall of holes rather than bottom, the stop band range will be smaller.
- With the same position of resonators and the same holes, there are almost no difference in the stop band between square resonators and circular resonators.
- With the same holes, there are almost no difference between the stop band frequency of the model with resonators and without resonators.

7.3 Correlation between simulation and experiment results

In this section, the experimental results and simulation results of the same model will be compared and analyzed. The main focus is to optimize the simulation process, so that the results of simulation are as close as possible to the experimental results.

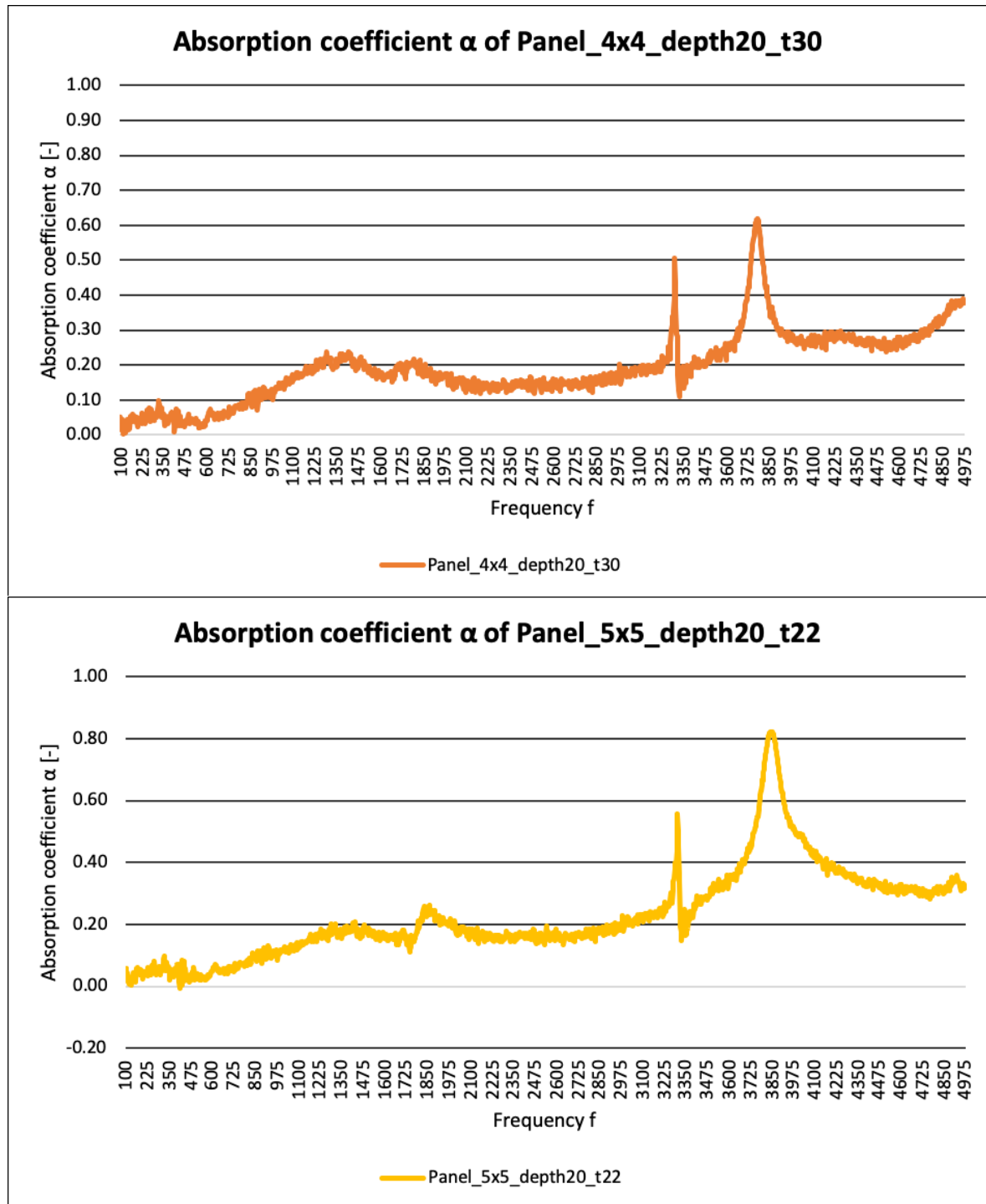


Figure 7.9: Experimental results of model 2a and model 2b

By comparing these two diagrams from experiment, the stop band of the model with 4x4

holes is between 3600Hz and 3850Hz, the stop band of the model with 5x5 holes is between 3725Hz and 3975Hz. The more holes in the model, the larger value of the stop band. This conclusion is same to the simulation results. However, the frequency band values from experiments are smaller than the simulation.

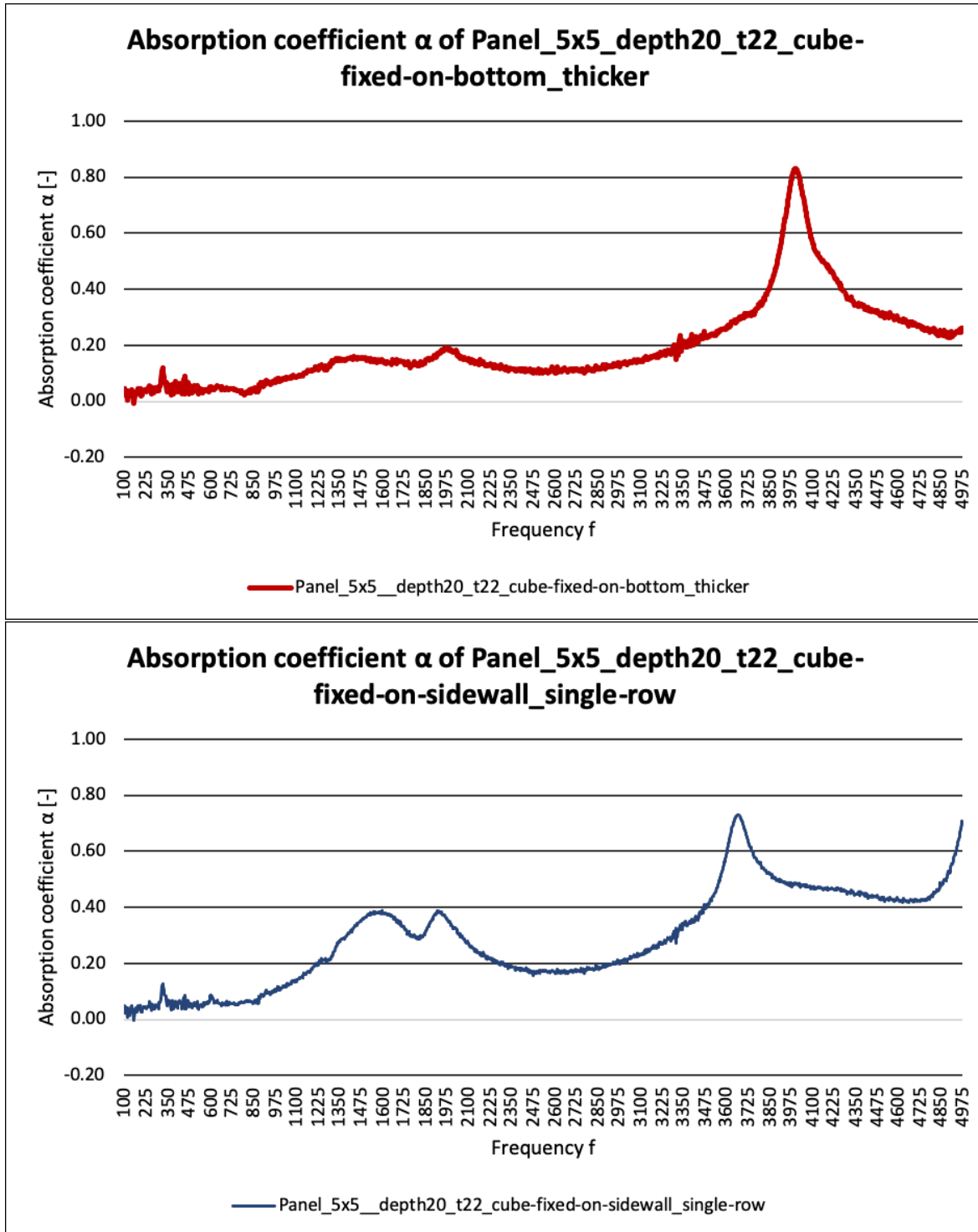


Figure 7.10: Experimental results of model 5a and model 5b

By comparing these two diagrams from experiment, the stop band of the model with resonators connected to the bottom of holes is between 3850Hz and 4100Hz, the stop band of

the model with resonators connected to the side wall of holes is between 3600Hz and 3800Hz. The former has a larger frequency band range, which matches to the simulation. Different from the simulation, the latter has obviously smaller stop band values.

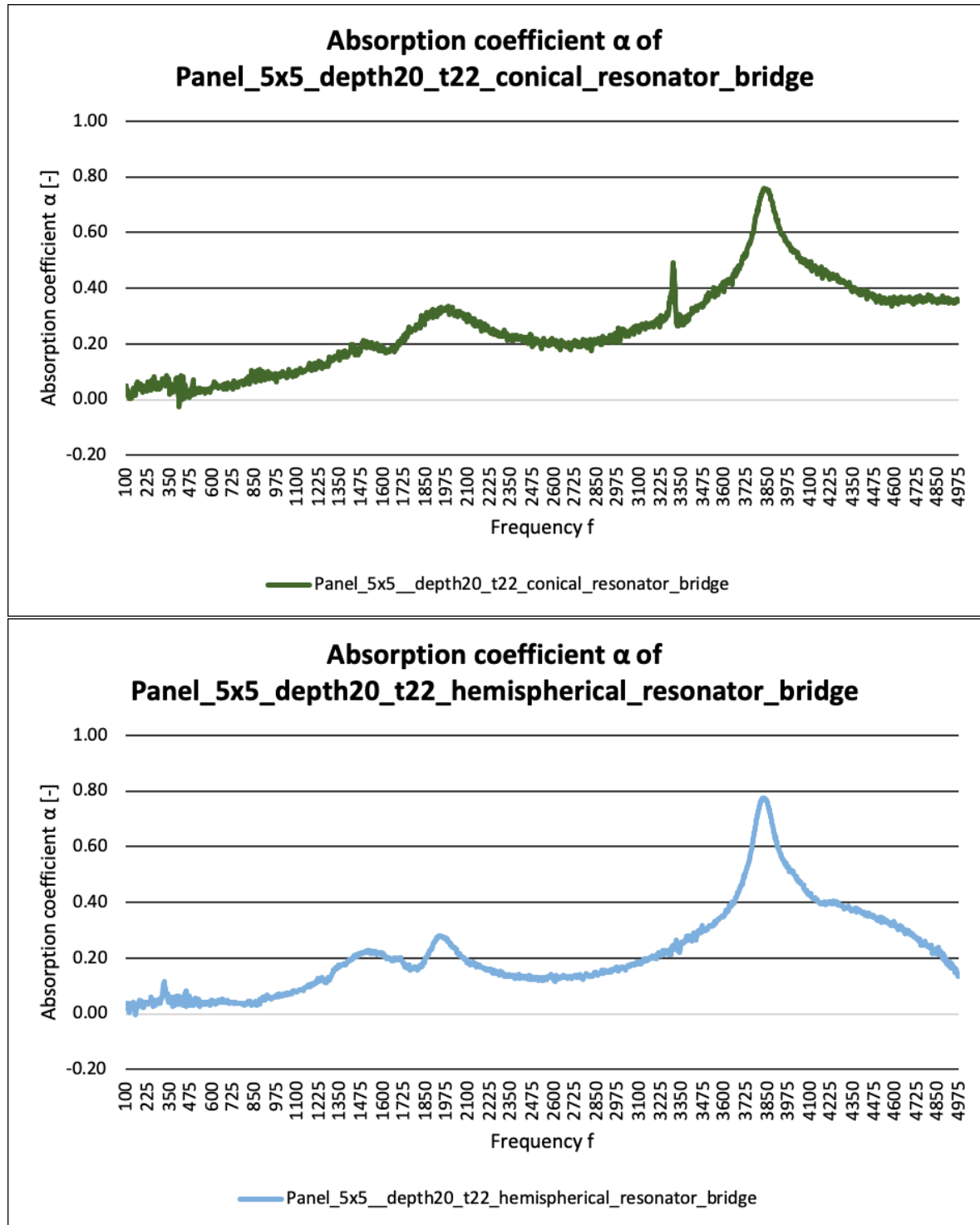


Figure 7.11: Experimental results of model 6a and model 7b

By comparing these two diagrams from experiment, the stop band of the model with square resonators is between 3725Hz and 3925Hz, which is almost exactly the same as the model

with circular resonators and same holes. This finding matches to the simulation but with larger frequency values.

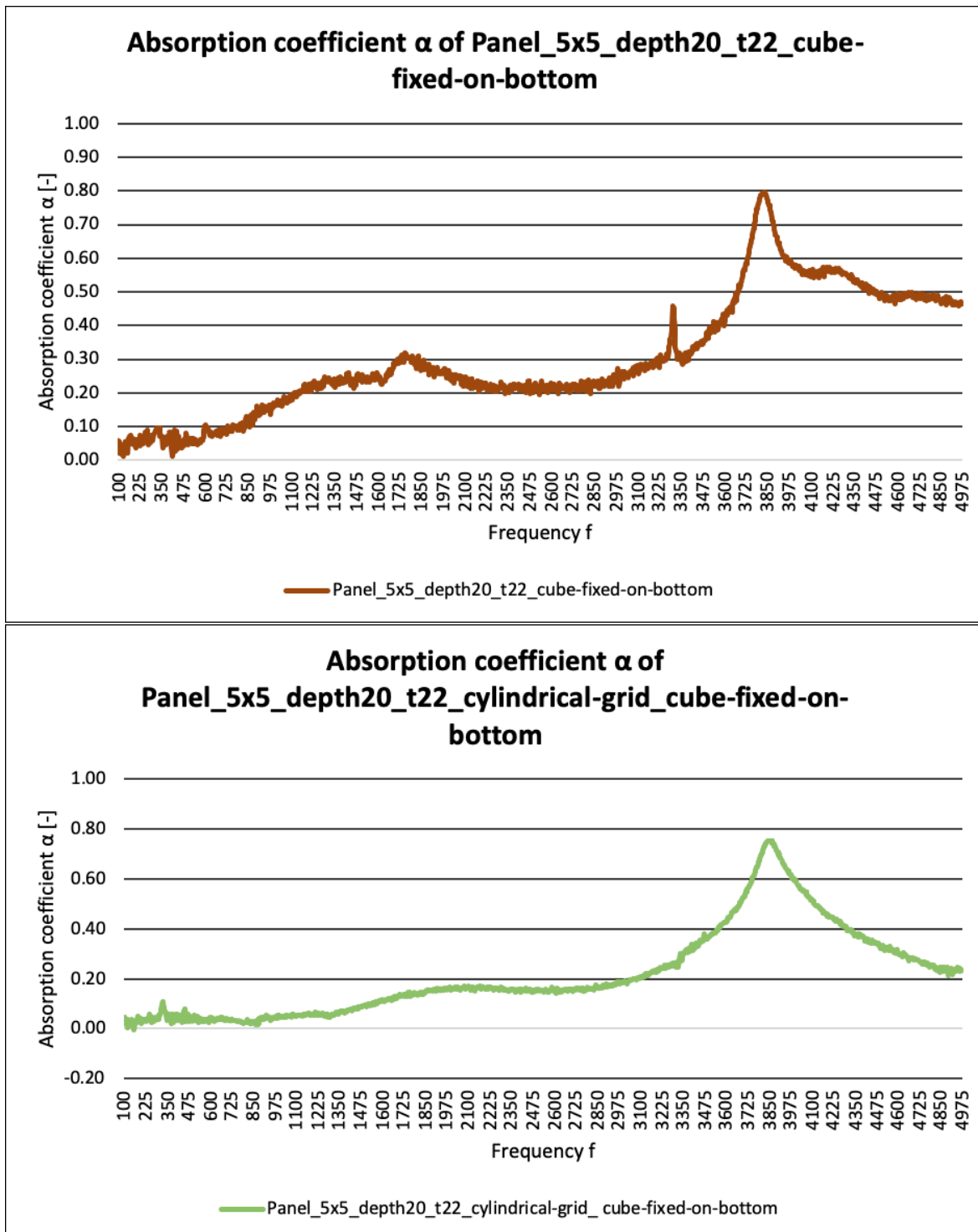


Figure 7.12: Experimental results of model 9a and model 9b

These two diagrams of models with 1x1mm resonators from experiments show a good absorption of noise in the frequency range 3725Hz–3925Hz, which can not be found in the simulation.

- **Similarities and differences of experimental and simulation results:**

The overall variation trend and characteristics of the frequency band are the same. The experimental results are generally smaller than the simulation. It should be noted that the influence of some parameters can not be found and evaluated in the simulation results.

7.4 Potentials for convergence study

- **Causes for the differences:**

The main reason why the frequency band values are different in the experiments and simulations is that the simulation model is only built in two-dimension. Some parameters which have great influence on the 3D-model can not be considered, such as the connecting part between resonators and holes, the depth of holes and resonators and the resonators which consists of several parts. Moreover, the simulation environment is idealized, that means, the interference of environmental factors was ignored, which leads to a larger frequency band value. Further more, by using the Floquet boundary condition the model is assumed to be periodically infinite, which is different from the experiment panel.

- **Potentials for the convergence study**

Firstly, for the model with smaller resonators in the length of 1mm, the mesh size of the resonators can be selected smaller to get an even finer meshing. With a finer meshing the interference of resonators with the basic structure can be better evaluated. Moreover, in order to ensure the geometry of simulation models is as close as possible to experiments, the four corners of model can be rounded to match the experiment panel.

8 Convergence study

In this chapter, the convergence study is executed for several chosen models based on the conclusion of last chapter. On the one hand, the models with smaller resonators in the length of 1mm are simulated with a finer meshing on the resonator surface. On the other hand, the four corners of basic square can be rounded to match the experimental results. In the following sections, the process of convergence study is showed and the results are compared with the last chapter. In the end, further suggestions for the research of acoustic metamaterials are summarized.

The principle of a convergence study is to find the most comprehensive result by changing only one variable parameter. In the following, the process of convergence study is firstly divided into two steps in order to keep only one variable parameter in each simulation. The two parameters are: mehsing size of smaller resonators, model geometry. After each simulation, the results are compared with the last chapter in order to prove the effectiveness of convergence study.

8.1 Convergence study of the meshing size for small resonators

In this section, only the parameter meshing size of resonators is changed. The meshing size of other model areas remains with the size of old models. In order to take a more visualized look, a single unit of resonators with the length of 1mm is showed in different meshing sizes in the following pictures. It is obvious that the number of triangle mesh units is much bigger. There are two simulated models (5b and 9b) from the chapter 5 have those smaller resonators. Each model is simulated with the finer meshing size and compared with the results from the last chapter.

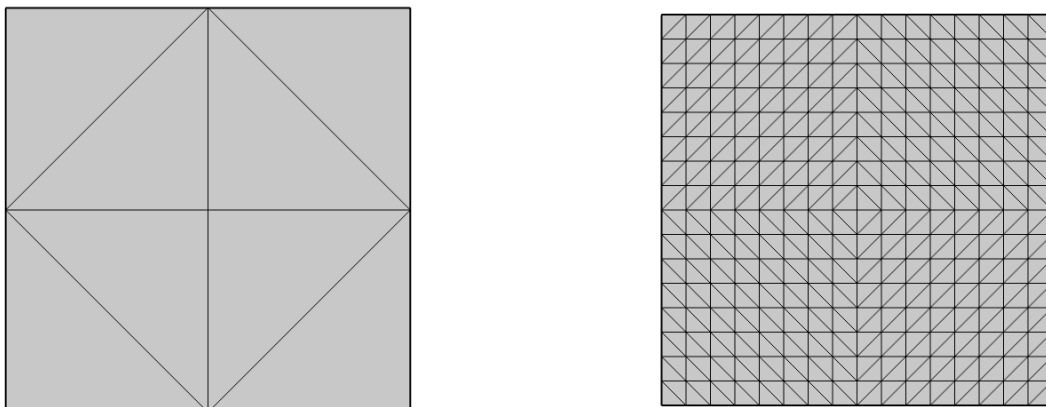


Figure 8.1: Comparison of different mesh size of resonators with the length of 1mm: rough mesh (left), finer mesh (right)

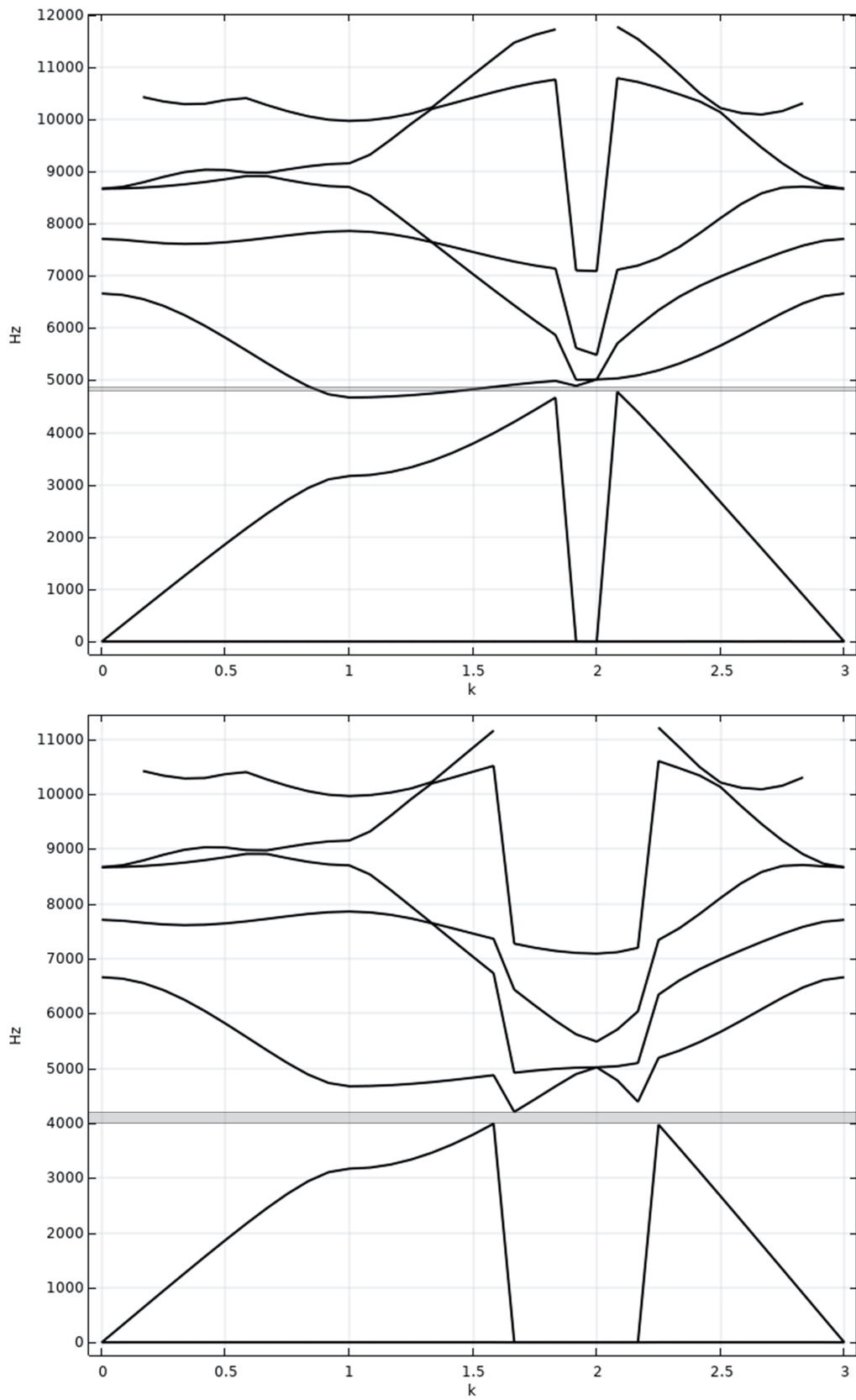


Figure 8.2: Comparison of simulation results of model 5b: rough mesh (upon), finer mesh (bottom)

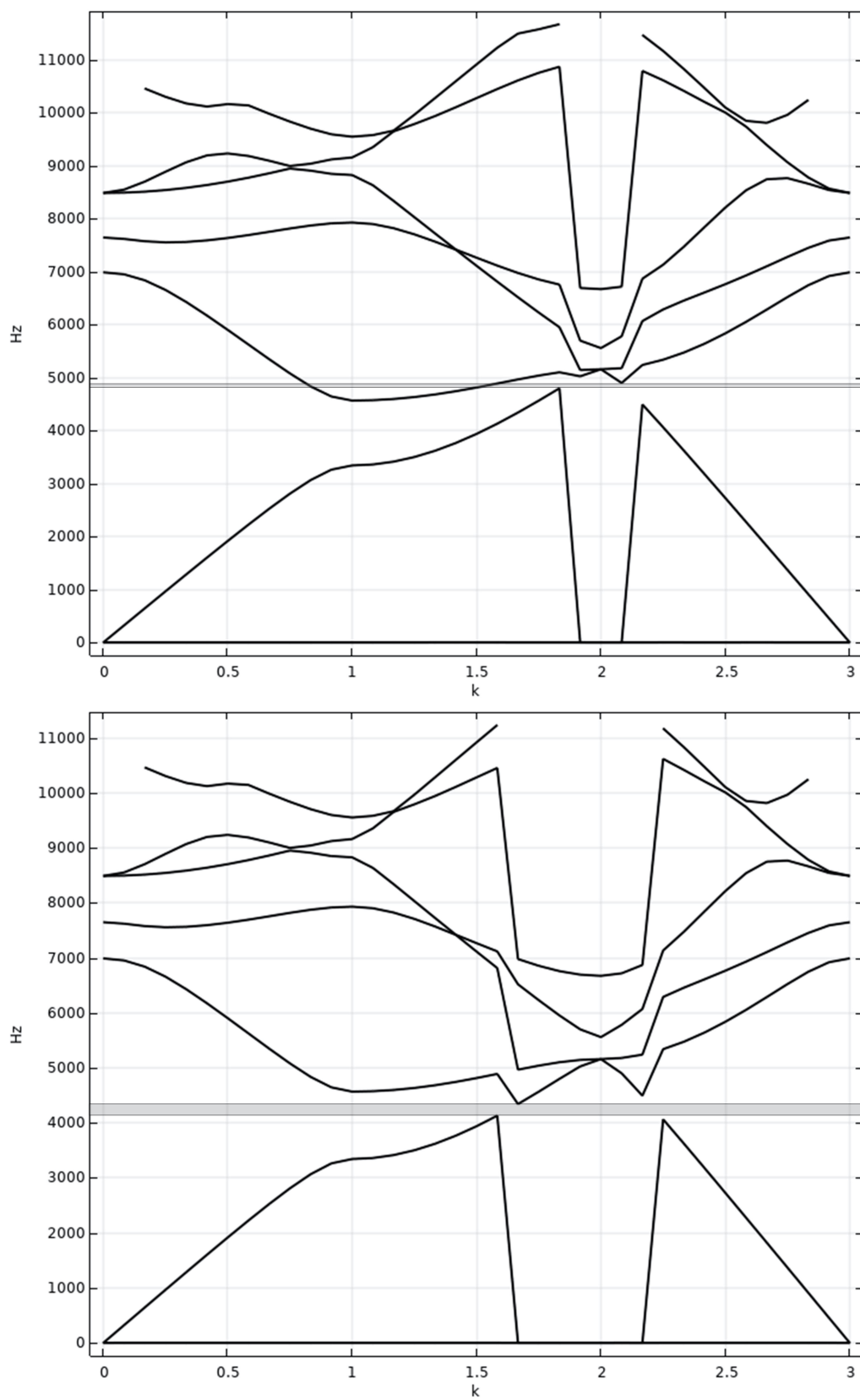


Figure 8.3: Comparison of simulation results of model 9b: rough mesh (upon), finer mesh (bottom)

In the pictures above the differences are showed between the model with rough and with finer meshing. The first two pictures are results of model 5b, which has 5x5 square holes with the small resonators. The last two pictures are results of model 9b, which has 5x5 circular holes with the small resonators. It is obvious that with a finer meshing size of resonators the stop band is wider and the frequency value is smaller, which means the eigenfrequency values of simulation are closer to the experiments. The stop band of improved model 5b is between 4000Hz–4250Hz. The stop band of improved model 9b is between 4250Hz–4400Hz.

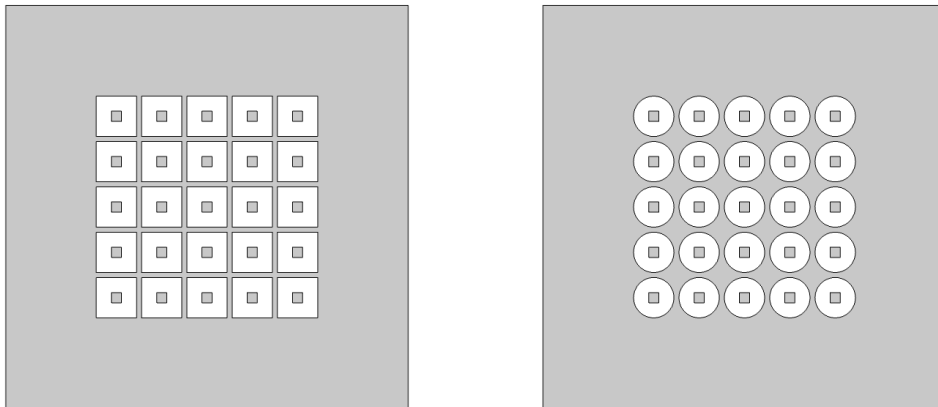


Figure 8.4: The simulation models with smaller resonators: model 5b (left), model 9b (right)

8.2 Convergence study of the model geometry

In this section, the model 2c and model 5a with 5x5 holes are taken as exsamples to prove the effectiveness of geometry improvement. The four corners of those models are rounded with a radius of 4mm, which is same as the hole length. Because the Floquet-Bloch boundary conditions can not be applied on the curved sides, only the straight sides of model are considered under the periodic boundary condition. The rest curved parts of sides are then automatically considered as sound hard boundaries.

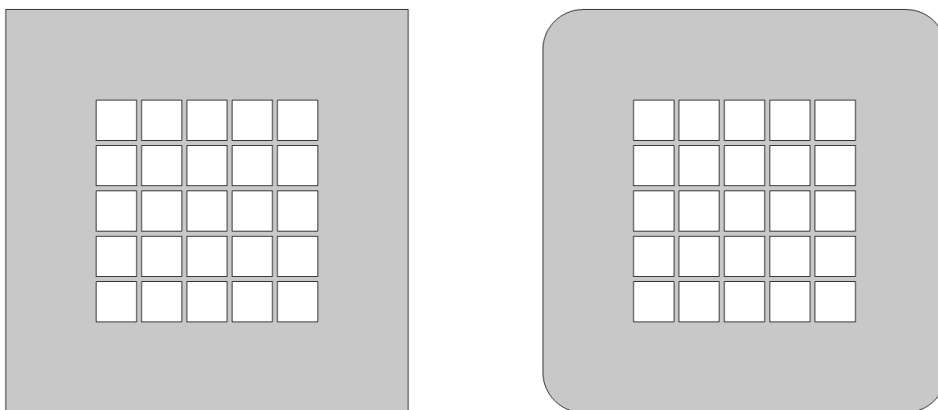


Figure 8.5: Model 2c before optimization (left) and after optimization (right)

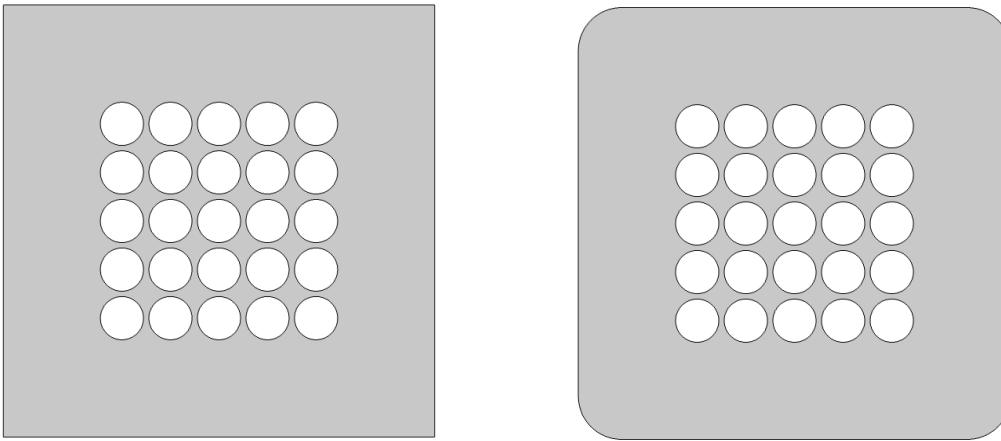


Figure 8.6: Model 5a before optimization (left) and after optimization (right)

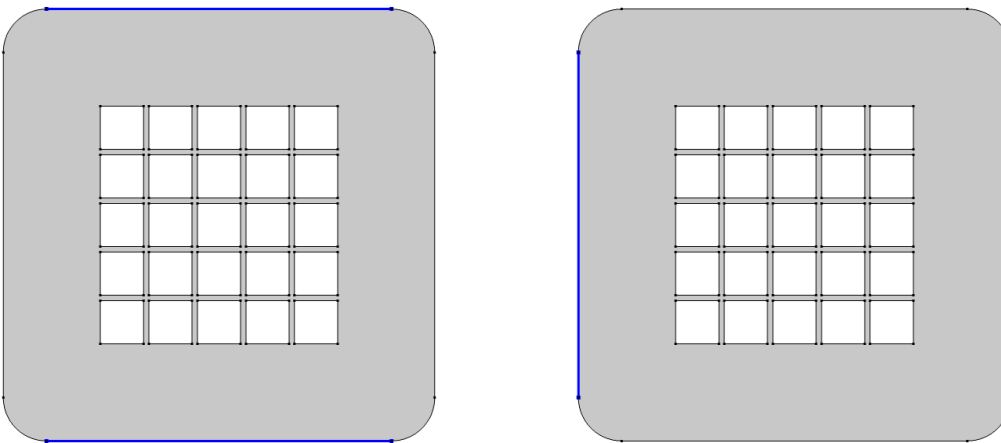


Figure 8.7: The Floquet-Bloch boundary conditions of optimized model 2c

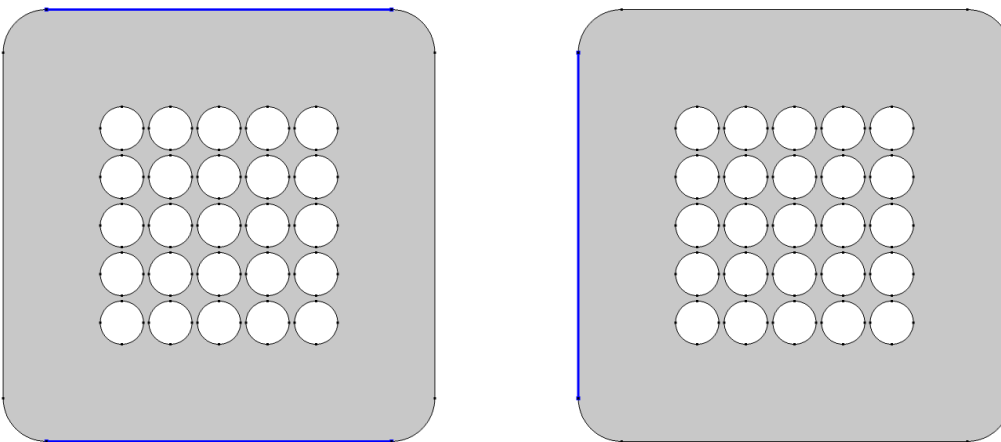


Figure 8.8: The Floquet-Bloch boundary conditions of optimized model 5a

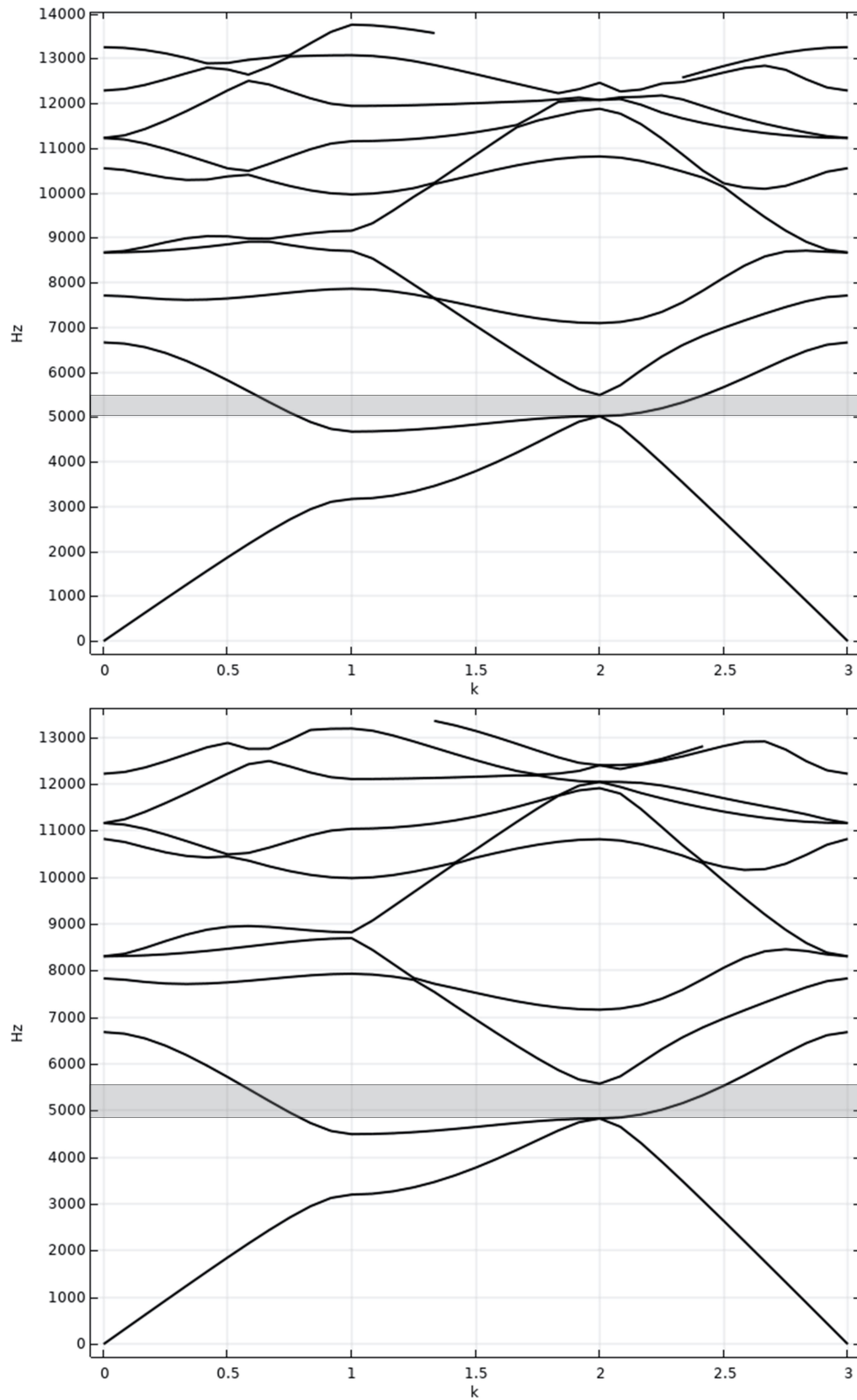


Figure 8.9: The simulation results of model 2c before (upon) and after (bottom) optimization

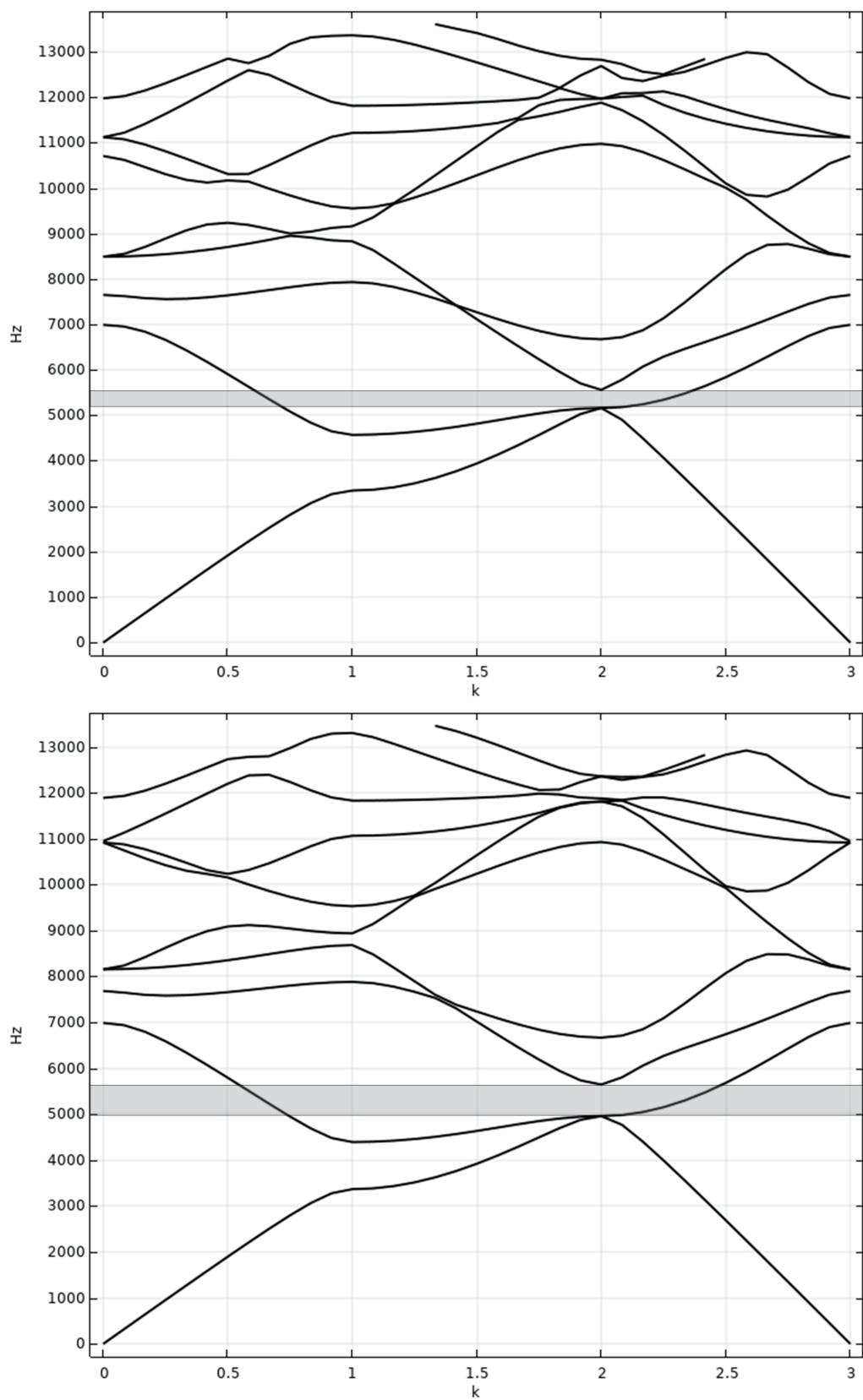


Figure 8.10: The simulation results of model 5a before (upon) and after (bottom) optimization

Except geometry and the Floquet-Bloch boundary condition of the simulation model, other parameters and properties remain unchanged comparing with the old model. By comparing the results before and after optimization, it is obvious that the stop band range is becoming bigger, and the minimum value of eigenfrequency is smaller, which is closer to the experimental results. The stop band of model 2c after optimization is between 4900Hz–5600Hz. The stop band of model 5a after optimization is between 5000Hz–5700Hz. In the following sections, the optimization process will be discussed and summarized. The challenges in simulating acoustic metamaterials will be illustrated. Some opinions for the future work will be suggested.

9 Discussion and summary

9.1 Discussion of results

To sum up, the overall variation trend and characteristics of the frequency band in the simulation are same as experiments. However, the eigenfrequencies of experiments are generally smaller than the simulation. Moreover, the influence of some parameters specially for three-dimensional models can not be evaluated in the simulation. It can be concluded that the simulation results agree with experimental results.

In the last chapter, two improvement methods are applied in the simulation process to match the experimental results. For the model with small resonators in the length of 1mm, the meshing size of resonators are reduced. For the model without resonators, four corners of basic square are rounded with a radius of 4mm. However, each method has its advantages and disadvantages. The first method can only be used for the model with relative small resonators, whose mesh units are much fewer than basic model panel. For the model with normal resonators, the meshing of resonator is just as same as the basic model. For the moment another method can only be applied for the model without resonators, the curved corners have to some extent influence on the eigenfrequency of resonators.

Obviously, both improvement methods can eliminate the influence of some factors on simulation results. With them the simulation results are more closer to the experiments. Nevertheless, none of them is perfect and can be applied for all kinds of models. As a result, there are still improvement potentials in the field of simulating acoustic metamaterials. In the following section, the challenges and suggestions will be explained.

9.2 Conclusion and outlook

Still, there are some challenges in the simulation of acoustic metamaterials:

- For the dispersion curve, the most simulations in literatures are achieved based on two-dimensional models. It is necessary to execute simulations with three-dimensional models, which match experimental prototypes. However, in order to simulate three-dimensional models for the dispersion curve, for each face and side of models the corresponding boundary conditions and initial conditions must be considered, which is still a challenge for today's work. Moreover, the most important factor for dispersion curve is the Floquet-Bloch boundary condition, which is mostly based on two-dimensional coordinate systems.
- In this thesis, only the band gap is compared with experiments as the results of simulations. For the most simulation models in the literature, it is difficult to get both dispersion curve and sound transmission loss. These two properties are based on different principles and formulas. But for a more powerful and persuasive result it is necessary to simulate both properties with a same model in the future work.
- Commonly, there are deviations between experimental and simulation results, whether the simulated property is dispersion curve or sound transmission loss. On the one

hand, the model itself can lead to this deviation, since the manufacturing method (for example 3D-printing technique) has errors, if the geometry of prototype is relatively small. On the other hand, the simulated environment is idealized, which is different from experimental environment. During experiments there are unavoidable constraints and influence factors. So it is necessary for the future work to build up a simulation environment which is as close to experiments as possible.

References

- Al-Zubi, M., Ayorinde, E., Witus, G., Dundar, M., Warriach, M., & Murty, Y. (2013). Vibro-acoustic characterization and optimization of periodic cellular material structures (pcms) for nvh applications. *Journal of Materials Science Research*, 2(4), 64.
- Amado-Mendes, P., Godinho, L., Dias, A. B., Amaral, P., & Pinho, N. (2018). A numerical study on the behavior of partition panels with micro-resonator-type metamaterials.
- Ang, L. Y. L., Koh, Y. K., & Lee, H. P. (2016). Acoustic metamaterials: A potential for cabin noise control in automobiles and armored vehicles. *Journal of Applied Mechanics*, 8(05), 1650072.
- Application of the plane wave expansion method to a two-dimensional, hexagonal photonic crystal.* (2013).
- Bin, J., Wen-Jun, Z., Wei, C., An-Jin, L., & Wan-Hua, Z. (2011). Improved plane-wave expansion method for band structure calculation of metal photonic crystal. *Chinese Physics Letters*, 28(3), 034209.
- Cai, L., Xiaoyun, H., & Xisen, W. (2006). Band-structure results for elastic waves interpreted with multiple-scattering theory. *Physical Review B*, 74(15), 153101.
- Cao, Y., Hou, Z., & Liu, Y. (2004). Finite difference time domain method for band-structure calculations of two-dimensional phononic crystals. *Solid state communications*, 132(8), 539–543.
- Chen, H., Zeng, H., Ding, C., Luo, C., & Zhao, X. (2013). Double-negative acoustic metamaterial based on hollow steel tube meta-atom. *Journal of Applied Physics*, 113(10), 104902.
- Chen, Y., Huang, G., Zhou, X., Hu, G., & Sun, C. T. (2014). Analytical coupled vibroacoustic modeling of membrane-type acoustic metamaterials: membrane model. *The Journal of the Acoustical Society of America*, 136(3), 969–979.
- Claeys, C., Deckers, E., Plutmers, B., & Desmet, W. (2016). A lightweight vibro-acoustic metamaterial demonstrator: Numerical and experimental investigation. *Mechanical systems and signal proceeding*, 70, 853–880.
- Danner, A. J. (2002). An introduction to the plane wave expansion method for calculating photonic crystals band diagrams. *University of Illinois*.
- Dastjerdi, S. R., & Ghanaatshoar, M. (2013). Finite difference time domain method for calculating the band structure of a 2d photonic crystal and simulating the lensing effect. *In Journal of Physics: Conference Series*, 454(1), 012011.
- Deng, J., Guasch, O., & Zheng, L. (2019). Ring-shaped acoustic black holes for broadband vibration isolation in plates. *Journal of Sound and Vibration*.
- Deymier, P. A. (Ed.). (2013). *Acoustic metamaterials and phononic crystals* (Vol. 173). Springer Science & Business Media.
- Dong, H. W., Zhao, S. D., Wei, P., Cheng, L., Wang, Y. S., & Zhang, C. (2019). Systematic design and realization of double-negative acoustic metamaterials by topology optimization. *Acta Material*, 172, 102–120.
- Dowling, L., Flanagan, L., Rice, H., Trimble, D., & Kennedy, J. (n.d.). The use of a benchmark periodic metamaterial to inform numerical modelling and additive manufacturing approaches.
- Elford, D. P., Chalmers, L., Kusmartsev, F. V., & Swallowe, G. M. (2011). Matryoshka locally resonant sonic crystal. *The Journal of the Acoustical Society of America*, 130(5),

- 2746–2755.
- Guild, M., Rohde, C., Tothko, M., & Sieck, C. (2018). 3d printed acoustic metamaterial sound absorbers using functionally-graded sonic crystals. *In Proceedings of Euronoise*.
- Gupta, A. (2014). A review on sonic crystal, its applications and numerical analysis techniques. *Acoustical Physics*, 60(2), 223–234.
- Huang, T. Y., Shen, C., & Jing, Y. (2016). Membrane- and plate-type acoustic metamaterials. *The Journal of the Acoustical Society of America*, 139(6), 3240–3250.
- Jung, J., Kim, H.-G., Chol, D. R., & Wang, S. (2018). An application of acoustic metamaterial for reducing noise transfer through car body panels. *SAE Technical Paper*.(No. 2018-01-1566).
- Li, J., & Chan, C. (2004). Double-negative acoustic metamaterial. *Physical Review E*, 70(5), 055602.
- Liu, Z., Zhang, X., Mao, Y., Zhu, Y., Yang, Z., Chan, C., & Sheng, P. (2000). Locally resonant sonic materials. *science*, 289(5485), 1734–1736.
- LU, L., OTOMORI, M., YAMADA, T., YAMAMOTO, T., IZUI, K., & NISHIWAKI, S. (2014). Topology optimization of acoustic metamaterials with negative mass density using a level set-based method. *Mechanical Engineering Journal*, 1(4), DSM0040–DSM0040.
- Lu, Z., Yu, X., Lau, S.-K., Khoo, B. C., & Cui, F. (2020). Membrane-type acoustic metamaterial with eccentric masses for broadband sound isolation. *Applied Acoustics*, 157, 107003.
- Ma, G., & Sheng, P. (2016). Acoustic metamaterials: From local resonances to broad horizons. *Science advances*, 2(2), e1501595.
- Maldovan, M., & Thomas, E. L. (2009). *Periodic materials and interference lithography for photonics, phononics and mechanics*. John Wiley & Sons.
- Matlack, K. H., Bauhofer, A., Kröder, S., Palermo, A., & Daraio, C. (2016). Composite 3d-printed metastructures for low-frequency and broadband vibration absorption. *Proceedings of the National Academy of Sciences*, 113(30), 8386–8390.
- Mavropoulos, P., & Papanikolaou, N. (2006). The korringa-kohn-rostoker (kkR) green function method i. electronic structure of periodic systems. *NIC Series*, 31, 131–158.
- Mei, J., Ma, G., Yang, M., Yang, Z., Wen, W., & Sheng, P. (2012). Dark acoustic metamaterials as super absorbers for low-frequency sound. *Nature communications*, 3(1), 1–7.
- Melo, N. F., Claeys, C., Deckers, E., Pluymers, B., & Desmet, W. (2016). Dynamic metamaterials for structural stopband creation. *SAE International Journal of Passenger Cars Mechanical Systems*, 9(2016-01-1791), 1013–1019.
- Mohammadi, S., Eftekhar, A. A., Khelif, A., & Adibi, A. (2010). Simultaneous two-dimensional phononic and photonic band gaps in opto-mechanical crystal slabs. *Optics express*, 18(9), 9164–9172.
- Naify, C. J., Chang, C.-M., McKnight, G., & Nutt, S. (2010). Transmission loss and dynamic response of membrane-type locally resonant acoustic metamaterials. *Journal of Applied Physics*, 108(11), 114905.
- Nateghi, A., Van Belle, L., Claeys, C., Deckers, E., Pluymers, B., & Desmet, W. (2017). Wave propagation in locally resonant cylindrically curved metamaterial panels. *International Journal of Mechanical Sciences*, 127, 73–90.
- Nouh, M., Aldraihem, O., & Baz, A. (2015). Wave propagation in metamaterial plates with periodic local resonances. *Journal of Sound and Vibration*, 341, 53–73.
- Oltmann, J., Hartwich, T., & Krause, D. (2018). Design of particle dampers for lightweight

- structures using frequency based substructuring. *International Conference on Uncertainty in Structural Dynamics*(pp. 4049-4062).
- Qiu, M., & He, S. (2000). A nonorthogonal finite-difference time-domain method for computing the band structure of a two-dimensional photonic crystal with dielectric and metallic inclusions. *Journal of applied physics*, 87(12), 8268–8275.
- Rice, H. J., Kennedy, J., Göransson, P., Dowling, L., & Trimble, D. (2020). Design of a kelvin cell acoustic metamaterial. *Journal of Sound and Vibration*(115167).
- Sangluliano, L., Claeys, C., Deckers, E., Pluymers, B., & Desmet, W. (2018). Force isolation by locally resonant metamaterials to reduce nvh. *SAE Technical Papers*, 2018(June).
- Shadrivov, I. V., Kozyrev, A. B., van der Weide, D. W., & Kivshar, Y. S. (2008). Nonlinear magnetic metamaterials. *Optics Express*, 16(25), 20266–20271.
- Shi, S., Chen, C., & Prather, D. (2004). Plane-wave expansion method for calculating band structure of photonic crystal slabs with perfectly matched layers. *JOSA A*, 21(9), 1769–1775.
- Singh, A., & Jain, P. K. (2012). Fdtd analysis of the dispersion characteristics of the metal pbg structures. *Progress in Electromagnetics Research*, 39, 71–88.
- Stenger, N., Wilhelm, M., & Wegner, M. (2012). Experiments on elastic cloaking in thin plates. *Physical Review Letters*, 108(1), 014301.
- Wang, X., Chen, Y., Zhou, G., Chen, T., & Ma, F. (2019). Synergetic coupling large-scale plate-type acoustic metamaterial panel for broadband sound insulation. *Journal of Sound and Vibration*, 459, 114867.
- Watts, C. M., Liu, X., & Padilla, W. J. (2012). Metamaterial electromagnetic wave absorbers. *Advanced materials*, 24(23), OP98–OP120.
- Wu, J. H., Ma, F., Zhang, S., & L., S. (2016). Application of acoustic metamaterials in low-frequency vibration and noise reduction [j]. *Journal of Mechanical Engineering*, 52(13), 68–78.
- Xiao, X., He, Z., Li, E., & Cheng, A. (2019). Design multi-stopband laminate acoustic metamaterials for structural-acoustic coupled system. *Mechanical Systems and Signal Processing*, 115, 418–433.
- Yang, Z., Mei, J., Yang, M., Chan, N. H., & Sheng, P. (2008). Membrane-type acoustic metamaterial with negative dynamic mass. *Physical review letters*, 101(20), 204301.
- Yeh, S.-L., & Harne, R. L. (2019). Origins of broadband vibration attenuation empowered by optimized viscoelastic metamaterial inclusions. *Journal of Sound and Vibration*.
- Yu, D., Liu, Y., Zhao, H., Wang, G., & Qiu, J. (2006). Flexural vibration band gaps in euler-bernoulli beams with locally resonant structures with two degrees of freedom. *Physical Review B*, 73(6), 064301.
- Zhang, W., Chan, C. T., & Sheng, P. (2001). Multiple scattering consisting of coated spheres. *Optics express*, 8(3), 203–208.
- Zhou, M., Pan, C. P., Liu, L. P., Yuan, R., Ren, R. F., & Cai, L. (2007). Finite difference time domain method for computing the band-structure of 3d photonic crystals. *In Solid State Phenomena*, 121, 599–602.
- Zhou, X., Liu, X., & Hu, G. (2012). Elastic metamaterials with local resonances: an overview. *Theoretical and Applied Mechanics Letters*, 2(4), 041001.

List of Figures

2.1	Example of elastic metamaterial: pentamode metamaterial.....	7
2.2	Photograph of the nonlinear tunable magnetic created by a square lattice of nonlinear SRR. resonator	7
2.3	Schematic of the two canonical metamaterial unit cells used to create magnetic and electric response.....	8
2.4	Locally Resonant Sonic Crystals	9
3.1	Principle of mass-spring-unit in 3D-version.....	12
3.2	A spring-coupled mass-in-mass oscillator	13
3.3	Two-dimensional solid-vacuum phononic crystals.....	14
3.4	Two-dimensional air-solid phononic crystals	14
3.5	Two types of rod-type acoustic metamaterials according to Wu et al.....	15
3.6	Principles of two rod-type acoustic metamaterials.....	16
3.7	Single membrane with negative effective mass density	16
3.8	Schematics of the simulation configuration for the membrane-type acoustic metamaterial.....	17
3.9	Membrane or plate clamped in a waveguide: a) Without mass attached. b) With mass attached. c) The corresponding mass-spring diagram for a). d) The corresponding mass-spring diagram for b).	18
3.10	Schematic of acoustic meta-atom model of hollow steel tube: 2D and 3D model	18
3.11	CAD Sample based on a Kelvin Cell; 3D-printed Sample based on a benchmark structure.....	19
3.12	Compact 3D printed functionally-graded acoustic metamaterial sound absorber, consisting of 3 sections.....	19
4.1	Band structure of a 1D Photonic Crystal based on PWEM.....	21
4.2	Band diagramm based on FDTD.	23
4.3	Categories of finite elements.....	25
4.4	Finite-element discretization of radiator model	25
5.1	Sketch of the first prototype.....	27
5.2	Schematic representation of mass-spring system	28
5.3	Model 1: Panel-Flat-Sides	29
5.4	Model 2a: Panel-4x4-Length6-T30; Model 2b: Panel-4x4-Length6.....	29
5.5	Model 2c: Panel-Grid-Without-Resonator; Model 3a: Panel-Grid-13x13	30
5.6	Model 4a: Panel-Grid-5x5-Depth-5; Model 4b: Panel-Grid-5x5-Depth-10	31

5.7	Model 5a: Panel-Grid-Cube-Fixed-On-Bottom; Model 5b: Panel-Grid-Cube-Fixed-On-Bottom-5b	32
5.8	Model 6a: Panel-Grid-Cube-Fixed-On-Sidewall-6a; Model 6b: Panel-Grid-Cube-Fixed-On-Sidewall-6b	33
5.9	Model 7a: Panel-Grid-With-Cubic-Bridge; Model 7b: Panel-Grid-With-Conical-Resonator	34
5.10	Model 7c: Panel-Grid-Hemispherical-Resonator; Model 8a: Panel-8x8-Length2.5	35
5.11	Model 8b: Panel-5x5-Length4-Without-Bottom; Model 8c: Panel-5x5-Length4-Lattice-Edges	36
5.12	Model 9a: Panel-Cylindricalgrid; Model 9b: Panel-Cylindricalgrid-Cube-Fixed-On-Bottom	37
6.1	Sound absorption of some periodic cellular material structures based on Abaqus and Matlab	39
6.2	Band structure for a C-shaped locally resonant sonic crystal based on COMSOL ®Multiphysics.....	40
6.3	Results of STL. based on COMSOL ®Multiphysics	41
6.4	Results of frequency responses based on COMSOL ®Multiphysics.....	42
6.5	The typical Brillouin zone for two dimensional models: a) Square Brillouin zone; b) Hexagon Brillouin zone	43
6.6	The critical points in two dimensional Brillouin zones	44
6.7	Unit cell with Floquet boundary condition.....	45
6.8	Workflow of simulation steps in COMSOL Multiphysics	45
6.9	Model 2a (left) and model 2c (right)	47
6.10	Model 5a (left) and model 5b (right).....	47
6.11	Model 6a (left) and model 7b (right).....	47
6.12	Model 9a (left) and model 9b (right).....	48
6.13	The Brillouin zone for the simulation model.....	49
6.14	The Floquet-Bloch boundary condition for the model 2c	50
6.15	The Floquet-Bloch boundary condition for the model 6a.....	50
6.16	Sound hard boundaries of model 2c (left) and model 6a (right)	50
6.17	Sound hard boundaries of model 9b (left) and model 7b (right).....	51
6.18	Meshing for the structure (left) and for the boundaries (right) of model 2c	51
6.19	the Floquet-Bloch boundary condition for the meshing of model 2c	52
6.20	Meshing of model 6a (left) and model 9a (right)	52
6.21	Comparison of the band structure between the paper (left) and simulation (right) in this thesis.....	53

7.1	The band structure of the model 2a: with 4x4 holes and without resonators.....	54
7.2	The band structure of the model 2b: with 5x5 holes and without resonators.....	55
7.3	The band structure of the model 5a: with circle holes and without resonators ...	55
7.4	The band structure of the model 5b: with 5x5 holes and with resonators in the length of 1x1mm.....	56
7.5	The band structure of the model 6a: with 5x5 holes and with resonators in the length of 2x2mm.....	56
7.6	The band structure of the model 7b: with 5x5 holes and with 2x2mm resonators on the side.....	57
7.7	The band structure of the model 9a: with 5x5 holes and circle resonators.....	57
7.8	The band structure of the model 9b: with circle holes and with resonators in the length of 1x1mm.....	58
7.9	Experimental results of model 2a and model 2b	59
7.10	Experimental results of model 5a and model 5b	60
7.11	Experimental results of model 6a and model 7b	61
7.12	Experimental results of model 9a and model 9b	62
8.1	Comparison of different mesh size of resonators with the length of 1mm: rough mesh (left), finer mesh (right)	64
8.2	Comparison of simulation results of model 5b: rough mesh (upon), finer mesh (bottom)	65
8.3	Comparison of simulation results of model 9b: rough mesh (upon), finer mesh (bottom)	66
8.4	The simulation models with smaller resonators: model 5b (left), model 9b (right)	67
8.5	Model 2c before optimization (left) and after optimization (right)	67
8.6	Model 5a before optimization (left) and after optimization (right)	68
8.7	The Floquet-Bloch boundary conditions of optimized model 2c.....	68
8.8	The Floquet-Bloch boundary conditions of optimized model 5a.....	68
8.9	The simulation results of model 2c before (upon) and after (bottom) optimization.....	69
8.10	The simulation results of model 5a before (upon) and after (bottom) optimization.....	70

List of Tables

5.1	Parameters of Model 1	29
5.2	Parameters of Model 2a	30
5.3	Parameters of Model 2b	30
5.4	Parameters of Model 2c	31
5.5	Parameters of Model 3a	31
5.6	Parameters of Model 4a	32
5.7	Parameters of Model 4b	32
5.8	Parameters of Model 5a	33
5.9	Parameters of Model 5b	33
5.10	Parameters of Model 6a	34
5.11	Parameters of Model 6b	34
5.12	Parameters of Model 7a	35
5.13	Parameters of Model 7b	35
5.14	Parameters of Model 7c	36
5.15	Parameters of Model 8a	36
5.16	Parameters of Model 8b	37
5.17	Parameters of Model 8c	37
5.18	Parameters of Model 9a	38
5.19	Parameters of Model 9b	38
6.1	Global parameters for the simulation model	48
6.2	Material parameters for the simulation model	49
6.3	Parameter sweep for the wave vector k	52

List of abbreviations

BEM	Boundary Element Method
FDM	Fused Deposition Modelling
FDTD	Finite Difference Time Domain
FEM	Finite Element Method
FSS	Frequency Selective Surface
KKR	Korringa Kohn Rostoker
MSM	Multiple scattering method
NVH	Noise Vibration and Harshness
PCMS	Periodic Cellular Material Structures
PWEM	Plane wave expansion method
SLM	Selective Laser Melting
SLS	Selevtive Laser Sintering
STL	Sound Transimission Loss
SRR	Split Ring Resonator